

3.5 GHz Exclusion Zone Analyses and Methodology

E. Drocella
J. Richards
R. Sole
F. Najmy
A. Lundy
P. McKenna



report series

3.5 GHz Exclusion Zone Analyses and Methodology

**E. Drocella
J. Richards
R. Sole
F. Najmy
A. Lundy
P. McKenna**



U.S. DEPARTMENT OF COMMERCE

June 2015
Reissued March 2016

DISCLAIMER

Certain commercial equipment and materials are identified in this report to specify adequately the technical aspects of the reported results. In no case does such identification imply recommendation or endorsement by the National Telecommunications and Information Administration, nor does it imply that the material or equipment identified is the best available for this purpose.

PREFACE

The National Telecommunications and Information Administration's Office of Spectrum Management (OSM) and Institute for Telecommunication Sciences (ITS) would like to acknowledge and thank the staff of the Federal Communications Commission and the Department of Defense for their hard work and dedication in the preparation of this report that will lead to sharing the 3550-3650 MHz band between federal radar operations and commercial broadband systems. OSM and ITS would also like to acknowledge the assistance received from the Navy and Army spectrum management offices.

NOTE ON REISSUE

This report was reissued in March 2016 to correct a typographical error in (A-21) and to clarify certain terms in Sections 4 and 5.

CONTENTS

Preface.....	v
Note on Reissue	v
Figures.....	ix
Tables	xii
Abbreviations/Acronyms	xiii
Executive Summary	xv
1. Introduction.....	1
2. CBSD Technical and Deployment Parameters	3
2.1 Small Cell Device Technical Characteristics.....	3
2.2 Small Cell Device Deployment Characteristics.....	4
3. Radar Technical and Deployment Parameters	7
3.1 Radar Technical Parameters	7
3.2 Radar Deployment Parameters	8
4. Description of Shipborne Radar Analysis Methodology	9
4.1 Analysis Overview.....	9
4.2 Interference Link Budget	9
4.3 Radar Receiver Interference Threshold	10
4.4 AP and UE EIRP Values	11
4.5 Radar Receive Antenna Gain.....	11
4.6 Transmitter and Receiver Insertion Losses.....	11
4.7 Propagation and Clutter Loss.....	11
4.8 Building Attenuation Loss	13
4.9 Frequency Dependent Rejection.....	13
4.10 Shipborne Radar Exclusion Zone Distance Analysis Output	14
5. Description of Ground-Based Radar Analysis Methodology	18
5.1 Interference Link Budget	19
5.2 AP EIRP and Antenna Height	20
5.3 Radar Receive Antenna Gain.....	20
5.4 Basic Transmission Loss	20
5.5 Clutter Loss.....	20
5.6 FDR.....	20
5.7 Radar Receiver Interference Threshold	21
5.8 Ground-Based Radar Exclusion Zone Distance Analysis Output	21
6. Summary of Exclusion Zone Distance Analysis	23

7. References.....	25
Appendix A Description of Propagation and Clutter Loss Model.....	27
A.1 Introduction.....	27
A.2 Propagation Model Overview	27
A.3 The Extended Hata Model	28
A.4 The Irregular Terrain Model (ITM)	35
A.4.1 The Reference Attenuation.....	39
A.4.2 The Coefficients of the Diffraction Range	40
A.4.3 The Diffraction Range Attenuation Function.....	40
A.4.4 The Coefficients of the Line-of-Sight Range	42
A.4.5 The Line-of-Sight Range Attenuation Function.....	46
A.4.6 The Coefficients of the Forward (or Tropospheric) Scatter Range	47
A.4.7 The Scatter Range Attenuation Function	48
A.4.8 Variability and the Quantiles of the Attenuation.....	50
A.5 References	54
Appendix B Shipborne Radar Analysis Results	56
B.1 Introduction	56
B.2 Shipborne Radar Analysis Results	56
B.3 References	75
Appendix C Ground-Based Radar Analysis Results	76
C.1 Introduction	76
C.2 Ground-Based Radar Analysis Results	76
C.3 References	82

FIGURES

Figure 1. Example—Exclusion zone distances referenced to the coastline for different confidence intervals.	15
Figure 2. Example—Exclusion zone distances for different confidence intervals for a shipborne radar at S2.	16
Figure 3. Example of Visualyse simulation area.	19
Figure 4. AP emission spectra measurement used for the model and the analysis.	21
Figure 5. Example output— <i>IN</i> cumulative distribution of interference probability.	22
Figure B-1. Shipborne Radar 1—exclusion zone lower 48 states (yellow line—fast track exclusion zone and blue line—revised exclusion zone).	56
Figure B-2. Shipborne radar 1—Exclusion zone upper west coast (yellow line—fast track exclusion zone and blue line—revised exclusion zone).	57
Figure B-3. Shipborne Radar 1—Exclusion zone middle west coast (yellow line—fast track exclusion zone and blue line—revised exclusion zone).	57
Figure B-4. Shipborne Radar 1—Exclusion zone lower west coast (yellow line—fast track exclusion zone and blue line—revised exclusion zone).	58
Figure B-5. Shipborne Radar 1—Exclusion zone upper east coast (yellow line—fast track exclusion zone and blue line—revised exclusion zone).	58
Figure B-6. Shipborne Radar 1—Exclusion zone middle east coast (yellow line—fast track exclusion zone and blue line—revised exclusion zone).	59
Figure B-7. Shipborne Radar 1—exclusion zone lower east coast (yellow line—fast track exclusion zone and blue line—revised exclusion zone).	59
Figure B-8. Shipborne Radar 1—Exclusion zone eastern gulf coast (yellow line—fast track exclusion zone and blue line—revised exclusion zone).	60
Figure B-9. Shipborne Radar 1—Exclusion zone western gulf coast (yellow line—fast track exclusion zone and blue line—revised exclusion zone).	60
Figure B-10. Shipborne Radar 4—Exclusion zone lower 48 states (yellow line—fast track exclusion zone and blue line—revised exclusion zone).	61
Figure B-11. Shipborne Radar 4—Exclusion zone upper west coast (yellow line—fast track exclusion zone and blue line—revised exclusion zone).	61

Figure B-12. Shipborne Radar 4–Exclusion zone middle west coast (yellow line–fast track exclusion zone and blue line–revised exclusion zone).	62
Figure B-13. Shipborne Radar 4–Exclusion zone lower west coast (yellow line–fast track exclusion zone and blue line–revised exclusion zone).	62
Figure B-14. Shipborne Radar 4–Exclusion zone upper east coast (yellow line–fast track exclusion zone and blue line–revised exclusion zone).	63
Figure B-15. Shipborne Radar 4–Exclusion zone middle east coast(yellow line–fast track exclusion zone and blue line–revised exclusion zone).	63
Figure B-16. Shipborne Radar 4–exclusion zone lower east coast (yellow line–fast track exclusion zone and blue line–revised exclusion zone).	64
Figure B-17. Shipborne Radar 4–Exclusion zone eastern gulf coast (yellow line–fast track exclusion zone and blue line–revised exclusion zone).	64
Figure B-18. Shipborne Radar 4–Exclusion zone eastern gulf coast (yellow line–fast track exclusion zone and blue line–revised exclusion zone).	65
Figure B-19. Shipborne Radar 5–Exclusion zone lower 48 states(yellow line–fast track exclusion zone and blue line–revised exclusion zone).	65
Figure B-20. Shipborne Radar 5–Exclusion zone upper west coast(yellow line–fast track exclusion zone and blue line–revised exclusion zone).	66
Figure B-21. Shipborne Radar 5–Exclusion zone middle west coast (yellow line–fast track exclusion zone and blue line–revised exclusion zone).	66
Figure B-22. Shipborne Radar 5–Exclusion zone lower west coast (yellow line–fast track exclusion zone and blue line–revised exclusion zone).	67
Figure B-23. Shipborne Radar 5–Exclusion zone upper east coast (yellow line–fast track exclusion zone and blue line–revised exclusion zone).	67
Figure B-24. Shipborne Radar 5–Exclusion zone middle east coast (yellow line–fast track exclusion zone and blue line–revised exclusion zone).	68
Figure B-25. Shipborne Radar 5–Exclusion zone lower east coast (yellow line–fast track exclusion zone and blue line–revised exclusion zone).	68
Figure B-26. Shipborne Radar 5–Exclusion zone eastern gulf coast (yellow line–fast track exclusion zone and blue line–revised exclusion zone).	69
Figure B-27. Shipborne Radar 5–Exclusion zone western gulf coast (yellow line–fast track exclusion zone and blue line–revised exclusion zone).	69

Figure B-28. Composite shipborne radar exclusion zone lower 48 states (yellow line–fast track exclusion zone and blue line–revised exclusion zone).	70
Figure B-29. Composite shipborne radar exclusion zone upper west coast (yellow line–fast track exclusion zone and blue line–revised exclusion zone).	70
Figure B-30. Composite shipborne radar exclusion zone middle west coast (yellow line–fast track exclusion zone and blue line–revised exclusion zone).	71
Figure B-31. Composite shipborne radar exclusion zone lower west coast (yellow line–fast track exclusion zone and blue line–revised exclusion zone).	71
Figure B-32. Composite shipborne radar exclusion zone upper east coast (yellow line–fast track exclusion zone and blue line–revised exclusion zone).	72
Figure B-33. Composite shipborne radar exclusion zone middle east coast (yellow line–fast track exclusion zone and blue line–revised exclusion zone).	72
Figure B-34. Composite shipborne radar exclusion zone lower east coast(yellow line–fast track exclusion zone and blue line–revised exclusion zone).	73
Figure B-35. Composite shipborne radar exclusion zone eastern gulf coast (yellow line–fast track exclusion zone and blue line–revised exclusion zone).	73
Figure B-36. Composite shipborne radar exclusion zone western gulf coast (yellow line–fast track exclusion zone and blue line–revised exclusion zone).	74
Figure C-1. Ground-based radar exclusion zone lower 48 states.	78
Figure C-2. Ground-based radar exclusion zone upper west coast.....	78
Figure C-3. Ground-based radar exclusion zone middle west coast.....	79
Figure C-4. Ground-based radar exclusion zone upper central.	79
Figure C-5. Ground-based radar exclusion zone lower central.	80
Figure C-6. Ground-based radar exclusion zone upper east coast.....	80
Figure C-7. Ground-based radar exclusion zone middle east coast.....	81
Figure C-8. Ground-based radar exclusion zone lower east coast.....	81

TABLES

Table 1. Small Cell Device (CBSD) Technical Characteristics Used in Exclusion Zone Analysis	3
Table 2. Example Calculation for Number of APs	6
Table 3. Antenna Directivity Parameters	7
Table 4. Peak and Average Mask Pattern Equations	7
Table 5. Summary of Shipborne Radar Analysis Results	23
Table 6. Summary of Shipborne Radar Analysis Results	23
Table 7. Summary of Shipborne Radar Analysis Results	23
Table 8. Summary of Ground-Based Radar Analysis Results	24
Table A-1. Okumura et al. Location Variability Standard Deviations	34
Table A-2. Irregular Terrain Model Input Parameters/Data and Preliminary Calculations	35
Table A-3. Longley-Rice Low Probability or “Ducting” Constants	53
Table B-1. Summary of Shipborne Radar Analysis Results	74
Table B-2. Comparison of Summary of Shipborne Radar Analysis Results	75
Table B-3. Summary of Shipborne Radar Analysis Results by Area Affected	75
Table C-1. Ground-Based Radar 1 Locations	76
Table C-2. Ground-Based Radar 3 Locations	77
Table C-3. Results of Ground-Based Radar Analyses	77

ABBREVIATIONS/ACRONYMS

AP	access point
CBRS	Citizens Broadband Radio Service
CBSD	Citizens Broadband Radio Service Device
dB	decibel
dB_i	decibels relative to an isotropic antenna
dB_m	decibels relative to a milliwatt
DoD	Department of Defense
EIRP	equivalent isotropically radiated power
FCC	Federal Communications Commission
FDR	frequency dependent rejection
GHz	gigahertz
GIS	Geographic Information System
$\frac{I}{N}$	interference-to-noise ratio (dB)
IF	Intermediate Frequency
ITM	ITS Irregular Terrain Model
ITS	Institute for Telecommunication Sciences
log	common logarithm
ln	natural logarithm
MHz	megahertz
NLCD	National Land Cover Database
NTIA	National Telecommunications and Information Administration
OFR	off-frequency rejection
OTR	on-tune rejection
TDD	time division duplex
UE	user equipment

EXECUTIVE SUMMARY

The National Telecommunications and Information Administration (NTIA) Fast Track Report [1] identified the 3550–3650 MHz band (3.5 GHz band) as potentially suitable for commercial broadband use. The 3.5 GHz band was one of the candidate bands identified by NTIA in response to the President’s initiative [2] to identify 500 megahertz of spectrum for commercial wireless broadband. NTIA believes that the 3.5 GHz band is well suited to exploring the next generation of shared spectrum technologies, to drive greater productivity and efficiency in spectrum use.

The Federal Communications Commission (FCC) voted to approve a rulemaking proceeding in GN Docket No. 12-354 [3] to address sharing issues associated with the establishment of a new Citizens Broadband Radio Service (CBRS) in the 3.5 GHz band. The Report and Order [4] was adopted on April 17, 2015.

In its Fast Track Report [1], NTIA concluded that large geographic separation and frequency offsets could be used to minimize interference between a deployment of commercial high-power macro-cell networks seeking access to the 3.5 GHz band and incumbent federal shipborne, ground-based, and airborne radar systems that operate or are planned to operate in and adjacent to the 3.5 GHz band. In the 3.5 GHz Band Further Notice of Proposed Rulemaking [3], the FCC stated that it would work with NTIA to reassess these exclusion zone distances using lower-powered small cell technology. NTIA, working in collaboration with the FCC and the Department of Defense (DoD), performed the analysis to re-evaluate the exclusion zone distances needed to protect federal shipborne and ground-based radar systems. This report presents the results of this 3.5 GHz Study. This report also provides a description of the technical and deployment parameters of Citizens Broadband Radio Service Device (CBSD) access points (APs) and user equipment (UE), technical characteristics of federal radar systems, and the analysis methodology used to compute the distances that establish revised exclusion zones necessary to protect federal radar systems operating in and adjacent to the 3.5 GHz band.

The coastal exclusion zones developed by the 3.5 GHz Study were derived from the composite characteristics of existing or planned shipborne radars. The associated maps show the minimum separation distances that the devices must be set back from the coastlines so that the aggregate interference power of the small-cell base stations does not exceed the interference protection criteria of the shipboard radar receivers. The UE devices were also analyzed and shown not to be of concern in terms of generating interference in the shipboard radar receivers. The updated analysis results in a reduction of 77 percent of the total geographic area impacted by the coastal exclusion zones (averaged across three shipborne radar systems) compared to the Fast Track Report’s findings.

The 3.5 GHz Study also calculated exclusion zones for the ground-based radar systems; the resulting protection zones are polygons encompassing selected sites where the ground-based radars operate. As a result of the updated analysis, a protection zone of 3 kilometers is required around the perimeter boundary of the installations where the ground-based radars are deployed. The Fast Track Report recommended much larger exclusion zones ranging from 40 to 60 kilometers.

3.5 GHZ EXCLUSION ZONE ANALYSES AND METHODOLOGY

E. Drocella, J. Richards, R. Sole, F. Najmy, A. Lundy,¹ and P. McKenna²

This report describes the 3.5 GHz Study. It explains the assumptions, methods, analyses, and system characteristics used to generate the revised exclusion zones for small-cell commercial broadband systems to protect federal radar operations (ship and land based) from aggregate interference in the band 3550–3650 MHz. The 3.5 GHz Study’s exclusion zones are compared with the exclusion zones that were generated in the Fast Track Report, which considered macro-cell operations.

Keywords: NTIA, FCC, radar, exclusion zones, CBRS, CBSD, spectrum sharing, 3550–3650 MHz, 3.5 GHZ band

1. INTRODUCTION

The National Telecommunications and Information Administration (NTIA) Fast Track Report [1] identified the 3550–3650 MHz band (3.5 GHz band) as potentially suitable for commercial broadband use. The 3.5 GHz band is one of the candidate bands identified by NTIA in response to the President’s initiative to identify 500 megahertz of spectrum for commercial wireless broadband [2]. NTIA believes that the 3.5 GHz band is well suited to exploring the next generation of shared spectrum technologies, to drive greater productivity and efficiency in spectrum use.

The Federal Communications Commission (FCC) voted to approve a rulemaking proceeding under GN Docket No. 12-354 to address sharing issues associated with the establishment of a new Citizens Broadband Radio Service (CBRS) in the 3.5 GHz band [3]. The Report and Order [4], adopted on April 17, 2015, established a roadmap for making the entirety of the 3.5 GHz Band available for commercial use in phases. It described a broad, three-tiered sharing framework enabled by a Spectrum Access System, adopting a hybrid framework that selects, automatically, the best authorization approach based on local supply and demand.

In its Fast Track Report, NTIA concluded that geographic separation and frequency offsets could be used to minimize interference between a deployment of commercial high-power macro-cell networks seeking access to the 3.5 GHz band and incumbent federal shipborne, ground-based, and airborne radar systems that operate or are planned to operate in and adjacent to the 3.5 GHz band [1, 1.6]. Based on the Fast Track Report’s analysis, NTIA recommended large exclusion zones along U.S. coastlines (East, West, and Gulf) and exclusion zones around selected ground-based radar sites. In the 3.5 GHz Further Notice of Proposed Rulemaking, the FCC stated that it

¹ The first five authors are with the Office of Spectrum Management (OSM), National Telecommunications and Information Administration, U.S. Department of Commerce, Washington, D.C. 20230.

² The author is with the Institute for Telecommunication Sciences (ITS), National Telecommunications and Information Administration, U.S. Department of Commerce, Boulder, CO 80305.

would work with NTIA to reassess the exclusion zone distances using lower-powered small cell technology [3, 31249].

NTIA, working in collaboration with the FCC and the Department of Defense (DoD), re-evaluated the exclusion zone distances needed to protect federal shipborne and ground-based radar systems. This report describes that study, which is referred to as the 3.5 GHz Study. This report describes the technical and deployment parameters of Citizens Broadband Radio Service Device (CBSD) access points (APs) and user equipment (UE), technical characteristics of federal radar systems, the analysis methodology for computing the revised exclusion zone distances necessary to protect federal radar systems operating in and adjacent to the 3.5 GHz band, and the results of the exclusion zone distance analysis.

2. CBSD TECHNICAL AND DEPLOYMENT PARAMETERS

2.1 Small Cell Device Technical Characteristics

The 3.5 GHz Study's exclusion zone distance analysis examined small cell technology for the Citizens Band Radio Service Devices (CBSD) technical and deployment parameters. The technical parameters for the small cell CBSD APs and UE used in the exclusion zone distance analysis are provided in Table 1.

Table 1. Small Cell Device (CBSD) Technical Characteristics Used in Exclusion Zone Analysis

Parameter	Value
Access Points	
Transmitted Power to Antenna (dBm)	24 (Outdoor) 20 (Indoor)
Mainbeam Antenna Gain (dBi)	6
Equivalent Isotropically Radiated Power - Outdoor CBSD (dBm)	30
Equivalent Isotropically Radiated Power - Indoor CBSD (dBm)	26
Channel Bandwidth (MHz)	10
Signal Bandwidth (MHz)	9
Channel Usage (%)	
Dense Urban/Urban	60
Suburban	40
Rural	20
Antenna Height (m)	
Outdoor	6
Indoor - Dense Urban	50%: 3 to 15; 25%: 18 to 30; and 25%: 33 to 60
Indoor - Urban	50%: 3 and 50%: 6 to 18
Indoor - Suburban	70%: 3 and 30%: 6 to 12
Indoor - Rural	80%: 3 and 20%: 6
Cable, Insertion, or Other Losses (dB)	2 (Outdoor)
User Equipment	
Transmitted Power to Antenna (dBm)	24
Mainbeam Antenna Gain (dBi)	0
Equivalent Isotropically Radiated Power (dBm)	24
Channel Bandwidth (MHz)	10
Signal Bandwidth (MHz)	9
Channel Usage (%)	
Dense Urban/Urban	60
Suburban	40
Rural	20
Antenna Height (m)	1.5 (Outdoor) 1.5 below their associated CBSD (Indoor)

The CBSD in the 3.5 GHz band considered in this analysis use a time division duplex (TDD) access scheme so the APs and UE will not be transmitting simultaneously. In the exclusion zone

distance analysis the interference effects from APs and UE were computed separately. In performing the exclusion zone distance analysis for federal radar systems operating below 3550 MHz, the measured emission spectrum of a representative TDD microcell base station was used [5].

The maximum allowable equivalent isotropically radiated power (EIRP) level for outdoor APs used in the analysis is 30 dBm, which includes a 24 dBm transmitted power to the antenna and 6 dBi mainbeam antenna gain. In the analysis a fractional transmit power is applied to each AP in the dense urban/urban, suburban, and rural regions to account for partial utilization of subcarriers (e.g., LTE resource blocks) within a 10 MHz carrier bandwidth. Such partial utilization is expected due to traffic dynamics and resource partitioning between small cells to reduce intra-system interference. These fractions applied to the outdoor APs are based on the channel loading percentages shown in Table 1: 60 percent for dense urban and urban regions, 40 percent for suburban regions, and 20 percent for rural regions. Using these fractional power adjustments the EIRP values for the outdoor APs used in the analysis are: 27.8 dBm for dense urban/urban regions; 26 dBm for suburban regions; and 23 dBm for rural regions. For all indoor APs the EIRP used in the analysis is 26 dBm based on a 20 dBm transmitted power to the antenna and a 6 dBi mainbeam antenna gain. Similar partial loading percentages (60/40/20) are also applied to indoor small cells in different regions.

2.2 Small Cell Device Deployment Characteristics

Geographic Information System (GIS) 2011 National Land Cover Database (NLCD) data and overlaid 2010 U.S. Census population data (provided in average population density) were used in a multi-step distance analysis process to distribute the small cell APs considered in the exclusion zone distance analysis.³

The GIS data used in the exclusion zone distance analysis extends 150 kilometers inland and 120 kilometers along the coast on each side of possible locations for the shipborne radar systems. The NLCD area classification codes were grouped and mapped to dense urban, urban, suburban, and rural regions and applied to 90 meter by 90 meter bins. Next the raw population density data for each classification was determined. For the dense urban and urban regions, a daytime traveling factor expressed in terms of a percentage was included to account for the higher population densities that occur in cities during daytime.⁴

To be conservative and assuming a mature deployment phase, a market penetration factor of 20 percent was assumed for this band. To account for distribution of users across ten available 10 MHz channels in the 3.5 GHz band, a scaling factor of 10 percent was also included to determine the number of effective users potentially operating in each 10 MHz channel of interest.

³The population data is based on the 2010 U.S. Census data available at <http://www.census.gov/geo/maps-data/data/gazetteer2010.html> and 2011 National Land Cover Database data is available at <http://www.mrlc.gov/>.

⁴The daytime commuter factors available at <https://www.census.gov/hhes/commuting/data/daytimepop.html> were used as a baseline.

The relative percentages of indoor and outdoor APs and UE varies depending on the classification regions. For APs and UE in dense urban/urban regions, 80 percent of the APs and UE were assumed to be deployed indoors, while 20 percent of the APs and UE were assumed to be deployed outdoors. For APs and UE in suburban and rural regions, 99 percent of the APs and UE were assumed to be deployed indoors, while 1 percent of the APs and UE were assumed to be deployed outdoors. The locations and antenna height of the AP and UE were treated as random variables in the analysis.

The antenna height for outdoor APs was fixed at 6 meters. For indoor APs an antenna height distribution across different floors was assumed with higher probability of lower floors, as they apply to more buildings, and lower probability of higher floors, as they apply to fewer buildings in city environments.

Given the limited time and available data, and for simplicity, no region-specific building data was used. The same sets of assumptions were equally applied to all regions and cities considered in the analysis.

In addition, the following factors were associated with the number of effective users per AP corresponding to each region classification:

- For the dense urban/urban classification, 50 effective users per AP
- For the suburban classification, 20 effective users per AP
- For the rural classification, 3 effective users per AP

More users share the coverage of each AP in enterprise and downtown areas. In rural areas, most APs serve a single family dwelling with an average of three family members per dwelling.

The total number of APs for each of the classification regions was computed using the following equations:

$$\text{Number of APs (Dense Urban/Urban)} = \frac{P \times \left(1 + \frac{D}{100}\right) \times \frac{MP}{100} \times \frac{CS}{100}}{50} \quad (1)$$

$$\text{Number of APs (Suburban)} = \frac{P \times \frac{MP}{100} \times \frac{CS}{100}}{20} \quad (2)$$

$$\text{Number of APs (Suburban)} = \frac{P \times \frac{MP}{100} \times \frac{CS}{100}}{3} \quad (3)$$

where

P is the raw census population for a region class;

D is the daytime commuter adjustment factor (percentage);

MP is the market penetration factor (percentage); and

CS is the channel scaling factor (percentage).

An example of the AP calculations for San Diego, CA is provided in Table 2, where in this case the population in the urban and dense urban regions was augmented by 15 percent to account for daytime commuter adjustment.

Table 2. Example Calculation for Number of APs

Region	Population	MP	CS	D	AP/User	Number of APs
Urban	4,715,098	0.2	0.1	115	0.02	2,169
Suburban	1,696,558	0.2	0.1	100	0.05	1,697
Rural	653,558	0.2	0.1	100	0.333	4,353

It is understood and expected that AP counts and distribution in each region vary widely based on deployment assumptions and service penetration growth over time. Given the critical nature of incumbent use in the 3.5 GHz band, and that the transition time to eventually implement sensing and dynamic protection zones is not known in advance, a conservative approach was used in the assumptions made in this analysis.

3. RADAR TECHNICAL AND DEPLOYMENT PARAMETERS

3.1 Radar Technical Parameters

In the Fast Track Report [1], NTIA performed an analysis to determine the exclusion zone distances necessary to protect federal shipborne and ground-based radar systems. The shipborne radars analyzed in the Fast Track Report were designated as Shipborne Radars 1 through 5 and the ground-based radars were designated GB-1 and GB-3. Shipborne Radars 2 and 3 operate below 3550 MHz and Shipborne Radars 1, 4, and 5 are capable of operating in the 3.5 GHz band. The ground-based radars both operate below 3550 MHz. The technical parameters for the radar receivers used in the exclusion zone distance analysis include: 3 dB intermediate frequency (IF) filter bandwidth, noise figure, mainbeam antenna gain, antenna 3 dB beamwidth (vertical and horizontal), insertion/cable losses, and antenna height. The 3.5 GHz Study uses these same assumptions and names.

In the 3.5 GHz Study analysis, the generalized mathematical model of the radar systems antenna described in Recommendation ITU-R M.1851 was used to determine the radar receive antenna gain in the azimuth and elevation orientations in the direction of the APs or UE [6]. Knowledge of the antenna 3 dB beamwidth and first peak side-lobe level, allowed selection of equations for both the azimuth and elevation patterns. Cosine patterns were used for the radar systems' antennas. The equations for the theoretical antenna directivity parameters of the model are provided in Table 3; the equations for the peak and average mask patterns used in the model are provided in Table 4.

Table 3. Antenna Directivity Parameters

Relative shape of field distribution $f(x)$ where $-1 \leq x \leq 1$	Directivity pattern $F(\mu)$	θ_3 , the 3 dB or half power beam-width (degrees)	μ as a function of θ_3	First side-lobe level below main lobe peak (dB)	Proposed mask floor level (dB)
$\cos\left(\frac{\pi}{2}x\right)$	$\frac{\pi}{2} \left[\frac{\cos \mu}{\left(\frac{\pi}{2}\right)^2 - \mu^2} \right]$	$68.8 \left(\frac{\lambda}{l}\right)$ λ is the wavelength l is the overall length of the aperture	$68.8\pi \frac{\sin \theta}{\theta_3}$	-23	-50

Table 4. Peak and Average Mask Pattern Equations

Pattern Type	Mask equation beyond pattern break point where mask departs from theoretical pattern (dB)	Peak pattern break point where mask departs from theoretical pattern (dB)	Average pattern break point where mask departs from theoretical pattern (dB)	Constant added to the peak pattern to convert it to average mask (dB)
Cosine	$-17.51 \ln\left(2.33 \frac{ \theta }{\theta_3}\right)$	-14.4	-20.6	-4.32

The following equation was used to model the off-axis antenna gain pattern for the shipborne radar systems:

$$G(\theta) = G_{Max} - 12 \left(\frac{\theta}{BW} \right)^2 \quad (4)$$

where

$G(\theta)$ is the antenna gain at the off-axis angle of θ in degrees (dBi);

G_{Max} is the mainbeam antenna gain (dBi); and

BW is the antenna beamwidth (degrees).

The interference thresholds used to assess compatibility are referred to as long-term thresholds because their derivation assumes that the interfering signal levels are present most of the time. The interference threshold, I_T , used in computing the exclusion distances to protect federal radar systems was determined using (5) (see [7] (15)):

$$I_T = N + \frac{I}{N} \quad (5)$$

where

$\frac{I}{N}$ is the maximum permissible interference-to-noise ratio at the receiver IF output necessary to maintain acceptable performance criteria (dB); and

N is the receiver noise power level at the receiver IF output in the IF bandwidth (dBm).

For a receiver 3 dB IF bandwidth and receiver noise figure the receiver noise power level is given by (6) (see [7] Section 3.2):

$$N = -114 + 10 \log BW_{rx} + NF \quad (6)$$

where

BW_{rx} is the receiver 3 dB IF bandwidth (MHz); and

NF is the receiver noise figure (dB).

3.2 Radar Deployment Parameters

In the analysis to compute the exclusion zone distances for the shipborne radar systems, virtual ships were positioned at the various locations along the East, West and Gulf coasts. A limited number of shipborne radar ports of call and test sites were also considered. Ground-based radars were positioned at their normal test and training sites. (In practice, ground-based radars may re-deploy periodically to conduct training or for homeland defense missions.)

4. DESCRIPTION OF SHIPBORNE RADAR ANALYSIS METHODOLOGY

4.1 Analysis Overview

A Monte Carlo analysis was used to compute exclusion zone distances on each of the individual azimuths from the shipborne radars.⁵ APs or UE were randomly located in the previously described 90 meter by 90 meter bins corresponding to the different regions (dense urban/urban, suburban, and rural) and exclusion distances were computed. The Monte Carlo analysis used 10,000 iterations to compute the exclusion zone distance on each azimuth, each time randomly varying the different parameters. The parameters randomized in the analysis included: AP and UE location, indoor AP antenna heights, building attenuation losses, clutter losses, time variability and location variability associated with the propagation loss and the radar receive antenna gain.

The analysis placed ships at coastal locations 10 kilometers offshore. At each ship's location, the azimuth angle of the radar receive antenna mainbeam was varied in 1 degree increments, pointed at areas along the coast. This set of inland azimuth angles of the radar antenna mainbeam toward the APs and UE remained fixed during each iteration of the Monte Carlo analysis. The aggregate interference calculations used to determine the exclusion zone distances were computed on each of the individual azimuth angles generated at each ship location.

4.2 Interference Link Budget

The interference power levels at the radar system receiver were calculated using (7) for each AP or UE transmitter considered in the analysis:

$$I = EIRP_{AP/UE} + G_R - L_T - L_R - L_P - L_C - L_B - FDR \quad (7)$$

where

I is the received interference power at the output of the antenna (dBm);

$EIRP_{AP/UE}$ is the EIRP of the AP or UE transmitter (dBm);

G_R is the radar receive antenna gain in the direction of the AP or UE transmitter (dBi);

L_T is the AP transmitter insertion loss (dB);

L_R is the radar receiver insertion loss (dB);

L_P is the basic transmission loss (dB);

L_C is the clutter loss (dB, only applied to rural sources);

⁵ Monte Carlo methods are a class of algorithms that rely on repeated random sampling to compute the solution to problems whose solution space is too large to explore systematically or whose systemic behavior is too complex to model.

L_B is the building attenuation loss (dB, only applied to indoor sources); and

FDR is the frequency dependent rejection (dB).

Using (7), the values of interference power level were calculated for each AP or UE transmitter considered in the analysis. These individual interference power levels were then used in the calculation of the aggregate interference to the radar system receiver and converted to dBm using (8).⁶

$$I_{AGG} = 10 \log \left[\sum_{j=1}^N I_j \right] + 30 \quad (8)$$

where

I_{AGG} is the aggregate interference level at the radar receiver from the AP or UE transmitters (dBm);

N is the number of AP or UE transmitters; and

I_j is the interference power level at the input of the radar receiver from an individual AP or UE transmitter (Watts)

The difference between the received aggregate interference power level computed using (8) and the radar receiver interference threshold represents the available margin. When the available margin is positive, compatible operation is possible. The distance at which the available margin is zero represents the minimum distance separation that is necessary for compatible operation. This distance was used to establish the exclusion zone distances to protect the federal radar systems.

4.3 Radar Receiver Interference Threshold

The desensitizing effect on a radar system due to interference from other services with a noise-like modulation such as those from the AP or UE transmitters is predictably related to its intensity. In any azimuth in which such interference arrives, its power spectral density can, to within a reasonable approximation, simply be added to the power density of the radar receiver thermal noise. In the exclusion zone distance analysis, the interference threshold for the shipborne radar was based on an $\frac{I}{N}$ criterion of -6 dB [4]. An $\frac{I}{N}$ of -6 dB corresponds to a 1 dB

⁶ The interference power calculated in (7) must be converted from dBm to Watts before calculating the aggregate interference seen by the radar receiver using (8). The constant term on the right-hand side of (8) provides the conversion back to dBm.

increase in the radar receiver noise level.⁷ The interference level was based on the aggregate interference from AP or UE transmitters.⁸

4.4 AP and UE EIRP Values

The EIRP for outdoor APs used in the analysis were assigned based on the dense urban/urban, suburban, and rural classifications. Outdoor APs in urban/urban regions were assigned an EIRP of 27.8 dBm. Outdoor APs in suburban regions were assigned an EIRP of 26 dBm. Outdoor APs in rural classifications were assigned an EIRP of 23 dBm.

Indoor APs were all assigned an EIRP of 26 dBm.

The UE in the analysis were all assigned an EIRP of 24 dBm.

4.5 Radar Receive Antenna Gain

The antenna gain model described in Recommendation ITU-R M.1851 was used to determine the antenna gain in the azimuth and elevation orientations for the radar systems. The radars have the ability to track down to the horizon, so a 0 degree up-tilt angle (e.g., 0 degree elevation angle) was used in the analysis.

4.6 Transmitter and Receiver Insertion Losses

In the analysis, an additional factor of 2 dB was included for insertion loss, cable loss, etc., for the outdoor APs. An additional 2 dB was used for additional losses associated with the radar receivers.

4.7 Propagation and Clutter Loss

In the aggregate interference analysis, it was recognized that interference predictions arising from sources in a small cell deployment in heavy traffic areas would be required to account for radio propagation in man-made and naturally cluttered environments, as well as other impediments to propagation, such as terrain obstructions. An extensive review was performed of existing propagation models. In general, it was found that most of the existing propagation models were used for predicting signal strength and propagation path loss in built-up urban/suburban areas where there are numerous man-made building structures. Typically these propagation models are based on measurements with a high antenna (e.g., base station) and a lower antenna (e.g., mobile station) immersed in clutter. Propagation models based on this methodology (i.e., using the mean/median of measurements at given distances between the two terminals) tend to underestimate interference for the small percentages of time/locations, which must be considered for interference calculations. It was understood that accurate interference and

⁷ An increase in the receiver noise can reduce the operating range or increase the tracking error of a radar system.

⁸ NTIA has published several reports that confirm a $\frac{1}{N}$ of -6 dB is the appropriate protection criterion for radar receivers in the presence of noise-like interfering signals [8]–[10].

propagation models should be developed and tuned based on real field measurement results. However, given limitations on time and resources and after consideration of possible alternative models and the aggressive schedule of the work, a compromise approach was adopted as the way forward. This compromise was to revisit the Okumura et al. [11] basic median attenuation curves, with the intention of extending Hata's [12] empirical formulae in both distance and frequency ranges, and then apply the "Urban Factor" approach suggested by Longley [13], a method referred to as the extended Hata model. A brief description of this approach is provided below.

To extend the Hata [12] model in frequency and distance, it was assumed that the base and mobile station height gain terms appearing in the empirical formulae were unchanged. Then it is sufficient to extend the frequency range of the formulae by refitting to frequencies from 1,500–3,000 MHz, based on the Okumura et al. [11] median basic attenuation curves at the reference base and mobile station heights (see [11] Figure 15). For path distances less than approximately 20 km, this was accomplished by simply refitting the basic median attenuation curve at 1 km distance. However, it is also important to consider path distances longer than approximately 20 km. For these distances, the approach was to fit the basic median attenuation curve at 100 km distance, and then use the long distance exponents shown in [11] Figure 12, Curve B, to determine the distance at which the two power laws intersect (i.e., the break-point distance). Effectively, for distances less than or equal to the break-point distance, the extended Hata model uses the original Hata power law exponent and the (refitted) Hata intercept, while for distances greater than the break-point distance, the extended Hata model uses the long distance power law exponent and the 100 km basic median attenuation curve fit.

In addition to the extensions in the frequency and distance ranges, the following site-specific corrections to the median attenuation ([11], Section 4) were implemented:

- AP/UE "effective height" corrections
- "Median" correction for rolling hilly terrain (applied in the vicinity of the AP/UE only)
- "Fine" correction for rolling hilly terrain (applied in the vicinity of the AP/UE only)
- General slope of terrain correction (applied in the vicinity of the AP/UE only)
- Isolated mountain (or isolated ridge) correction (applied only to single horizon paths)
- Mixed land-sea path correction

These corrections are site-specific in that they depend on the details of the terrain profile between the AP/UE. The environment surrounding the AP/UE (urban or suburban) was also accounted for via the [11] Figure 20 correction for suburban environments relative to urban environments.

For APs less than 18 meters in height above ground in urban and suburban environments, the extended Hata model median basic transmission loss was then compared to the ITS Irregular Terrain Model (ITM) predicted median basic transmission loss (in point-to-point mode) and the

larger value was used as the basis for Monte Carlo studies of the aggregate interfering power [14]. For APs in rural environments at all heights and in urban and suburban environments above 18 meters height, the ITM median basic transmission loss was the basis for the Monte Carlo studies. For rural APs, an additional clutter factor of 0–15 dB was randomly applied, with a uniform distribution, on each Monte Carlo iteration⁹. The specific implementation of the propagation loss models and clutter loss used in the exclusion zone distance analysis is described in Appendix A.

4.8 Building Attenuation Loss

In the dense urban/urban region, it was assumed that 80 percent of the APs and UE will operate indoors. In the suburban and rural regions, it is assumed that 99 percent of the APs and UE will operate indoors. For the indoor APs, a building attenuation loss in addition to the propagation loss was used in the exclusion zone distance analysis. The following random distribution was used to represent the building attenuation loss in the analysis: 20 percent were assigned a building attenuation loss of 20 dB; 60 percent were assigned a building attenuation loss of 15 dB; and 20 percent were assigned a building attenuation loss of 10 dB.

4.9 Frequency Dependent Rejection

Frequency dependent rejection (FDR) accounts for the fact that not all of the undesired transmitter energy at the receiver input will reach the detector. FDR is a calculation of the amount of undesired transmitter energy that is rejected by a victim receiver. This FDR attenuation is composed of two parts: on-tune rejection (OTR) and off-frequency rejection (OFR). The OTR is the rejection provided by a receiver selectivity characteristic to a co-tuned transmitter as a result of an emission spectrum exceeding the receiver bandwidth. A detailed description of how to compute FDR can be found in [15]. The transmitter emission spectrum and receiver selectivity curves used in the FDR calculation are defined in terms of a relative attenuation level specified in decibels as a function of frequency offset from center frequency in megahertz.

The FDR can be stated mathematically in decibel terms as:

$$FDR = 10 \log \left[\frac{\int_0^\infty p(f - f_{tx}) df}{\int_0^\infty p(f - f_{tx}) h(f - f_{rx}) df} \right] \quad (9)$$

where

f_{tx} is the undesired transmitter tuned frequency;

f_{rx} is the receiver tuned frequency;

$p(f)$ is the normalized emission spectrum of the undesired transmitter;

⁹The clutter factor is being applied to account for additional losses (e.g., due to vegetation) for low APs in rural environments.

$h(f)$ is the normalized transfer function of the receiver; and

f is the absolute frequency.

Numerical integration and convolution routines were used to solve (9).

In the special case of an undesired transmitter operating co-channel to a receiver, the following simplified form may be used.

$$FDR = \max\left(0, 10 \log\left(\frac{B_{tx}}{B_{rx}}\right)\right) \quad (10)$$

where

B_{tx} is the emission bandwidth of the undesired transmitter (MHz); and

B_{rx} is the IF bandwidth of the receiver (MHz).

For Shipborne Radars 1, 4, and 5, all of the APs or UE considered in the exclusion zone distance analysis were operating co-frequency with the radar systems and (10) was used to compute the FDR. For Shipborne Radars 2 and 3 an approximate frequency separation of 50 MHz from the APs or UE and (9) was used to compute the FDR.

4.10 Shipborne Radar Exclusion Zone Distance Analysis Output

The Monte Carlo analysis produced a distribution of results. Figure 1 shows an example plot for a single ship location, comparing the results for various confidence intervals. The minimum (blue curve), maximum (red curve), mean (yellow curve), and 95 percent (green curve) exclusion zone distances on each of the individual azimuths are shown on Figure 1. The maximum, minimum, and percentile values are derived for the 10,000 iterations for each azimuth. The minimum value is the smallest exclusion zone distance for the 10,000 iterations. The maximum is the largest exclusion zone distance for the 10,000 iterations at each azimuth. The 95 percent value is the exclusion zone distance that is exceeded by 5 percent of the iterations at that azimuth. Figure 2 is an example of the exclusion zone distance analysis output.

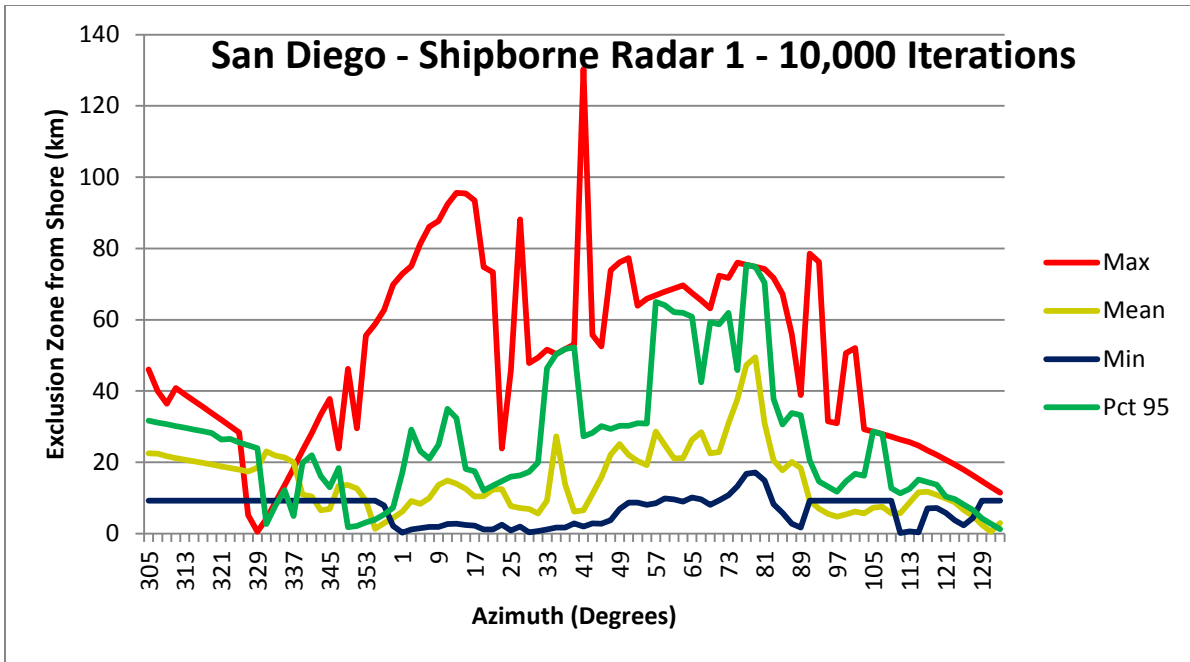


Figure 1. Example—Exclusion zone distances referenced to the coastline for different confidence intervals.

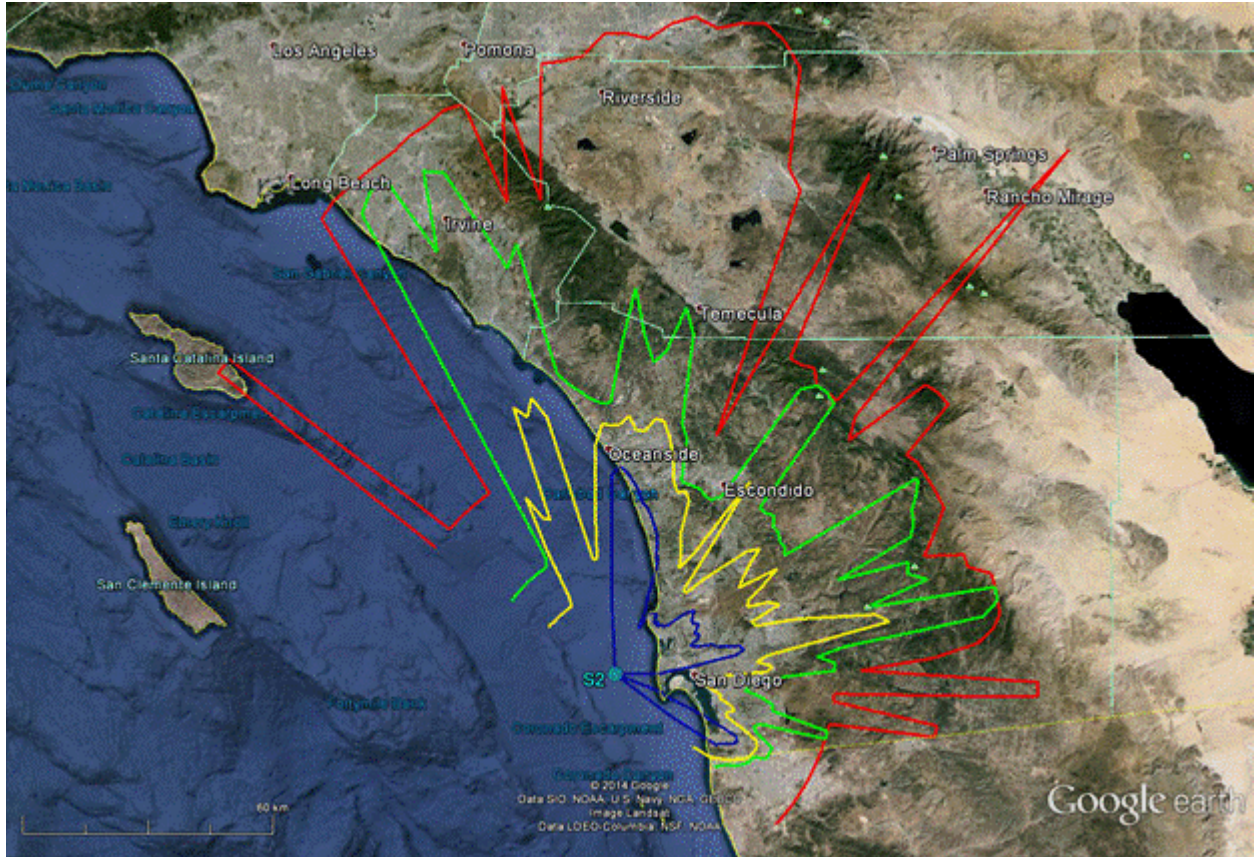


Figure 2. Example—Exclusion zone distances for different confidence intervals for a shipborne radar at S2.

The 95 percent distance calculations were used to establish the exclusion zones to protect the shipborne radar. The confidence interval was used to quantify the uncertainty in a Monte Carlo statistical analysis. The confidence interval can be computed by [16]:

$$Confidence\ Interval = p \pm z \sqrt{\frac{p(1-p)}{n}} \quad (11)$$

where

p is the estimated probability (0.95);

n is the number of samples (i.e., iterations in the Monte Carlo analysis (10,000)); and

z is the constant multiplier depending on the chosen confidence interval (1.96 for a normal distribution).¹⁰

¹⁰ The assumption of a normal distribution is reasonable as long as $np > 5$ and $n(1-p) > 5$.

Using these factors, the confidence interval for this analysis is 95 percent \pm 0.43 percent. The expected 95 percent value for the exclusion zone distance is between 94.6 percent and 95.4 percent for the 10,000 iterations with a confidence level of 95 percent.

It is understood that such a high percentage is not common for interference analysis in designing commercial systems. But, given the critical missions of federal incumbent systems operating in the 3550–3650 MHz band, it was agreed following some deliberations to take a conservative approach and use a higher percentage for establishing the exclusion zone distances. The results of the shipborne radar exclusion zone distance analysis are presented in Appendix B.

5. DESCRIPTION OF GROUND-BASED RADAR ANALYSIS METHODOLOGY

The analysis used to compute the exclusion zone distances for ground-based radars employed the Monte Carlo analysis capabilities of Visualyse (©Transfinite Systems Ltd.), a commercial modeling and simulation application. A less detailed analysis approach was taken for the ground based radars, since they operate below 3550 MHz and there will be additional interference rejection due to the filters used in the ground based radar receiver and the CBRS AP transmitter. The analysis only considered outdoor APs with the ground-based radar placed at the edge of a city near the base on which the radar could be deployed. The APs were randomly distributed within one or more square regions covering a portion of the heavily populated city area at which the radar antenna mainbeam was pointed, as illustrated in Figure 3. The number of APs in this area was calculated from the 2010 U.S. census population data using (12).

$$\text{Number of APs} = \frac{P \times MP \times SF \times OF \times CS}{20} \quad (12)$$

where

P is the raw census population for a city;

MP is the market penetration factor (fraction);

SF is the ratio of population in simulation area to total city population (fraction);

OF is the ratio of outdoor APs to total APs (fraction); and

CS is the channel scaling factor (fraction).

A market penetration factor of 40 percent, a 20 percent ratio of outdoor to indoor APs, a channel usage factor of 100 percent, and a factor of 20 users per AP were used to compute the number of APs considered in the analysis. A 100 percent channel usage factor was chosen since the CBSD out-of-band emission spectrum used was relatively constant over the allocated band and thus CBSDs operating on all channels contributed to the interference level at the radar receiver. The percentage of city population included in the simulation area was taken as the ratio of the simulation area that included the radar main beam and its near-in sidelobes to the area of the city that was heavily developed. The number of APs calculated in (12) was divided equally among multiple square areas, as depicted in Figure 3. Visualyse randomly distributed the AP locations within each square for each Monte Carlo analysis iteration. The analysis considered 1,000 random configurations for each exclusion zone distance. The randomized parameters in the analysis included: AP location within the specified simulation area, clutter loss (0 to 15 dB), and the reliability variability (0 to 100%) used in the propagation loss calculation. A uniform probability distribution was used to select the values for these parameters.

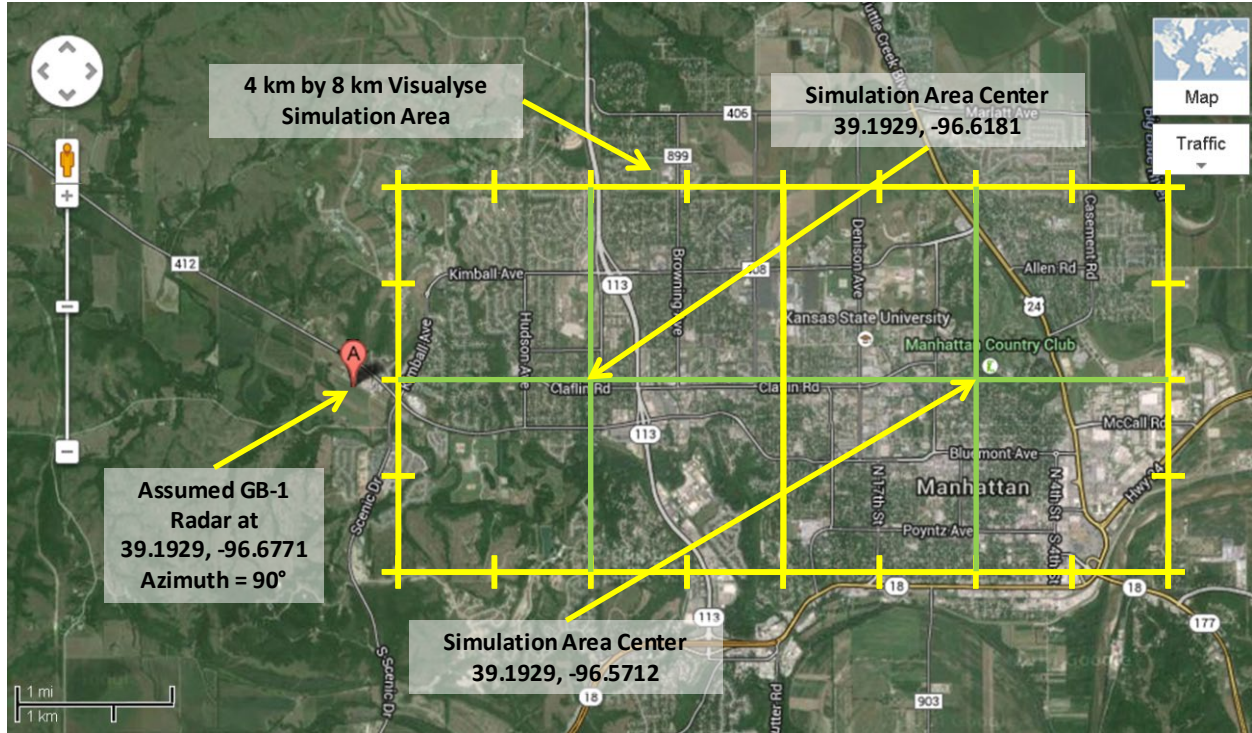


Figure 3. Example of Visualyse simulation area.

5.1 Interference Link Budget

The interference power levels at the radar receiver were calculated using (13) for each AP transmitter considered in the analysis.

$$I = EIRP_{AP} + G_R - L_P - L_C - L_R - FDR \quad (13)$$

where

I is the received interference power at the output of the antenna (dBm);

$EIRP_{AP}$ is the EIRP of the AP transmitter (dBm);

G_R is the radar receive antenna gain in the direction of the AP transmitter (dBi);

L_P is the basic transmission loss (dB);

L_C is the clutter loss (dB);

L_R is the radar line loss (dB); and

FDR is the frequency dependent rejection (dB).

The aggregate interference was computed using (8).

5.2 AP EIRP and Antenna Height

The EIRP used in the analysis for all of the APs was 30 dBm. An antenna height of 6 meters was assumed for all of the APs in the analysis.

5.3 Radar Receive Antenna Gain

The antenna gain model described in Recommendation ITU-R M.1851 was used to determine the antenna gain. A receive line loss of 2 dB was assumed. The radar receive antenna gain will vary depending on the location of the AP (distance from the radar) and antenna height of the AP. An antenna height of 5 meters was assumed for the center-line of the radar antenna. The ground-based radars have the ability to track down to the horizon, so a 0 degree up-tilt angle (e.g., 0 degree elevation angle) was assumed.

5.4 Basic Transmission Loss

The Longley-Rice terrain dependent propagation model was used to compute the basic transmission loss for the exclusion distance analysis. The reliability variability was treated as a random variable in the analysis, with a minimum value of 0 percent and a maximum value of 100 percent selected using a uniform probability distribution.

5.5 Clutter Loss

The clutter loss was treated as a random variable in the analysis with a minimum value of 0 dB and a maximum value of 15 dB, selected using a uniform probability distribution.

5.6 FDR

Interference calculations were performed assuming the radar was operating at 3490 MHz. Figure 4 (which is based on [5] Figure 74) displays the spectrum emission mask assumed for the AP in calculating the FDR. Radar receiver selectivity data was obtained from radar equipment certification records.

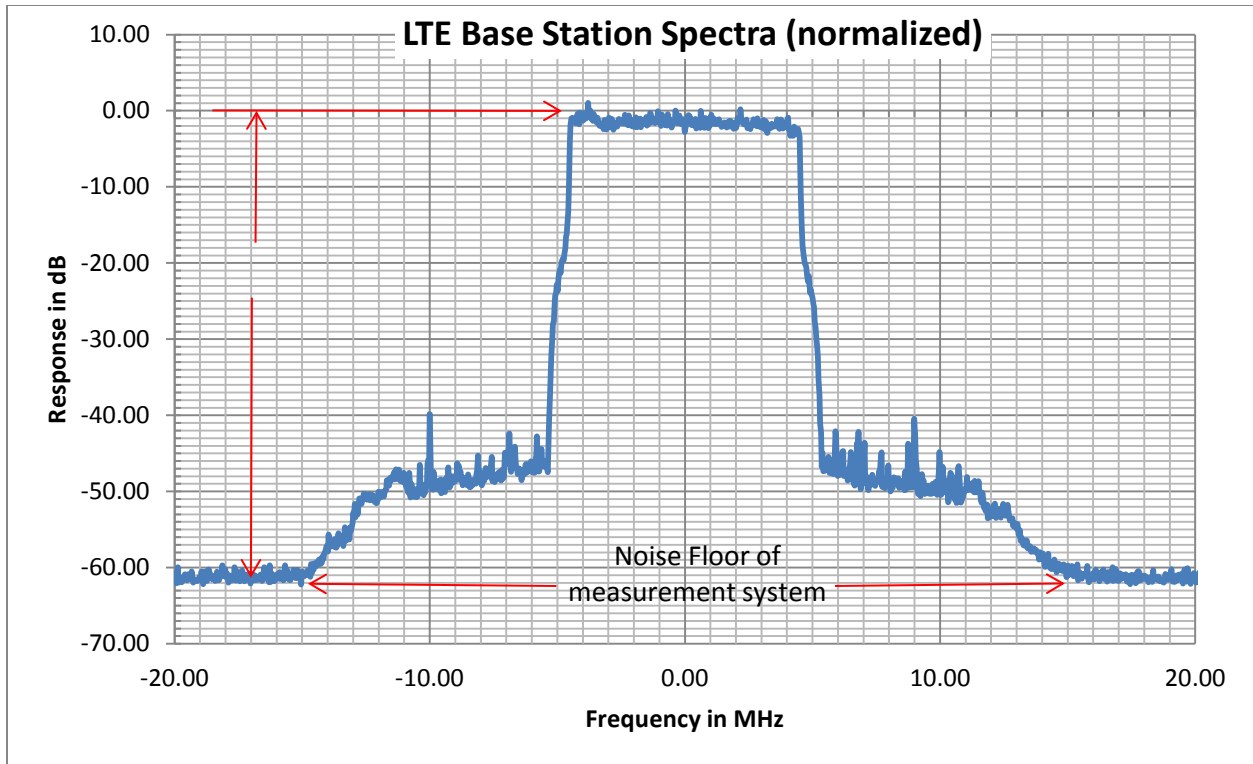


Figure 4. AP emission spectra measurement used for the model and the analysis.

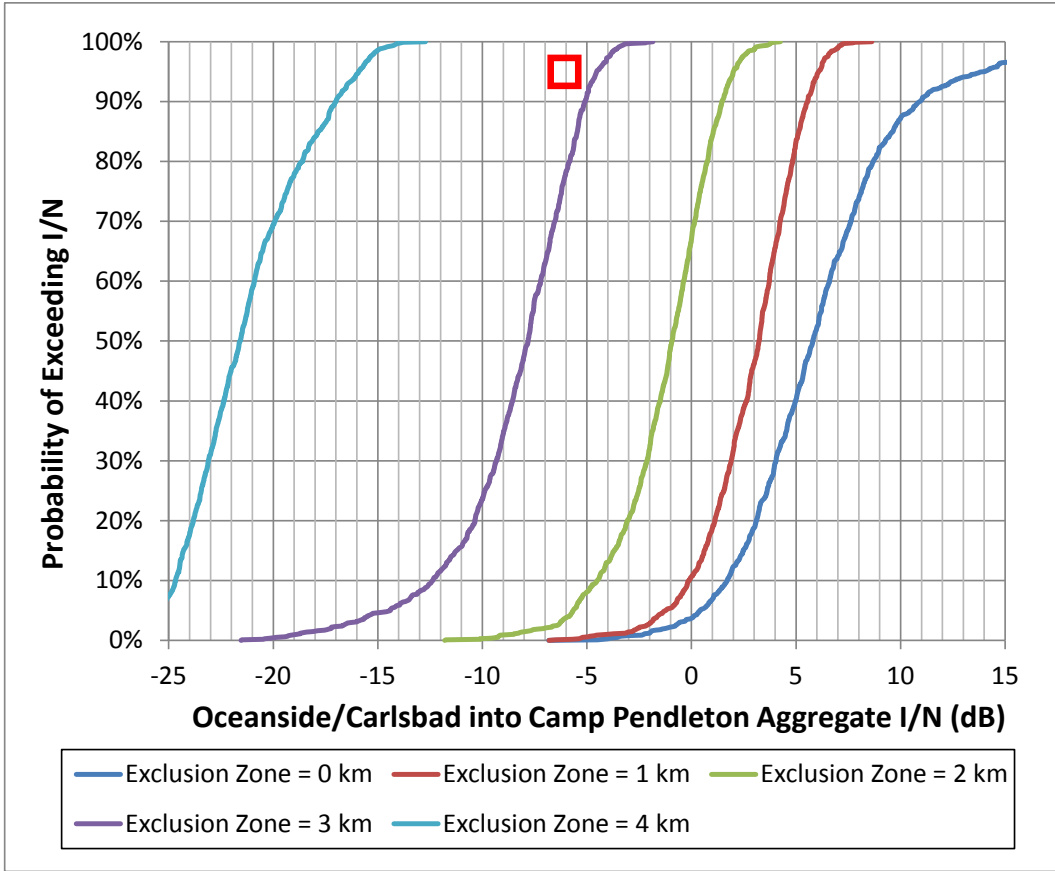
Using this emission spectrum for APs and the receiver selectivity of the ground-based radar, an FDR of 67.2 dB was computed for radar GB-1 and 59.3 dB for radar GB-3 and used in the analysis. This FDR was used for all the APs considered in the analysis.

5.7 Radar Receiver Interference Threshold

An $\frac{I}{N}$ of -6 dB was used as the interference criteria to compute the ground-based radar receiver threshold.

5.8 Ground-Based Radar Exclusion Zone Distance Analysis Output

The Monte Carlo analysis was used to compute plots of the cumulative distribution of the probability of not exceeding the $\frac{I}{N}$ criteria of -6 dB for different exclusion zone distances. Figure 5 is an example of the exclusion zone distance analysis output.



□ 95th percentile -6 dB aggregate I/N

Figure 5. Example output $\frac{I}{N}$ cumulative distribution of interference probability

The results of the exclusion zone distance analysis for the ground-based radars are presented in Appendix C. Based on the analysis, a 3 kilometer exclusion zone around the perimeter of each of the installations is needed to protect the ground-based radars.

6. SUMMARY OF EXCLUSION ZONE DISTANCE ANALYSIS

Based on the analysis results, it was determined that the exclusion zone distances to protect shipborne radars from APs would also provide adequate protection from UE. The analysis results presented for the shipborne and ground-based radars only consider interference from the APs.

The results for the shipborne radar exclusion zone distance analysis compared to the Fast Track Report exclusion zone distances are provided in Tables 5–7. The results are presented for three parameters: percentage of area impacted, percentage of population impacted, and average exclusion zone distance. Exclusion zones were not necessary to protect Shipborne Radar 2 and Shipborne Radar 3 analyzed in the Fast Track Report.

The 3.5 GHz Study’s exclusion zone distance analysis for the ground-based radar analysis is shown in Table 8. The exclusion zones for ground-based radars in the Fast Track Report were between 40 and 60 km.¹¹

Table 5. Summary of Shipborne Radar Analysis Results

Geographic Area	Percentage of Area Impacted (km ²)		
	Fast Track Report Analysis ¹²	Revised Analysis (3.5 GHz Study)	Percent Reduction of Area Impacted
East Coast	1,081,389	345,067	68
West Coast	956,435	118,035	88
Gulf Coast	880,096	217,902	75

Table 6. Summary of Shipborne Radar Analysis Results

Geographic Area	Fast Track Report Analysis		Revised Analysis		Reduction in Percentage of Total Population Impacted
	Population Impacted	Percentage of Total Population Impacted	Population Impacted	Percentage of Total Population Impacted	
East Coast	66,771,384	32	50,566,713	24	24
West Coast	45,145,947	22	32,404,740	16	28
Gulf Coast	29,342,307	14	13,360,186	6	54

Table 7. Summary of Shipborne Radar Analysis Results

Geographic Area	Average Exclusion Zone Distance (km)		
	Fast Track Report Analysis	Revised Analysis (3.5 GHz Study)	Reduction in Average Exclusion Zone Distance
East Coast	427	135	292
West Coast	423	60	363
Gulf Coast	427	68	359

¹¹ [1] Table 5-2.

¹² [1] Table 5-4.

Table 8. Summary of Ground-Based Radar Analysis Results

Military Base	Radar	Nearby City	Exclusion Zone
Fort Carson CO	GB-1	Colorado Springs CO	2 km
Fort Riley KS	GB-1	Junction City KS	3 km
Fort Riley KS	GB-1	Manhattan KS	2 km
Fort Sill OK	GB-3	Lawton OK	2 km
Camp Pendleton CA	GB-3	Oceanside/Carlsbad CA	4 km

7. REFERENCES

- [1] U.S. Department of Commerce, National Telecommunications and Information Administration, *An Assessment of the Near-Term Viability of Accommodating Wireless Broadband Systems in the 1675-1710 MHz, 1755-1780 MHz, 3500-3650 MHz, and 4200-4220 MHz, 4380-4400 MHz Bands* (Nov. 15, 2010) (*Fast Track Report*), available at http://www.ntia.doc.gov/reports/2010/FastTrackEvaluation_11152010.pdf.
- [2] Memorandum for the Heads of Executive Departments and Agencies, “Unleashing the Wireless Broadband Revolution” (rel. Jun. 28, 2010), published at 75 Fed. Reg. 38387 (Jul. 1, 2010), available at <http://www.whitehouse.gov/the-press-office/presidential-memorandum-unleashing-wireless-broadband-revolution>.
- [3] “Commission Seeks Comments on Shared Commercial Operations in the 3550–3650 MHz Band,” *Further Notice of Proposed Rulemaking* in GN Docket No. 12-354, FCC 14-49, Fed. Reg. Vol. 79, No. 105, 31247 (Jun. 2, 2014).
- [4] “Amendment of the Commission’s Rules with Regard to Commercial Operations in the 3550-3650 MHz Band,” *Report and Order and Second Further Notice of Proposed Rulemaking* in GN Docket No. 12-354 (Apr. 21, 2015).
- [5] Geoffrey Sanders, John E. Carroll, Frank H. Sanders, and Robert L. Sole, *Effects of Radar Interference on LTE (FDD) eNodeB and UE Receiver Performance in the 3.5 GHz Band*, National Telecommunications and Information Administration Technical Report TR-14-506 (Jul. 2014), available at <http://www.its.bldrdoc.gov/publications/2759.aspx>.
- [6] International Telecommunication Union-Radiocommunication Sector, Recommendation ITU-R M.1851, *Mathematical Models for Radio determination Radar Systems Antenna Patterns for use in Interference Analyses* (Jun. 2009).
- [7] International Telecommunication Union-Radiocommunication Sector, Recommendation ITU-R M.1461-1, *Procedures for Determining the Potential for Interference Between Radars Operating in the Radio determination Service and Systems in Other Services* (2000-2003), Annex 1.
- [8] Frank H. Sanders, Robert L. Sole, Brent L. Bedford, David Franc, and Timothy Pawlowitz, *Effects of RF Interference on Radar Receivers*, National Telecommunications and Information Administration Technical Report 06-444 (Feb. 2006), available at <http://www.its.bldrdoc.gov/publications/06-444.aspx>.
- [9] John E. Carroll, Geoffrey Sanders, Frank H. Sanders, and Robert L. Sole, *Case Study: Investigation of Interference into 5 GHz Weather Radars from Unlicensed National Information Infrastructure Devices, Part II*, National Telecommunications and Information Administration Technical Report 11-479 (Jul. 2011), available at <http://www.its.bldrdoc.gov/publications/2554.aspx>.

- [10] Frank H. Sanders, John E. Carroll, Geoffrey Sanders, Robert L. Sole, Robert J. Achatz, and Lawrence S. Cohen, *EMC Measurements for Spectrum Sharing Between LTE Signals and Radar Receivers*, National Telecommunications and Information Administration Technical Report 14-507 (Jul. 2014), available at <http://www.its.bldrdoc.gov/publications/2760.aspx>.
- [11] Y. Okumura, E. Ohmori, T. Kawano, and K. Fukuda, "Field strength and its variability in VHF and UHF land-mobile radio service," *Rev. Elec. Commun. Lab.*, 16, 9-10, pp. 825-873, (Sept.-Oct. 1968).
- [12] M. Hata, "Empirical formula for propagation loss in land mobile radio services," *IEEE Transactions on Vehicular Technology*, VT-29, 3, pp. 317-325 (Aug. 1980).
- [13] Anita G. Longley, *Radio Propagation in Urban Areas*, United States Department of Commerce, Office of Telecommunications, OT Report 78-144 (Apr. 1978), available at <http://www.its.bldrdoc.gov/publications/2674.aspx>.
- [14] George A. Hufford, Anita G. Longley, William A. Kissick, *A Guide to the Use of the ITS Irregular Terrain Model in the Area Prediction Mode*, National Telecommunications and Information Administration Technical Report 82-100, (Apr. 1982), available at <http://www.its.bldrdoc.gov/publications/2091.aspx>.
- [15] International Telecommunication Union-Radiocommunication Sector, Recommendation ITU-R SM.337-4, *Frequency and Distance Separations* (1997), Annex 1.
- [16] Allan Agresti and Brent A. Coull, "Approximate is Better than "Exact" for Interval Estimation of Binomial Proportions," *The American Statistician*, Vol. 52, No. 2, pp. 119-126 (May 1998), available at http://www.stat.ufl.edu/~aa/articles/agresti_coull_1998.pdf.

APPENDIX A DESCRIPTION OF PROPAGATION AND CLUTTER LOSS MODEL

A.1 Introduction

This appendix describes the implementation of the propagation loss and clutter loss models used in the exclusion zone distance analysis.

A.2 Propagation Model Overview

Two propagation models were used to predict the individual links' basic transmission losses used in the exclusion zone distance analyses: the extended Hata model and the ITS Irregular Terrain Model (ITM) [A-1]–[A-3]. The details of the specific implementations of these propagation models are described below. For either of these models, the site-specific or point-to-point mode of implementation was employed. Therefore, the great circle terrain elevation profile between the individual source's (access point (AP) or user equipment (UE)) location and the shipborne radar's location (usually 10 km out to sea) was extracted and used by the two models.

For the purposes of the aggregate interference power computation (see (8)), either model's basic transmission loss was treated as a random variable, which varied according to the statistics (i.e., location variability in the case of the extended Hata model and location and time variability in the case of ITM) described below. This randomness in the basic transmission losses was over and above other random aspects of the small cell device deployment characteristics, such as terminal heights, indoor vs. outdoor siting and, hence, the application of a random building entry loss, and whether a device at a given location was actively transmitting.

For APs and UE located in dense urban/urban and suburban environments (see the description of small cell device deployment characteristics in Section 2.2), the median basic transmission losses calculated using the extended Hata model and ITM were compared and the model yielding the greater median basic transmission loss was then used in the computation of the aggregate interference power statistics. For dense urban/urban and suburban APs and UE having terminal heights greater than 18 m, and all rural APs and UE, only the basic transmission loss from ITM was used in the computation of the aggregate interference power statistics. For rural APs and UE only, an additional, uniformly distributed, random "vegetative clutter" loss of 0 to 15 dB was added to the ITM basic transmission loss.

On any given Monte Carlo iteration, the active AP/UE locations, siting, and terminal heights were randomly assigned, as well as the corresponding basic transmission losses. There then commenced a sweep over all relevant (i.e., inland) radar antenna main beam azimuths. For each individual AP/UE-to-radar link, the (random) basic transmission loss was adjusted by the antenna gain of the radar in that direction and any other relevant losses (see (7)), and the individual link's interference powers were power summed as shown in (8), to yield the aggregate interference power for that radar antenna main beam azimuth.

To obtain the corresponding exclusion zone distance for that radar antenna main beam azimuth, AP/UE transmitters were then removed (i.e., excluded from the power sum calculation of the

aggregate interference) at successively greater distances from the ship's location, until the aggregate interference power fell below the interference-to-noise ratio of -6 dB.

A.3 The Extended Hata Model

Okumura et al. [A-1] conducted a series of land-mobile measurements made over varied, but principally quasi-smooth, terrain in urban, suburban and open/rural environments, and then used these measurements to derive curves and adjustment methods suitable for land mobile propagation predictions over the distance range 1–100 km, the frequency range 100–3,000 MHz, base station effective height range 20–1,000 m and mobile station effective height range 1–10 m. Hata [A-2] derived empirical formulae that closely approximated the curves-based methods, for quasi-smooth terrain only, for a distance range 1–20 km, a frequency range 150–1,500 MHz, a base station effective height range 30–200 m and a mobile station effective height range 1–10 m. In the interim, Longley [A-3] made use of the Basic Median Attenuations at base/mobile station effective antenna heights' reference values in [A-1] to develop an "Urban Factor" correction for the ITS Irregular Terrain Model (ITM) for quasi-smooth terrain. Longley noted that ITM and Okumura et al. yielded similar results with respect to base station effective heights [A-3].

The Hata [A-2] empirical formula for the median basic transmission loss for the mobile station located in a large city, L_p , in decibels is given as follows ($f \geq 400$ MHz):

$$L_p = 69.55 + 26.16 \log f - 13.82 \log h_b - a(h_m) + (44.9 - 6.55 \log h_b) \log d \quad (\text{A-1})$$

where

$$a(h_m) = 3.2(\log(11.75h_m))^2 - 4.97 \quad (\text{A-2a})$$

while for a mobile station in a medium-small city

$$a(h_m) = (1.1 \log f - 0.7)h_m - 1.56 \log f + 0.8 \quad (\text{A-2b})$$

and the units are: $[f]=\text{MHz}$, $[d]=\text{km}$ and $[h_b, h_m]=\text{m}$. For a mobile station located in a suburban area, [A-2] provides a fit to the [A-1] suburban correction factor:

$$L_{p,s} = L_p - 2 \left(\log \left(\frac{f}{28} \right) \right)^2 - 5.4 \quad (\text{A-3})$$

As noted in [A-2], (A-1) is a slope-intercept form for L_p with respect to the independent variable $\log d$, so the extension of the frequency range may be viewed as a matter of adjusting the first two terms on the right-hand side of (A-1) to match the intercept's behavior at higher frequencies, if the slope and height gains are unchanged. A quick inspection of Figure 15 in [A-1] suggests a new curve fit of the form: $\alpha + \beta \log f + \gamma(\log f)^2$. The coefficients of the fit can be found using the simultaneous solution of an equal number of equations and unknowns, given the values of the intercepts at three independent frequencies: 1,500 MHz, 2,000 MHz and 3,000 MHz.

Note that the values of the basic median attenuation relative to free space shown in Figure 15 of [A-1] are given at the reference antenna effective base and mobile stations' heights of 200 m and 3 m, i.e., h_b and h_m , respectively. The basic median attenuations at 1 km are 22 dB, 23.5 dB and 25.85 dB for the three frequencies: 1,500 MHz, 2,000 MHz and 3,000 MHz, respectively. Then the three equations in the three unknown coefficients are:

$$22 = \alpha_1 + \beta_1 \log(1500) + \gamma_1 (\log(1500))^2 - 13.82 \log(200) - 3.2(\log(35.25))^2 + 4.97 - L_{fs}(1500, R) \quad (\text{A-4a})$$

$$23.5 = \alpha_1 + \beta_1 \log(2000) + \gamma_1 (\log(2000))^2 - 13.82 \log(200) - 3.2(\log(35.25))^2 + 4.97 - L_{fs}(2000, R) \quad (\text{A-4b})$$

$$25.85 = \alpha_1 + \beta_1 \log(3000) + \gamma_1 (\log(3000))^2 - 13.82 \log(200) - 3.2(\log(35.25))^2 + 4.97 - L_{fs}(3000, R) \quad (\text{A-4c})$$

where

$$L_{fs}(f, R) \cong 20 \log \left(4\pi \frac{fR}{300} \right) = 20 \log \left(\frac{4\pi R}{300} \right) + 20 \log f \quad (\text{A-4d})$$

with

$$R = \sqrt{(1 \times 10^3)^2 + (h_b - h_m)^2} = \sqrt{10^6 + (200 - 3)^2} \quad (\text{A-4e})$$

The unknown coefficients are:

$$\alpha_1 = 97.62;$$

$$\beta_1 = 3.19;$$

$$\gamma_1 = 4.45.$$

The resulting extended Hata median basic transmission loss for a mobile station in a large city urban area is thus $1,500 \text{ MHz} \leq f \leq 3,000 \text{ MHz}$ and $1 \text{ km} \leq d \leq 20 \text{ km}$:

$$L_p^{EH} = 97.62 + 3.19 \log f + 4.45(\log f)^2 - 13.82 \log h_b - 3.2(\log(11.75h_m))^2 + 4.97 + (44.9 - 6.55 \log h_b) \log d \quad (\text{A-5})$$

The corresponding basic median attenuation relative to free space, A_b^{EH} ($1,500 \text{ MHz} \leq f \leq 3,000 \text{ MHz}$ and $1 \text{ km} \leq d \leq 20 \text{ km}$), is given by:

$$A_b^{EH}(f, d) \cong 30.52 - 16.81 \log f + 4.45(\log f)^2 + 9.83 \log d \quad (\text{A-6})$$

Turning next to the extension of the Hata model for distances greater than 20 km, it is more or less clear why Hata [A-2] limited his empirical formulas to the distance range 1–20 km originally. A careful review of [A-1] reveals that the measurements showed different distance power law exponents for distances greater than ~20–40 km (e.g., see Figures 11, 12 and 15 of [A-1]). The dependence of the median attenuation’s distance power law exponent on the base station effective height for distances above about 20 km, $n_h(h_b)$, is also fundamentally different from its behavior with base station effective antenna height for distances below 20 km, $n_l(h_b)$.

The distance extension begins with a curve fit of the basic median attenuation relative to free space at 100 km, $A(f, 100) = 10 \log a(f, 100)$, takes the functional form: $\alpha + \beta \log f + \gamma(\log f)^2$, using values taken from Figure 15 of [A-1] at 1,500 MHz, 2,000 MHz and 3,000 MHz. These are 63.5 dB, 65.75 dB and 69.5 dB, respectively. The resulting values for the curve fit coefficients are:

$$\alpha_{100} = 120.78;$$

$$\beta_{100} = -52.71;$$

$$\gamma_{100} = 10.92.$$

From (A-1) and (A-5), the base station effective height dependence of the lower distance range power law exponent of the median attenuation relative to free space, $n_l(h_b)$, is $n_l(h_b) = 0.1(24.9 - 6.55 \log h_b)$. To obtain the higher distance range power law exponent of the median attenuation relative to free space, n_h , use Curve B in Figure 12 of [A-1]. The required curve fit of this exponent to a functional form is written as:

$$\frac{n_h}{2} + 1 = \varrho + \sigma \log h_b + \tau(\log h_b)^2 \quad (\text{A-7})$$

The curve fit uses the following three $\left(h_b, \frac{n_h}{2} \right)$ ordered pairs: (24.5, 2.5), (70.0, 3) and (200, 3.22). The resulting values for the curve fit coefficients are:

$$\varrho = -0.75;$$

$$\sigma = 3.27;$$

$$\tau = -0.67.$$

For this study, the benefits of constructing a smoothly varying distance power law exponent were outweighed by the difficulties inherent in such a construction. Instead, a “two-slope” solution was chosen: the slope would be determined by the original Hata values below 20 km, and a second slope based on the power law exponents in Figure 12, Curve B, of [A-1] are applied to the (frequency extrapolated) basic median attenuation relative to free space, a_{bm} , at the reference base and mobile stations effective heights to find a distance “break-point”, assuming that the other height gain functions were unchanged. In this scheme the attenuations (in physical terms) can be rewritten as:

$$\begin{aligned}
a_{bm,l}(f, d) &= a_{bm,l}(f, d_l^{ref}) \left(\frac{d}{d_l^{ref}} \right)^{0.1(24.9-6.55 \log h_b)} \\
&= a_{bm,l}(f, d_l^{ref}) \left(\frac{d}{d_l^{ref}} \right)^{n_l(h_b)}
\end{aligned} \tag{A-8a}$$

for $1 \leq d \lesssim 20 \text{ km}$, and

$$a_{bm,h}(f, d) = a_{bm,h}(f, d_h^{ref}) \left(\frac{d}{d_h^{ref}} \right)^{n_h(h_b)} \tag{A-8b}$$

for $20 \lesssim d \leq 100 \text{ km}$.

For convenience, set $d_l^{ref} = 1 \text{ km}$ and $d_h^{ref} = 100 \text{ km}$. To find the ‘‘break-point’’ distance, equate (A-8a) and (A-8b) (and suppress all but the essential functional dependences):

$$a_{bm}(f, 1) d_{bp}^{n_l} = 10^{-2n_h} a_{bm}(f, 100) d_{bp}^{n_h} \tag{A-9a}$$

or, after a little manipulation

$$d_{bp} = \left(10^{2n_h} \frac{a_{bm}(f, 1)}{a_{bm}(f, 100)} \right)^{\frac{1}{(n_h - n_l)}} \tag{A-9b}$$

Given the ‘‘break-point’’ distance, d_{bp} , rewrite the extended Hata median basic transmission loss, L_p^{EH} ($1,500 \text{ MHz} \leq f \leq 3,000 \text{ MHz}$, $1 \text{ km} \leq d \leq 100 \text{ km}$, $30 \text{ m} \leq h_b \leq 200 \text{ m}$, $1 \text{ m} \leq h_m \leq 10 \text{ m}$), as:

$$\begin{aligned}
L_p^{EH}(f, d, h_b, h_m) & \\
&= A_{bm}^{EH}(f, d_{bp}) + 10n \log \left(\frac{d}{d_{bp}} \right) + 13.82 \log \left(\frac{200}{h_b} \right) + a(3) \\
&\quad - a(h_m) + L_{fs}(f, R(d, h_b, h_m))
\end{aligned} \tag{A-10}$$

$$\begin{aligned}
A_{bm}^{EH}(f, d_{bp}) &= 30.52 - 16.81 \log f + 4.45(\log f)^2 \\
&\quad + (24.9 - 6.55 \log h_b) \log d_{bp}
\end{aligned} \tag{A-11}$$

$$R(d, h_b, h_m) = \sqrt{(d \times 10^3)^2 + (h_b - h_m)^2} \tag{A-12}$$

$$n = \begin{cases} 0.1(24.9 - 6.55 \log h_b) & \text{for } 1 \text{ km} \leq d \leq d_{bp} \\ 2(3.27 \log h_b - 0.67(\log h_b)^2 - 1.75) & \text{for } d_{bp} < d \leq 100 \text{ km} \end{cases} \tag{A-13}$$

and it is understood that (A-2a) is used for the mobile station’s reference height correction, $a(3)$.

The lower frequency limit on the extended Hata formula in (A-10) is not absolute but only supplied in acknowledgement of the excellent agreement between the Hata formulae and the Okumura et al. results from 150 MHz to 1,500 MHz. If it is tolerable to allow small differences between these results and (A-1), then it is easy to show that the difference between the two is within 1.6 dB over virtually all of the original Hata model's frequency range.

The suburban factor shown in Figure 20 of [A-1] can be treated in a similar fashion to the method used to extend the frequency range of the formula in [A-2]. Fitting the suburban factor to a functional form of $\alpha + \beta \log f + \gamma(\log f)^2$ at the frequencies 1,500 MHz, 2,000 MHz, and 3,000 MHz yields the coefficients:

$$\alpha_s = 54.19;$$

$$\beta_s = -33.30;$$

$$\gamma_s = 6.25.$$

The corresponding extended Hata median basic transmission loss for a mobile station in a suburban area is thus $1,500 \text{ MHz} \leq f \leq 3,000 \text{ MHz}$ and $1 \text{ km} \leq d \leq 100 \text{ km}$:

$$L_{p,s}^{EH} = L_p^{EH} - (54.19 - 33.30 \log f + 6.25(\log f)^2) \quad (\text{A-14})$$

which can be seen to alter the frequency dependence of the intercept.

The extended Hata results given above are intended for use in predicting the median basic transmission loss in quasi-smooth terrain. Okumura et al. [A-1] also introduced various corrections to the median field strength curves, many of which were intended for use in situations where the terrain becomes irregular and rugged. These corrections provide a set of site-specific adjustments to be applied when terrain data is available for the path in question. These corrections are:

- The terminals' "effective height" corrections
- The "median" correction for rolling hilly terrain (applied in the vicinity of the mobile station only)
- The "fine" correction for rolling hilly terrain (applied in the vicinity of the mobile station only)
- The general slope of terrain correction (applied in the vicinity of the mobile station only)
- The isolated mountain (or isolated ridge) correction (applied only to single horizon paths)
- The mixed land-sea path correction

The terminals' "effective height" corrections are defined as the difference between the height of the terminal above mean sea level (the sum of the terminal's structural height above ground and the height of the terrain below the terminal above mean sea level) and the average height of

terrain above mean sea level from 3 to 15 km distance from the terminal in question. These quantities are to be used in the height gain terms in the extended Hata formulas. For paths less than 3 km, the terminal's structural height is used. For path distances between 3 and 15 km length, the average ground height is weighted by fraction of the path distance relative to 15 km.

For both the “median” and “fine” rolling hilly terrain corrections, it is necessary to compute the terrain irregularity parameter, Δh , for the terrain within 10 km of the mobile station. Note that Okumura et al. [A-1] refer to Δh as the terrain undulation parameter. The terrain irregularity parameter is defined as the interdecile range (i.e., the terrain height which is exceeded for 10% of the terrain elevations minus the terrain height which is exceeded for 90% of the terrain elevations) of terrain heights above mean sea level. If the path is less than 10 km in distance, then the asymptotic value for the terrain irregularity is computed:

$$\Delta h = \Delta h(d) \frac{(1 - 0.8e^{-0.2})}{(1 - 0.8e^{-0.02d})} \quad (\text{A-15})$$

For the “median” rolling hilly terrain correction, the median basic transmission loss is increased (and presented graphically in [A-1] Figure 28(c)) by:

$$K_h = 1.507213 - 8.458676 \log \Delta h + 6.102538(\log \Delta h)^2 \quad (\text{A-16})$$

For the “fine” rolling hilly terrain correction, it is necessary to compare the mobile station's terrain height to the value of median terrain height for the terrain within 10 km of the mobile station (i.e., the terrain height which is exceeded for 50% of the terrain elevations). The “fine” rolling hilly terrain correction is negative/positive in terms of its contribution to the median basic transmission loss depending on whether the mobile station's terrain height is greater/less-than the median terrain height exceedance level. The maximum magnitude of the correction is given by (and presented graphically in [A-1] Figure 29):

$$K_{hf} = -11.728795 + 15.544272 \log \Delta h - 1.8154766(\log \Delta h)^2 \quad (\text{A-17})$$

which is achieved for mobile station terrain heights equal to the terrain heights exceeded for 10% or 90% of terrain elevations, respectively, passing through zero at the median terrain height, with linear interpolations between these values. For path distances less than 10 km, the 10%, 50%, and 90% terrain height exceedance levels follow the asymptotic form used for the terrain irregularity parameter in (A-15).

For the general slope of terrain correction, [A-1] found that this correction depends on the average slope of the terrain for at least 5 km and up to 10 km on the mobile station's end of the path and the overall path distance (see [A-1] Figure 34). In this correction, terrain which rises, on average, in the direction from the base station to the mobile station reduces the median basic transmission loss for the flat, or zero slope, case, while terrain which falls, on average, in the direction from the base station to the mobile station increases the median basic transmission loss for the zero slope case. However, unlike the “fine” rolling hilly terrain correction, the general slope of terrain correction is not perfectly antisymmetric. In the current implementation, a least squares fit was performed on the terrain elevations in intervals of 5, 6, 7, 8, 9, and 10 km on the mobile station's end of the path. There are then three possible outcomes: all six slopes are

positive, all six slopes are negative, or the slopes have a mixture of signs. If all six are positive, then we use the maximum slope; if all six are negative, then we use the minimum slope; if the six have a mixture of signs, then we use the slope found for the 5 km portion of the path. Note, if the path distance is less than 5 km, then no general slope of terrain correction is applied. Piecewise linear curve fits of the correction curves shown in Figure 34 of [A-1] are used, with linear interpolation for distances between the curves.

For the isolated ridge correction, [A-1] found that the corrections given above were inadequate if the path contained a single isolated ridge. For those paths, they provided a family of three correction curves for a ridge height normalized to 200 m, based on the distance of the mobile station to the peak of the isolated ridge. The three curves corresponding to distances of the base station to the peak of the isolated ridge: ≤ 15 km, 30 km and ≥ 60 km (see [A-1] Figure 31). In the current implementation this correction applies for single horizon paths only and piecewise linear fits are used based on discrete values taken from the curves. To correct for the actual ridge height ([A-1] Figure 32) the height of the ridge above the line between the electrical centers of the base and mobile stations was used. For distances between 15 km and 30 km and 30 km and 60 km, interpolate between the applicable curves.

For the mixed land-sea path correction, Okumura et al. (see [A-1] Figure 35) observed that there was a dependence on the fraction of the path over sea, the overall path distance (less than 30 km and greater than 60 km) and which terminal, either the base station or the mobile station, was principally adjacent to the sea. For intermediate cases, Okumura et al. suggested that linear interpolation gives satisfactory results. The current implementation uses piecewise linear fits to the curves in [A-1] Figure 35. In all cases where the fraction of the path over sea is non-zero, the mixed land-sea path correction reduces the median basic transmission loss.

To complete the discussion of the extended Hata model, note that [A-1] also provided estimates of the standard deviation of the location variability for urban and suburban environments in [A-1] Figure 39. A version of these curves suitable for computation/extrapolation is required. Noting that the frequency dependence is non-linear in $\log f$, one tries a fit of the form: $\alpha + \beta \log f + \gamma(\log f)^2$ using the values in Table A-1 that were extracted from the curves.

Table A-1. Okumura et al. Location Variability Standard Deviations

f (MHz)	σ_u (dB)	σ_r (dB)
1500	7.1	8.95
2000	7.5	9.5
3000	8.1	10.1

These values yield the following three simultaneous equations for σ_u in the unknowns α_u , β_u and γ_u :

$$7.1 = \alpha_u + \beta_u \log(1500) + \gamma_u(\log(1500))^2 \quad (\text{A-18a})$$

$$7.5 = \alpha_u + \beta_u \log(2000) + \gamma_u(\log(2000))^2 \quad (\text{A-18b})$$

$$8.1 = \alpha_u + \beta_u \log(3000) + \gamma_u (\log(3000))^2 \quad (\text{A-18c})$$

which evaluate to:

$$\alpha_u = 4.0976291,$$

$$\beta_u = -1.2255656,$$

$$\gamma_u = 0.68350345.$$

Note also that it is probably sufficient to set $\sigma_r = \sigma_u + 2$.

A.4 The Irregular Terrain Model (ITM)

The ITS Irregular Terrain Model (ITM) is a general purpose radio propagation prediction algorithm intended for use on tropospheric radio circuits utilizing frequencies in the range 20 MHz–20 GHz. The model is based on electromagnetic theory and statistical analyses of terrain features and radio measurements. The model predicts the median signal strength as a function of distance and the variability of the signal strength in time (because of changing atmospheric conditions) and space (because of changes in terrain). The model does not include the fine details of channel characterization (e.g., fast fading).

This description of the ITM algorithm focuses first on the computation of the reference attenuation, that is, the median computed attenuation relative to free space, and then on a discussion of the how the cumulative distributions of attenuation are obtained. This description covers the use of the model in its point-to-point mode, although mention is made of area mode predictions. The distinction between the use of the model in the area prediction mode and the point-to-point prediction mode is chiefly in the additional input parameters/data that must be provided, generally through examination of the detailed terrain profile between the two terminals. Automated procedures for examining the detailed terrain profile to obtain the additional inputs are available.

The input parameters in Table A-2 are required to use ITM in either mode.

Table A-2. Irregular Terrain Model Input Parameters/Data and Preliminary Calculations

d	the (horizontal) distance between the terminals [m]
h_{g_1}, h_{g_2}	the terminals' antenna structural (i.e., electrical center) heights above ground [m]
k	the wavenumber [m^{-1}]
Δh	the terrain irregularity parameter (i.e., the inter-decile range of terrain elevations on the path) [m]
N_s	the minimum monthly mean surface refractivity [N-units]
γ_e	the earth's effective curvature [m^{-1}]
Z_g	the surface transfer impedance of the ground
<i>climate</i>	one of seven discrete radio climate types

The wavenumber, k , is given in terms of the wavelength in a vacuum, λ , by:

$$k = \frac{2\pi}{\lambda} = \frac{2\pi f}{c} \quad (\text{A-19})$$

where the speed of light in a vacuum, $c = \frac{1}{\sqrt{\mu_0 \epsilon_0}} \cong 2.997 \times 10^8 \text{ m s}^{-1}$. If one measures the frequency, f , in units of MHz, rather than Hz, then it is convenient to write the wavenumber as:

$$k = \frac{f}{f_0} \quad (\text{A-20})$$

where $f_0 = 47.7 \text{ MHz m}$.

The surface refractivity, N_s , is sometimes given in terms of the surface refractivity reduced to sea-level, N_0 . If the surface refractivity is specified as its value at sea level, then it should be adjusted to account for the general elevation of the region involved, z_{sys} [m]:

$$N_s = N_0 e^{-\frac{z_{sys}}{9.46 \times 10^3}} \quad (\text{A-21})$$

The earth's effective curvature, γ_e [m^{-1}], is determined from the surface refractivity, N_s , using the empirical formula from [A-4] (4.4):

$$\gamma_e = \gamma_a \left(1 - 0.04665 e^{\frac{N_s}{N_1}} \right) = \frac{\gamma_a}{K} \quad (\text{A-22})$$

where K is the "effective earth's radius factor", $\gamma_a = \frac{\pi}{2} \times 10^{-7} \text{ m}^{-1}$ is the physical earth's curvature, and $N_1 = 179.3 \text{ N-units}$. The effective earth's radius, a_e , is given by:

$$a_e = \gamma_e^{-1} = K a \quad (\text{A-23})$$

where the physical earth's radius, a , is given by $a = \gamma_a^{-1} \cong 6.37 \times 10^6$.

The surface transfer impedance of the ground is a complex, dimensionless constant which depends on the relative dielectric permittivity of the ground, $\epsilon_r = \frac{\epsilon}{\epsilon_0}$, and electrical conductivity, of the ground, σ , and the polarization of the radio signal's electric field vector (i.e., horizontal, which is defined as perpendicular to the plane of incidence at the ground reflection point, or vertical, which is defined as parallel to the plane of incidence at the ground reflection point). The complex relative dielectric permittivity, ϵ' , is given by:

$$\epsilon' = \epsilon_r + i \frac{\sigma}{k} \sqrt{\frac{\mu_0}{\epsilon_0}} \quad (\text{A-24})$$

and, then, the surface transfer impedance of the ground, Z_g , is

$$Z_g = \begin{cases} \sqrt{\varepsilon' - 1} & \text{for horizontal polarization} \\ \frac{\sqrt{\varepsilon' - 1}}{\varepsilon'} & \text{for vertical polarization} \end{cases} \quad (\text{A-25})$$

For ITM in area prediction mode, the siting criteria for the terminals are required. These are qualitative measures of the care taken, at each terminal, to attempt to ensure good radio propagation conditions. There are three levels: at random, with care, and with great care.

For ITM in point-to-point prediction mode, a detailed terrain elevation profile must be provided at equally spaced horizontal distance increments between the two terminals. The sequence of elevations and their corresponding distances is then used to extract the terminals' irregular terrain radio horizon distances, d_{l_1}, d_{l_2} , the terminals' irregular terrain radio horizon elevation angles, $\theta_{e_1}, \theta_{e_2}$, the terminals' effective heights, h_{e_1}, h_{e_2} , and the terrain irregularity parameter, Δh .

The "effective height" of an antenna is its height above an "effective reflecting plane" or above the "intermediate foreground" between the antenna and its horizon. A difficulty with the model is that there is no explicit, quantitative, definition of this quantity, and the accuracy of the model sometimes depends on the skill of the user in estimating values for these effective heights. The terminals' effective antenna heights determine the terminals' smooth earth radio horizon distances. The ITM automated procedures are used in this analysis to compute the terminals' effective heights. Another user might override these procedures and, instead, specify these values based on his/her own educated estimates.

In ITM's point-to-point prediction mode, the terminals' irregular terrain radio horizon distances and elevation angles are found by geometric methods (see, e.g., [A-4]), given the line drawn between the two terminals' electrical centers and the terrain elevations' heights with respect to that line. The profile is assumed to lie along the great circle path containing the terminals and the curvature of the great circle path is γ_e , so that the effective loss of antenna height due to earth curvature through arc-length d is approximately $-\frac{\gamma_e d^2}{2}$. If none of the intermediate terrain elevations is higher than the line between the two terminals' electrical centers, then the path is line-of-sight. Otherwise, the path is trans-horizon.

In ITM's point-to-point prediction mode, this distinction between line-of-sight and trans-horizon paths is important. If the path is line-of-sight, then no horizons are detected during examination of the terrain profile. However, the model requires that these quantities be defined, so, for line-of-sight paths in the point-to-point mode only, the terminals' irregular terrain radio horizon distances and elevation angles are determined using the formulas from the area mode which are given below. In using the area mode formulas, it may happen that the point-to-point mode path distance, $d > d_l = d_{l_1} + d_{l_2}$, which, in turn, implies that the path is trans-horizon. To remedy this contradiction, it suffices to conjecture that the terminals' effective heights have been underestimated, and then these effective heights are increased by the common factor that yields $d \leq d_l$.

In the area prediction mode, the model does not require a terrain profile, but it should be emphasized that this does not mean that the model's area prediction mode does not account for

irregular terrain. Instead, the terminals' radio horizon distances, irregular terrain horizon elevation angles, and effective heights are determined by the terminals' antenna heights above ground, their siting criteria and the terrain irregularity parameter. This last quantity is user supplied, either from estimates based on many terrain profiles covering the region involved or from typical, suggested values ([A-5] Table 2.).

Beginning with the determination of the terminals' effective heights in the area prediction mode exclusively, if the terminal in question is sited at random, then:

$$h_{e_j} = h_{g_j} \text{ for } j = 1 \text{ or } 2 \quad (\text{A-26})$$

Otherwise, and again, exclusively in the area prediction mode, let

$$B_j = \begin{cases} 5 \text{ m} & \text{if terminal } j \text{ is sited with care} \\ 10 \text{ m} & \text{if terminal } j \text{ is sited with great care} \end{cases} \quad (\text{A-27a})$$

and

$$B'_j = (B_j - 1) \sin \left(\frac{\pi}{2} \min \left(\frac{h_{g_j}}{5}, 1 \right) \right) + 1 \quad (\text{A-27b})$$

Note that $B'_j = B_j$ if $h_{g_j} \geq 5 \text{ m}$. The j^{th} terminal's effective height, h_{e_j} ($j = 1 \text{ or } 2$), is then

$$h_{e_j} = h_{g_j} + B'_j e^{-\frac{2h_{g_j}}{\Delta h}} \quad (\text{A-27c})$$

In the area prediction mode (and in the point-to-point mode for line-of-sight paths), the terminals' observed median horizon distances and irregular terrain horizon elevation angles are then determined from their corresponding effective heights [A-6], the effective earth's curvature and the terrain irregularity parameter. First, one computes the smooth earth horizon distances, d_{ls_j} ($j = 1,2$):

$$d_{ls_j} = \sqrt{\frac{2h_{e_j}}{\gamma_e}} \quad (\text{A-28})$$

and then the terminals' irregular terrain radio horizon distances, d_{l_j} ($j = 1,2$), and elevation angles, θ_{e_j} ($j = 1,2$), are given by

$$d_{l_j} = d_{ls_j} e^{-0.07 \sqrt{\frac{\Delta h}{\max(h_{e_j}, 5)}}} \quad (\text{A-29})$$

(*Note:* in point-to-point mode for line-of-sight paths if $d > d_l = d_{l_1} + d_{l_2}$, then set $h_{e_j} = \left(\frac{d}{d_l}\right)^2 h_{e_j}$ ($j = 1,2$) and re-compute the smooth earth and irregular terrain radio horizon distances.)

Then set

$$\theta_{e_j} = - \frac{\left[2h_{e_j} + 0.65\Delta h \left(1 - e^{-0.07 \sqrt{\frac{\Delta h}{\max(h_{e_j}, 5)}}} \right) \right]}{d_{lsj}} \quad (\text{A-30})$$

In either the area or the point-to-point mode, the model requires the combined smooth earth radio horizon distance, d_{ls} , the combined irregular terrain radio horizon distance, d_l , and the combined irregular terrain radio horizon elevation angles, θ_e . From (A-28),

$$d_{lsj} = \sqrt{\frac{2h_{e_j}}{\gamma_e}} \text{ for } j = 1,2$$

$$d_{ls} = d_{ls1} + d_{ls2} \quad (\text{A-31})$$

$$d_l = d_{l_1} + d_{l_2} \quad (\text{A-32})$$

$$\theta_e = \max(\theta_{e_1} + \theta_{e_2}, -d_l\gamma_e) \quad (\text{A-33})$$

and the definition of a function of a distance, s , which asymptotically approaches the terrain irregularity parameter (see [A-6]):

$$\Delta h(s) = \Delta h \left(1 - 0.8e^{-\frac{s}{5 \times 10^4}} \right) \quad (\text{A-34})$$

A.4.1 The Reference Attenuation

The reference attenuation, A_{ref} , is given as a piecewise function of the path horizontal distance, d , by:

$$A_{ref} = \begin{cases} \max\left(0, A_{el} + K_1 d + K_2 \ln\left(\frac{d}{d_{ls}}\right)\right) & \text{for } d \leq d_{ls} \\ A_{ed} + m_d d & \text{for } d_{ls} \leq d \leq d_x \\ A_{es} + m_s d & \text{for } d_x \leq d \end{cases} \quad (\text{A-35})$$

where the coefficients A_{el} , K_1 , K_2 , A_{ed} , m_d , A_{es} , m_s , and the tropospheric scatter cross-over distance, d_x , are given in the following. The three distance ranges/intervals given above are

referred to as the line-of-sight range, the diffraction range and the scatter range, respectively. The function is continuous, so at the second interval's endpoints, $d = d_{ls}, d_x$, respectively, the lower and higher distance intervals' expressions are required to yield equal values for A_{ref} . Therefore, there are only five independent coefficients.

A.4.2 The Coefficients of the Diffraction Range

The coefficients for the diffraction range are found by evaluating the diffraction attenuation, $A_{diff}(d)$, at two distances, d_3 and d_4 , which are beyond line-of-sight. Set

$$d_3 = \max(d_{ls}, d_l + 1.3787X_{ae}) \quad (\text{A-36})$$

$$d_4 = d_3 + 2.7574X_{ae} \quad (\text{A-37})$$

$$A_3 = A_{diff}(d_3) \quad (\text{A-38})$$

$$A_4 = A_{diff}(d_4) \quad (\text{A-39})$$

where

$$X_{ae} = (k\gamma_e^2)^{-\frac{1}{3}} = a_e \left(\frac{2\pi a_e}{\lambda} \right)^{-\frac{1}{3}} \quad (\text{A-40})$$

Then the desired coefficients are given by:

$$m_d = \frac{A_4 - A_3}{d_4 - d_3} \quad (\text{A-41})$$

$$A_{ed} = A_3 - m_d d_3 = \frac{A_3 d_4 - A_4 d_3}{d_4 - d_3} \quad (\text{A-42})$$

A.4.3 The Diffraction Range Attenuation Function

The diffraction attenuation function is a weighted combination of both knife-edge and rounded-earth diffraction attenuations plus a terrain "clutter" attenuation:

$$A_{diff}(s) = (1 - w(s))A_k(s) + w(s)A_r(s) + A_{fo} \quad (\text{A-43})$$

The idea is to design the weighting factor, $w(s)$, in such a way that it is unity when the distance dependent terrain irregularity parameter, $\Delta h(s)$, vanishes and that the weighting factor vanishes when the distance dependent terrain irregularity parameter becomes large. To achieve this result, define

$$w(s) = \frac{1}{1 + 0.1\sqrt{Q(s)}} \quad (\text{A-44})$$

with

$$Q(s) = \min\left(\frac{\Delta h(s)}{\lambda}, 1000\right) \left[\sqrt{\frac{h_{e_1}h_{e_2} + C}{h_{g_1}h_{g_2} + C}} + \frac{d_l + a_e\theta_e}{s} \right] \quad (\text{A-45})$$

and

$$C = \begin{cases} 0 \text{ m}^2 & \text{in area prediction mode} \\ 10 \text{ m}^2 & \text{in point - to - point mode} \end{cases} \quad (\text{A-46})$$

In the diffraction range attenuation function, $A_{diff}(s)$, the additional terrain “clutter” attenuation, A_{fo} , is intended to approximately account for the median additional diffraction attenuation due to additional knife-edges between the terminals’ irregular terrain radio horizons that may obstruct the convex hull between the two irregular terrain radio horizons. Its median value is empirically determined and is given by

$$A_{fo} = \min\left(15, 5 \log\left(1 + 4.77 \times 10^{-4} k h_{g_1} h_{g_2} \sigma_h(d_{ls})\right)\right) \quad (\text{A-47})$$

where

$$\sigma_h(d_{ls}) = \frac{\Delta h(d_{ls})}{1.282} e^{-\frac{\sqrt[4]{\Delta h(d_{ls})}}{2}} \quad (\text{A-48})$$

The median double knife-edge diffraction attenuation for the two irregular terrain radio horizons is then given by a double knife-edge Epstein-Peterson like [A-7] approximation:

$$A_k(s) = Fn(v_1(s)) + Fn(v_2(s)) \quad (\text{A-49})$$

with

$$Fn(v) = 20 \log\left(\left|\frac{1}{\sqrt{2i}} \int_v^\infty e^{i\frac{\pi}{2}u^2} du\right|\right) \quad (\text{A-50})$$

and

$$v_j(s) = \frac{\theta(s)}{2} \sqrt{\frac{2d_{l_j}(s - d_l)}{\lambda(s - d_l + d_{l_j})}} \text{ for } j = 1, 2 \quad (\text{A-51})$$

where

$$\theta(s) = \theta_e + s\gamma_e \quad (\text{A-52})$$

The rounded-earth diffraction attenuation is based on a “three radii” method applied to Vogler’s formulation of the solution of the smooth spherical earth diffraction problem [A-8]. The three curvatures, i.e., the inverses of the three radii, are given by:

$$\gamma_0 = \frac{\theta(s)}{s - d_l} \quad (\text{A-53a})$$

and

$$\gamma_j = \frac{2h_{e_j}}{d_{l_j}^2} \text{ for } j = 1,2 \quad (\text{A-53b})$$

Next, set

$$\alpha_j = \left(\frac{k}{\gamma_j}\right)^{\frac{1}{3}} \text{ for } j = 0,1,2 \quad (\text{A-54})$$

and

$$K_j = \frac{1}{i\alpha_j Z_g} \text{ for } j = 0,1,2 \quad (\text{A-55})$$

In the next step, define the dimensionless distances:

$$x_j = AB(K_j)\alpha_j\gamma_j d_{l_j} \text{ for } j = 1,2 \quad (\text{A-56a})$$

and

$$\begin{aligned} x_0 &= AB(K_0)\alpha_0\gamma_0(s - d_l) + x_1 + x_2 \\ &= AB(K_0)\alpha_0\theta(s) + x_1 + x_2 \end{aligned} \quad (\text{A-56b})$$

where A is a dimensionless constant equal to 151.03. Of the dimensionless distances defined above, note that only x_0 depends on s . The rounded-earth diffraction attenuation, $A_r(s)$, is given by:

$$A_r(s) = G(x_0) - F(x_1, K_1) - F(x_2, K_2) - C_1(K_0) \quad (\text{A-57})$$

where the functions $G(x)$, $F(x, K)$, $C_1(K)$ and $B(K)$ are defined by [A-8].

A.4.4 The Coefficients of the Line-of-Sight Range

As noted above, in the line-of-sight range, the idea is to devise a curve for the reference attenuation of the form:

$$A_{ref} = A_{el} + K_1 d + K_2 \ln\left(\frac{d}{d_{ls}}\right) \quad (\text{A-58})$$

with the added constraints that $K_1, K_2 \geq 0$ and that continuity is ensured at the endpoint of the interval. To ensure continuity, set:

$$d_2 = d_{ls} \quad (\text{A-59})$$

and

$$A_2 = A_{ed} + m_d d_2 \quad (\text{A-60})$$

There are two general cases, depending upon the sign of A_{ed} .

First, consider the general case $A_{ed} \geq 0$. To determine the coefficients, the attenuations at two additional distances within the line-of-sight range are required, so set:

$$d_0 = \min\left(\frac{d_l}{2}, 1.908kh_{e_1}h_{e_2}\right) \quad (\text{A-61})$$

$$d_1 = \frac{3}{4}d_0 + \frac{d_l}{4} \quad (\text{A-62})$$

$$A_0 = A_{los}(d_0) \quad (\text{A-63})$$

$$A_1 = A_{los}(d_1) \quad (\text{A-64})$$

Solving simultaneously first for the unknowns K_1, K_2 yields the provisional values:

$$K'_2 = \max\left(0, \frac{(A_1 - A_0)(d_2 - d_0) - (A_2 - A_0)(d_1 - d_0)}{(d_2 - d_0) \ln\left(\frac{d_1}{d_0}\right) - (d_1 - d_0) \ln\left(\frac{d_2}{d_0}\right)}\right) \quad (\text{A-65})$$

$$K'_1 = \frac{A_2 - A_0 - K'_2 \ln\left(\frac{d_2}{d_0}\right)}{d_2 - d_0} \quad (\text{A-66})$$

If $K'_1 \geq 0$, then the added constraints are satisfied, so set:

$$K_1 = K'_1 \quad (\text{A-66a})$$

$$K_2 = K'_2 \quad (\text{A-66b})$$

However, if $K'_1 < 0$, then more work is required so, provisionally discard K_1, A_1 , which yields a pure power-law dependence with distance in the line-of-sight range:

$$K_2'' = \frac{A_2 - A_0}{\ln\left(\frac{d_2}{d_0}\right)} \quad (\text{A-67})$$

If $K_2'' \geq 0$, then

$$K_1 = 0 \quad (\text{A-68a})$$

$$K_2 = K_2'' \quad (\text{A-68b})$$

If, on the other hand, $K_2'' < 0$, then $A_0 > A_2$, so discard both A_0, A_1 and set

$$K_1 = m_d \quad (\text{A-69a})$$

$$K_2 = 0 \quad (\text{A-69b})$$

This last alternative corresponds to extrapolating the diffraction range attenuation back into the line-of-sight range and, given that $A_{ed} \geq 0$, ensures that the reference attenuation will always be greater than or equal to zero.

Now consider the second general case: $A_{ed} < 0$. As before, the attenuations at two additional distances in the line-of-sight range are required. As a starting point, set

$$d_0 = 1.908kh_{e_1}h_{e_2} \quad (\text{A-70})$$

$$d_1 = \max\left(-\frac{A_{ed}}{m_d}, \frac{d_l}{4}\right) \quad (\text{A-71})$$

Note that the first of the two distances in the comparative expression for d_1 is the distance at which the extrapolated diffraction range attenuation vanishes. The procedure for computing the unknown coefficients is now a bit more involved than before, because there is no a priori guarantee that $d_0 < d_1$.

If $d_0 < d_1$, then, as before, begin by attempting to use all three distances. Set

$$A_0 = A_{los}(d_0) \quad (\text{A-72})$$

$$A_1 = A_{los}(d_1) \quad (\text{A-73})$$

and then solve simultaneously for provisional values of K_1, K_2 , as before:

$$K_2' = \max\left(0, \frac{(A_1 - A_0)(d_2 - d_0) - (A_2 - A_0)(d_1 - d_0)}{(d_2 - d_0)\ln\left(\frac{d_1}{d_0}\right) - (d_1 - d_0)\ln\left(\frac{d_2}{d_0}\right)}\right) \quad (\text{A-74})$$

If $K_2' = 0$, then immediately branch to the $d_0 \geq d_1$ case given below. Otherwise, evaluate

$$K_1' = \frac{A_2 - A_0 - K_2' \ln\left(\frac{d_2}{d_0}\right)}{d_2 - d_0} \quad (\text{A-75})$$

Now, if $K_1' \geq 0$ (and since $K_2' > 0$), the constraints are satisfied:

$$K_1 = K_1' \quad (\text{A-76a})$$

$$K_2 = K_2' \quad (\text{A-76b})$$

However, if $K_1' < 0$, then more work is required so discard K_1, A_1 (which, as before, yields a pure power-law dependence with distance in the line-of-sight range):

$$K_2'' = \frac{A_2 - A_0}{\ln\left(\frac{d_2}{d_0}\right)} \quad (\text{A-77})$$

If $K_2'' \geq 0$, then

$$K_1 = 0 \quad (\text{A-78a})$$

$$K_2 = K_2'' \quad (\text{A-78b})$$

If, on the other hand, $K_2'' < 0$, then $A_0 > A_2$, so discard both A_0, A_1 and set:

$$K_1 = m_d \quad (\text{A-79a})$$

$$K_2 = 0 \quad (\text{A-79b})$$

If $d_0 \geq d_1$ or $K_2' = 0$, then discard A_0 :

$$A_1 = A_{los}(d_1) \quad (\text{A-80})$$

$$K_1'' = \frac{A_2 - A_1}{d_2 - d_1} \quad (\text{A-81})$$

Now, if $K_1'' > 0$, then

$$K_1 = K_1'' \quad (\text{A-82a})$$

$$K_2 = 0 \quad (\text{A-82b})$$

Otherwise, it becomes necessary to discard both A_0, A_1 :

$$K_1 = m_d \quad (\text{A-83a})$$

$$K_2 = 0 \quad (\text{A-83b})$$

To complete the calculation of the line-of-sight range coefficients, note that it is sufficient to set

$$A_{el} = A_2 - K_1 d_2 \quad (\text{A-84})$$

A.4.5 The Line-of-Sight Range Attenuation Function

The line-of-sight range attenuation function, $A_{los}(s)$, is given by a weighted combination of the “extrapolated/extended diffraction range attenuation”, $A_d(s)$, and the “two-ray attenuation”, $A_t(s)$:

$$A_{los}(s) = (1 - w)A_d(s) + wA_t(s) \quad (\text{A-85})$$

The idea here is to devise a weighting function, w , which varies from unity as the terrain irregularity parameter, Δh , vanishes and down to zero as Δh becomes large compared to the wavelength:

$$w = \frac{1}{1 + \frac{47.7k\Delta h}{\max(D_2, d_{ls})}} \quad (\text{A-86})$$

where $D_2 = 10$ km. The extended diffraction range attenuation is given by:

$$A_d(s) = A_{ed} + m_d s \quad (\text{A-87})$$

To obtain the two-ray attenuation, it is necessary to obtain an estimate of the effective reflection coefficient of the ground plane. Set

$$\sin \psi(s) = \frac{h_{e1} + h_{e2}}{\sqrt{s^2 + (h_{e1} + h_{e2})^2}} \quad (\text{A-88})$$

and then set the provisional effective reflection coefficient to the product of the Fresnel reflection coefficient (for small grazing angles) and a correction for surface roughness in the first Fresnel zone of the ground reflection point based on the Rayleigh criterion

$$R'_e(s) = \frac{\sin \psi(s) - Z_g}{\sin \psi(s) + Z_g} e^{-k\sigma_h(s) \sin \psi(s)} \quad (\text{A-89})$$

where

$$\sigma_h(s) = \frac{\Delta h(s)}{1.282} e^{-\frac{\sqrt[4]{\Delta h(s)}}{2}} \quad (\text{A-90})$$

Also, provisionally approximate the phase difference due to the path length differences between the direct and ground-reflected rays as

$$\delta'(s) \approx 2 \frac{kh_{e1}h_{e2}}{s} \quad (\text{A-91})$$

In ITM, the effective reflection coefficient, $R_e(s)$, is given by

$$R_e(s) = \begin{cases} R_e'(s) & \text{for } |R_e'(s)| \geq \max(0.5, \sqrt{\sin \psi(s)}) \\ \frac{R_e'(s)}{|R_e'(s)|} \sqrt{\sin \psi(s)} & \text{otherwise} \end{cases} \quad (\text{A-92})$$

The phase difference, $\delta(s)$, is then given by

$$\delta(s) = \begin{cases} \delta'(s) & \text{for } \delta'(s) \leq \frac{\pi}{2} \\ \pi - \frac{(\frac{\pi}{2})^2}{\delta'(s)} & \text{otherwise} \end{cases} \quad (\text{A-93})$$

which corrects for the approximation when the distance, s , is small.

The two-ray attenuation, $A_t(s)$, is then given by:

$$A_t(s) = -20 \log |1 + R_e(s)e^{i\delta(s)}| \quad (\text{A-94})$$

which is a good approximation as long as the distance, s , is not too small (i.e., the direct ray's path length and the ground reflected ray's path length are nearly equal).

A.4.6 The Coefficients of the Forward (or Tropospheric) Scatter Range

To find the coefficients of the scatter range, first set:

$$d_5 = d_l + D_s \quad (\text{A-95})$$

$$d_6 = d_5 + D_s \quad (\text{A-96})$$

with $D_s = 200$ km and then compute the tropospheric scatter attenuations at these distances

$$A_5 = A_{scat}(d_5) \quad (\text{A-97})$$

$$A_6 = A_{scat}(d_6) \quad (\text{A-98})$$

If both A_5 and A_6 are defined, then

$$m_s = \frac{A_6 - A_5}{D_s} \quad (\text{A-99})$$

$$d_x = \max\left(d_{ls}, d_l + X_{ae} \log(47.7k), \frac{A_5 - A_{ed} - m_s d_5}{m_d - m_s}\right) \quad (\text{A-100})$$

$$A_{es} = A_{ed} + (m_d - m_s)d_x \quad (\text{A-101})$$

If either A_5 or A_6 is undefined, then set

$$d_x = \infty \quad (\text{A-102})$$

A.4.7 The Scatter Range Attenuation Function

This function is computed using modified and abbreviated methods for computing the forward scatter loss found in [A-4] in Chapter 9 of Volume I and Appendix III.5 of Volume II. The following geometric parameters are set

$$\theta = \theta_e + \gamma_e s \quad (\text{A-103})$$

$$\theta' = \theta_{e_1} + \theta_{e_2} + \gamma_e s \quad (\text{A-104})$$

$$r_j = 2k\theta' h_{e_j} \text{ for } j = 1, 2 \quad (\text{A-105})$$

If both r_1 and r_2 are less than 0.2, then the function A_{scat} is undefined (or infinite). For other combinations of the values of r_1 and r_2 , the function is given by:

$$A_{scat}(s) = 10 \log(47.7k\theta^4) + F(\theta s, N_s) + H_0 \quad (\text{A-106})$$

where the attenuation function, $F(\theta s, N_s)$, and the “frequency gain” function, H_0 , are given below.

To obtain the attenuation function, $F(\theta s, N_s)$, it is useful to note that Rice et al. [A-4] give the reference value, L_{bsr} , of the long-term median basic transmission loss due to forward scatter ([A-4] (9.1)) as:

$$L_{bsr} = 30 \log f - 20 \log d + F(\theta d) - F_0 + H_0 + A_a \quad (\text{A-107})$$

where f is the frequency (MHz), d is the sea-level arc-length distance (km) and θ is the angular distance (radians). Neglecting the last three terms on the right-hand side of (A-107), the reference long-term median *attenuation relative to free space* due to forward scatter is then

$$L_{bsr} - L_{fs} = 30 \log f - 20 \log d + F(\theta d) - 20 \log(2ks) \quad (\text{A-108})$$

where $s = d \times 10^3$. After some manipulation, it can be shown that

$$L_{bsr} - L_{fs} = 10 \log(47.7k\theta^4) - 32.44 + F(\theta d) - 40 \log(\theta d) \quad (\text{A-109})$$

with

$$F(\theta d) = \begin{cases} 135.82 + 0.332\theta d + 30 \log(\theta d) & 0.01 \leq \theta d \leq 10 \\ 129.5 + 0.212\theta d + 37.5 \log(\theta d) & 10 \leq \theta d \leq 70 \\ 119.2 + 0.157\theta d + 45 \log(\theta d) & \text{otherwise} \end{cases} \quad (\text{A-110})$$

for $N_s = 301$ (see [A-4], Volume II, (III.46)–(III.48)). Absorbing the last three terms on the right-hand side of (A-109) into the sought after attenuation function, $F(\theta s, N_s)$, with $D \equiv \theta s = \theta d \times 10^3$, yields:

$$F(D, 301) = \begin{cases} 133.4 + 0.332 \times 10^{-3}D - 10 \log(D) & 0 \leq D \leq 10^4 \\ 104.6 + 0.212 \times 10^{-3}D - 2.5 \log(D) & 10^4 \leq D \leq 7 \times 10^4 \\ 71.8 + 0.157 \times 10^{-3}D + 5 \log(D) & \text{otherwise} \end{cases} \quad (\text{A-111})$$

and

$$F(D, N_s) = F(D, 301) - 0.1(N_s - 301)e^{-\frac{D}{4 \times 10^4}} \quad (\text{A-112})$$

The “frequency gain” function, H_0 , is a function of r_1 , r_2 , the scatter efficiency factor η_s , and the asymmetry factor, s_s , of the cross-over point. The cross-over point is assumed to be midway between the terminals’ radio horizons, so the asymmetry factor, s_s , is then given by:

$$s_s = \frac{d_{l_2} + \frac{(s - d_{l_1} - d_{l_2})}{2}}{d_{l_1} + \frac{(s - d_{l_1} - d_{l_2})}{2}} = \frac{s - (d_{l_1} - d_{l_2})}{s + (d_{l_1} - d_{l_2})} \quad (\text{A-113})$$

If it happens that the asymmetry factor, as defined above, is greater than unity, then two adjustments are made. Firstly, the asymmetry factor, s_s , is set to its reciprocal. Secondly, the ratio of the terminals’ effective heights, $\left(\frac{r_2}{r_1}\right)$, is also set to its reciprocal. The height of the cross-over point, z_0 , is:

$$z_0 = s\theta' \frac{s_s}{(1 + s_s)^2} \quad (\text{A-114})$$

and the scatter efficiency factor, η_s , is

$$\eta_s = \frac{z_0}{Z_0} \left[1 + (3.1 \times 10^{-2} - 2.32 \times 10^{-3}N_s + 5.67 \times 10^{-6}N_s^2)e^{-\left(\frac{z_0}{Z_1}\right)^6} \right] \quad (\text{A-115})$$

with $Z_0 = 1.756 \times 10^3$ m and $Z_1 = 8.0 \times 10^3$ m. The frequency gain function, H_0 , is given by

$$H_0 = H_{00}(r_1, r_2, \eta_s) + \Delta H_0(s_s, q, \eta_s) \quad (\text{A-116})$$

where

$$q = \frac{\left(\frac{r_2}{r_1}\right)}{s_s} \quad (\text{A-117})$$

$$\Delta H_0(s_s, q, \eta_s) = 6(0.6 - \log \eta_s) \log s_s \log q \quad (\text{A-118})$$

The function H_{00} is obtained by linear interpolation on integer values of the scatter efficiency, η_s . For $\eta_s = j = 1, \dots, 5$ the function takes the form:

$$H_{00}(r_1, r_2, j) = \frac{1}{2}(H_{01}(r_1, j) + H_{01}(r_2, j)) \quad (\text{A-119})$$

with

$$H_{01}(r, 1) = 10 \log \left(1 + \frac{24}{r^2} + \frac{25}{r^4}\right) \quad (\text{A-120a})$$

$$H_{01}(r, 2) = 10 \log \left(1 + \frac{45}{r^2} + \frac{80}{r^4}\right) \quad (\text{A-120b})$$

$$H_{01}(r, 3) = 10 \log \left(1 + \frac{68}{r^2} + \frac{177}{r^4}\right) \quad (\text{A-120c})$$

$$H_{01}(r, 4) = 10 \log \left(1 + \frac{80}{r^2} + \frac{395}{r^4}\right) \quad (\text{A-120d})$$

$$H_{01}(r, 5) = 10 \log \left(1 + \frac{105}{r^2} + \frac{705}{r^4}\right) \quad (\text{A-120e})$$

For $\eta_s > 5$, the value at $\eta_s = 5$ is used. For $\eta_s = 0$,

$$H_{00}(r_1, r_2, 0) = 10 \log \left(\left(1 + \frac{\sqrt{2}}{r_1}\right)^2 \left(1 + \frac{\sqrt{2}}{r_2}\right)^2 \frac{r_1 + r_2}{r_1 + r_2 + 2\sqrt{2}} \right) \quad (\text{A-121})$$

For all of this computation the values of s_s and q are truncated at 0.1 and 10.0.

A.4.8 Variability and the Quantiles of the Attenuation

The preceding discussion provided a method for computing the reference attenuation as a function of distance. Given the input quantities, the method is apparently deterministic, albeit with scattered empiricisms. However, as pointed out in [A-5] “it seems undeniable that received signal levels are subject to a wide variety of random variations and that proper engineering must take these variations into account.” In order to take these variations into account, ITM provides a simple model which uses random variables, each of which depends on only one of the three dimensions of variability: time, locations and situations.

When the signal levels are expressed in decibel notation, experience shows that the distributions involved are normal or nearly normal. Therefore, the calculations of the desired fractions (or quantiles) of the attenuation, $A(q_T, q_L, q_S)$, for time, q_T , locations, q_L , and situations, q_S , are rescaled in terms of “standard normal deviates”.

Following the convention of [A-4], Volume II, Annex V (see also, e.g., [A-5], Section 6.2), a positive deviation corresponds to an increase in signal level and, so, to a decrease in attenuation or loss. The complementary normal distribution for the value, z , which is exceeded for a given fraction (i.e., with probability), Q :

$$Q(z) = \frac{1}{\sqrt{2\pi}} \int_z^{\infty} e^{-\frac{t^2}{2}} dt \quad (\text{A-122})$$

with its inverse function giving the standard normal deviate, z , is given by:

$$z(q) = Q^{-1}(q) \quad (\text{A-123})$$

Thus one can say that if a random variable, x , is normally distributed with mean (and median) value, X_0 , and standard deviation, σ , then its quantiles are given by

$$X(q) = X_0 + \sigma z(q) \quad (\text{A-124})$$

Now set:

$$z_T = z(q_T) \quad (\text{A-125a})$$

$$z_L = z(q_L) \quad (\text{A-125b})$$

$$z_S = z(q_S) \quad (\text{A-125c})$$

and ask for the quantile of attenuation, $A(z_T, z_L, z_S)$. Given the sign convention for the deviations, let the provisional value of this quantile be:

$$A' \equiv A_{ref} - V_{med} - Y_T - Y_L - Y_S \quad (\text{A-126})$$

with V_{med} , Y_T , Y_L and Y_S defined below. The deviations, Y_T , Y_L and Y_S , have zero mean (and median) values.

To avoid predicting basic transmission loss values very much less than the free space loss, set:

$$A(z_T, z_L, z_S) = \begin{cases} A' & \text{if } A' \geq 0 \\ A' \frac{29 - A'}{29 - 10A'} & \text{otherwise} \end{cases} \quad (\text{A-127})$$

A.4.8.1 The Effective Distance

The “effective distance” is important in the evaluation of the median adjustment, V_{med} , and the deviations associated with the time variability, Y_T , and the situation variability, Y_S . The transition distance, d_{ex} , is given by:

$$d_{ex} = \sqrt{2a_1 h_{e1}} + \sqrt{2a_1 h_{e2}} + a_1 (kD_1)^{-\frac{1}{3}} \quad (\text{A-128})$$

with $a_1 = 9000$ km and $D_1 = 1266$ km. The effective distance, d_e , is a piecewise function of distance:

$$d_e = \begin{cases} d \frac{D_0}{d_{ex}} & \text{for } d \leq d_{ex} \\ D_0 + d - d_{ex} & \text{for } d > d_{ex} \end{cases} \quad (\text{A-129})$$

with $D_0 = 130$ km. Note that the effective distance depends on the terminals’ effective antenna heights and the frequency through d_{ex} . For example, with $h_{e1} = 50$ m, $h_{e2} = 6$ m and $f = 3500$ MHz, $d_{ex} \sim 60.3$ km.

A.4.8.2 The All Year Median Adjustment

The computed reference attenuation, A_{ref} , is adjusted by the all year median, $V_{med}(d_e, climate)$, to obtain the median quantile of attenuation. This adjustment is shown in Figure 10.13 of [A-4]. For effective distances less than ~ 80 km, the adjustment is less than 1 dB for all radio climates. For the maritime temperate oversea radio climate, the maximum adjustment is ~ 7 dB at an effective distance of ~ 220 km, falling gradually to ~ 3 dB at great effective distances.

A.4.8.3 The Deviation of Time Variability

The deviation of the time variability, Y_T , is piecewise linear in z_T . It takes the form of:

$$Y_T = \begin{cases} \sigma_{T-Z_T} & z_T \leq 0 \\ \sigma_{T+Z_T} & 0 \leq z_T \leq z_D \\ \sigma_{T+Z_D} + \sigma_{TD}(z_T - z_D) & z_D \leq z_T \end{cases} \quad (\text{A-130})$$

As is the case with the all year median adjustment, the “fading” and “enhancement” pseudo-standard deviations, σ_{T-} and σ_{T+} respectively, are both functions of the effective distance and the radio climate:

$$\sigma_{T-} = \sigma_{T-}(d_e, climate) \quad (\text{A-131})$$

$$\sigma_{T+} = \sigma_{T+}(d_e, climate) \quad (\text{A-132})$$

These pseudo-standard deviations are found by taking the curves shown in [A-4] Volume I, Section 10 and Volume II, Section III.7, and dividing the $Y(0.9)$ and $Y(0.1)$ long term power fading deviation quantiles by their corresponding standard normal deviates, -1.282 and 1.282 , respectively.

For the low probability or “ducting” case (i.e., $z_D \leq z_T$), there are two additional constants that depend on the radio climate:

$$z_D = z_D(\text{climate}) \quad (\text{A-133})$$

$$\sigma_{TD} = C_D(\text{climate})\sigma_{T+} \quad (\text{A-134})$$

Values for these constants are given in Table A-3 along with $q_D = Q(z_D)$.

Table A-3. Longley-Rice Low Probability or “Ducting” Constants

Radio Climate	q_D	z_D	C_D
Equatorial	0.10	1.282	1.224
Continental Subtropical	~ 0.015	2.161	0.801
Maritime Subtropical	0.10	1.282	1.380
Desert	0.00	∞	-
Continental Temperate	0.10	1.282	1.224
Maritime Temperate Overland	0.10	1.282	1.518
Maritime Temperate Oversea	0.10	1.282	1.518

A.4.8.4 The Deviation of Location Variability

The deviation of the location variability, Y_L , is given by:

$$Y_T = \sigma_L z_L \quad (\text{A-135})$$

with the standard deviation of location variability, σ_L , given by:

$$\sigma_L = \frac{10k\Delta h(d)}{13 + k\Delta h(d)} \quad (\text{A-136})$$

where d is the path length (i.e., distance). If the terrain irregularity parameter for this path distance is more than just a few wavelengths in size, then $\sigma_L \sim 10 \text{ dB}$. Of course, if both terminals are at known, fixed positions and the model is being used in point-to-point mode, then $z_L = 0$.

A.4.8.5 The Deviation of Situation Variability

The standard deviation of the situation variability, σ_S , is given by ([A-6], Annex 1, (1.16)):

$$\sigma_S = 5 + 3e^{-\frac{d_e}{10^5}} \quad (\text{A-137})$$

The deviation of the situation variability, Y_S , depends on the preceding quantity and terms dependent on the deviations of the time and location variabilities which account for the convolution of the three mutually independent random variables:

$$Y_S = z_S \sqrt{\sigma_S^2 + \frac{Y_T^2}{7.8 + z_S^2} + \frac{Y_L^2}{24 + z_S^2}} \quad (\text{A-138})$$

(For a discussion, see, e.g., [A-5] Section 6.2.)

A.5 References

- [A-1] Y. Okumura, E. Ohmori, T. Kawano, and K. Fukuda, "Field strength and its variability in VHF and UHF land-mobile radio service, *Rev. Elec. Commun. Lab.*, 16, 9-10, pp. 825-873, (Sept.-Oct. 1968).
- [A-2] M. Hata, "Empirical formula for propagation loss in land mobile radio services," *IEEE Transactions on Vehicular Technology*, VT-29, 3, pp. 317-325 (Aug. 1980).
- [A-3] A.G. Longley, *Radio Propagation in Urban Areas*, U.S. Department of Commerce, Office of Telecommunications, OT Report 78-144 (Apr.1978), available at <http://www.its.bldrdoc.gov/publications/2674.aspx>.
- [A-4] P.L. Rice, A.G. Longley, K.A. Norton, and A.P. Barsis, *Transmission Loss Predictions for Tropospheric Communication Circuits*, U.S. Department of Commerce, National Bureau of Standards, Technical Note 101 (Revised January 1, 1967), Vol. I available at <http://www.its.bldrdoc.gov/publications/2726.aspx>, Vol. II available at <http://www.its.bldrdoc.gov/publications/2727.aspx>.
- [A-5] G.A. Hufford, A.G. Longley, and W.A. Kissick, *A Guide to the Use of the ITS Irregular Terrain Model in Area Prediction Mode*, National Telecommunications and Information Administration Report 82-100 (April 1982), available at <http://www.its.bldrdoc.gov/publications/2091.aspx>.
- [A-6] A.G. Longley and P.L. Rice, *Prediction of Tropospheric Radio Transmission Loss Over Irregular Terrain: A Computer Method-1968*, U.S. Department of Commerce, Environmental Science Services Administration, ESSA Technical Report ERL 79-ITS 67 (July 1968), available at <http://www.its.bldrdoc.gov/publications/2784.aspx>.
- [A-7] J. Epstein and D.W. Peterson, "An experimental study of wave propagation at 850 Mc," *Proc. IRE* 41, pp. 595-611 (1953).

- [A-8] L. E. Vogler, "Calculation of groundwave attenuation in the far diffraction region," *Radio Science Journal of the Research NBS/USNC-URSI*, Vol. 68D, No. 7, pp. 819-826 (July 1964).

APPENDIX B SHIPBORNE RADAR ANALYSIS RESULTS

B.1 Introduction

This appendix provides the results of the exclusion zone distance analysis and the exclusion zones needed to protect the shipborne radars operating in the 3550–3650 MHz band.

B.2 Shipborne Radar Analysis Results

The initial analysis results indicated that the shipborne radar systems operating below 3550 MHz, Shipborne Radar 2 and Shipborne Radar 3, did not require exclusion zones for protection. The exclusion zone distance analysis results presented in this appendix are for Shipborne Radar 1, Shipborne Radar 4, and Shipborne Radar 5. The results are shown on Figures B-1 through B-9 for Shipborne Radar 1; Figures B-10 through B-18 for Shipborne Radar 4; and Figures B-19 through B-27 for Shipborne Radar 5. The yellow line on each plot is the exclusion zone distance based on the Fast Track Report and the blue line is the revised exclusion zone distance. The red and blue dots in the figures represent the ship location off-shore.



Figure B-1. Shipborne Radar 1—exclusion zone lower 48 states (yellow line—fast track exclusion zone and blue line—revised exclusion zone).

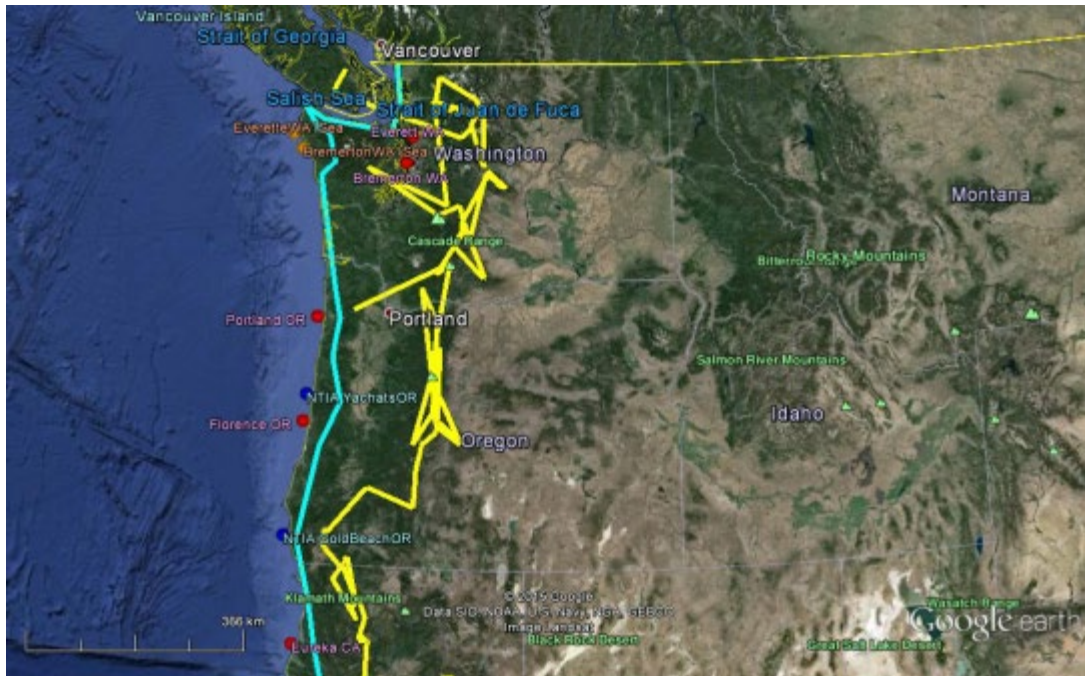


Figure B-2. Shipborne radar 1–Exclusion zone upper west coast (yellow line–fast track exclusion zone and blue line–revised exclusion zone).

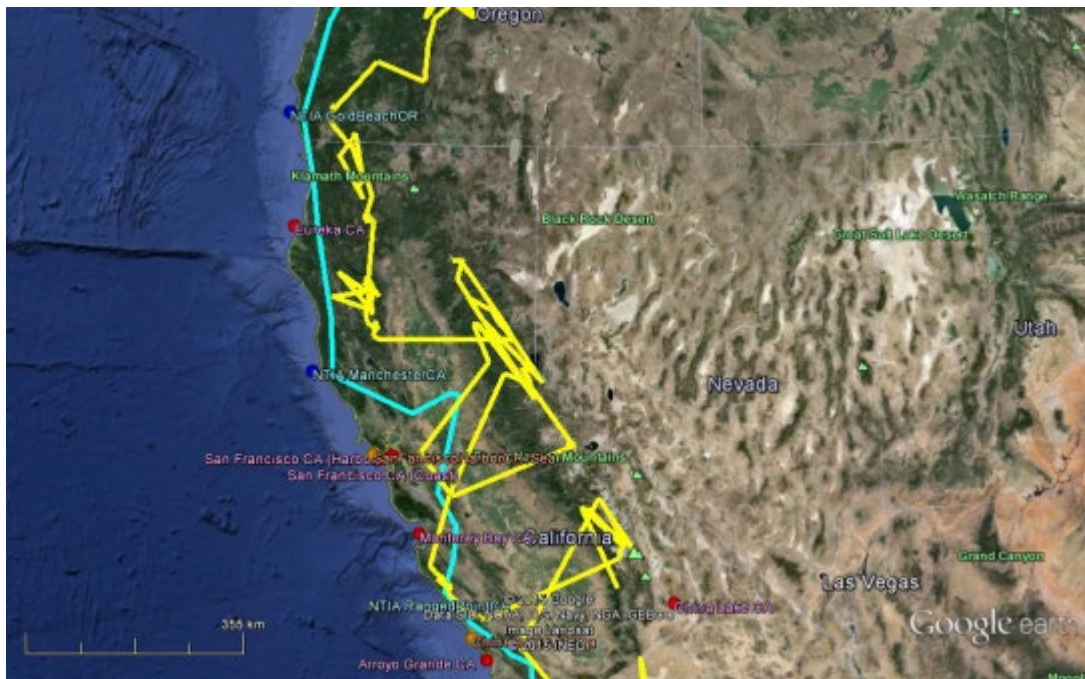


Figure B-3. Shipborne Radar 1–Exclusion zone middle west coast (yellow line–fast track exclusion zone and blue line–revised exclusion zone).

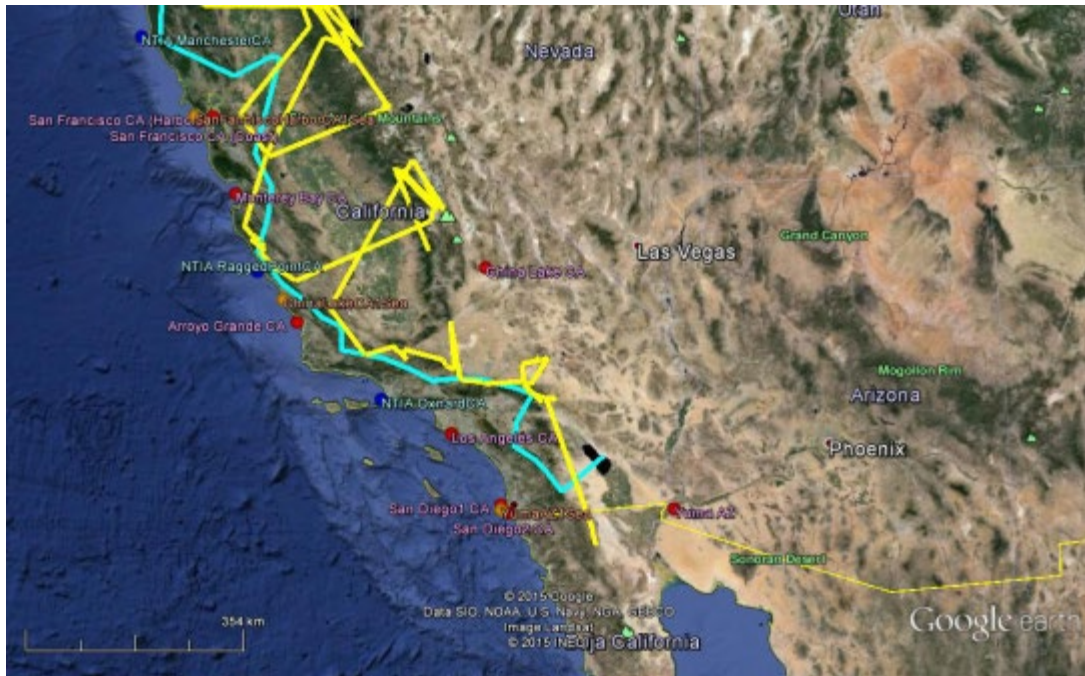


Figure B-4. Shipborne Radar 1–Exclusion zone lower west coast (yellow line–fast track exclusion zone and blue line–revised exclusion zone).

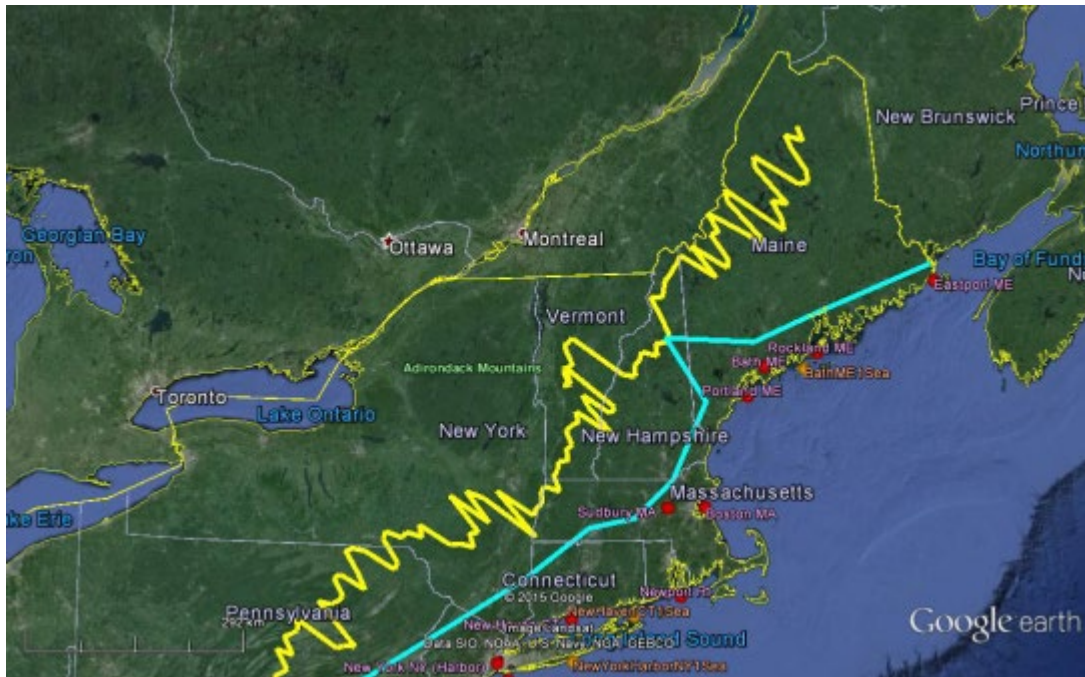


Figure B-5. Shipborne Radar 1–Exclusion zone upper east coast (yellow line–fast track exclusion zone and blue line–revised exclusion zone).



Figure B-6. Shipborne Radar 1–Exclusion zone middle east coast (yellow line–fast track exclusion zone and blue line–revised exclusion zone).

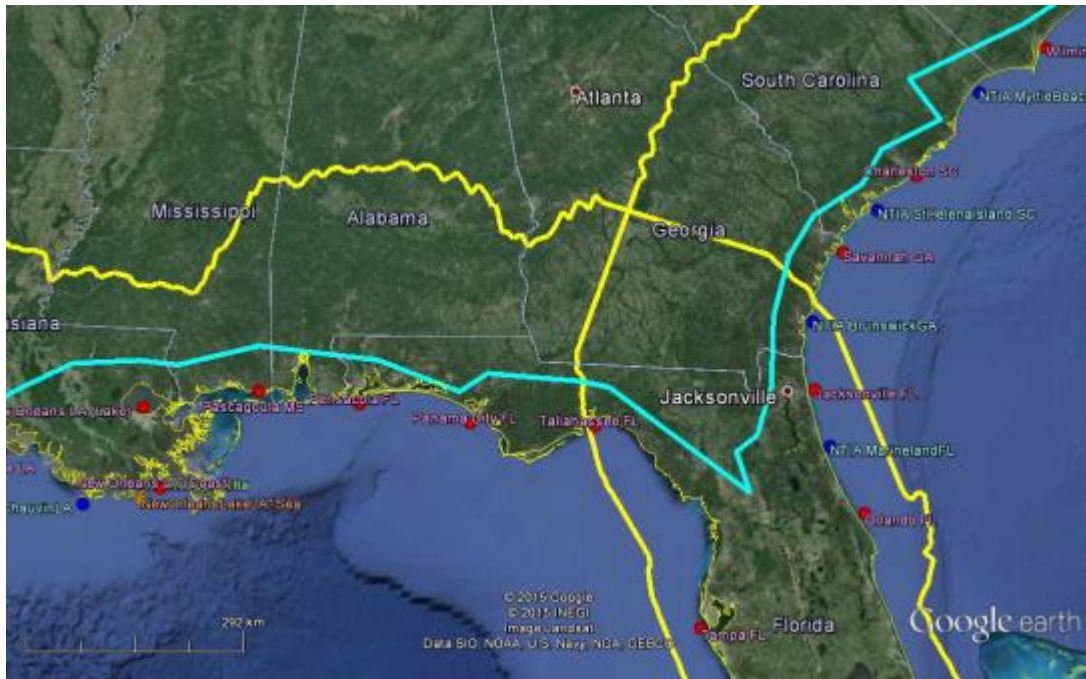


Figure B-7. Shipborne Radar 1–exclusion zone lower east coast (yellow line–fast track exclusion zone and blue line–revised exclusion zone).

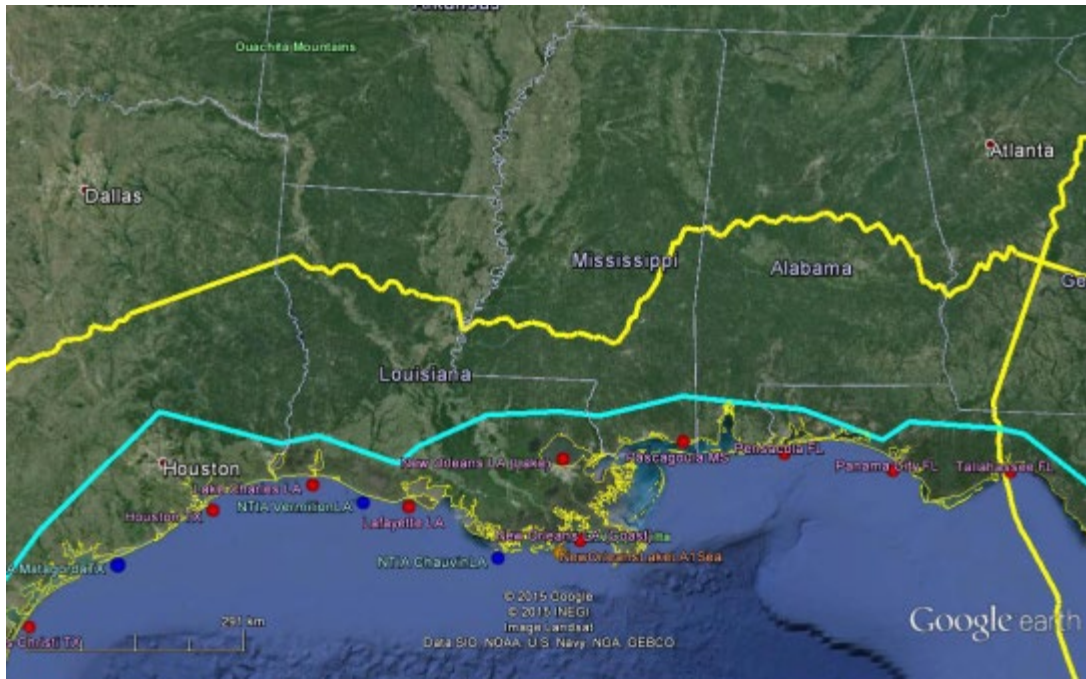


Figure B-8. Shipborne Radar 1–Exclusion zone eastern gulf coast (yellow line–fast track exclusion zone and blue line–revised exclusion zone).

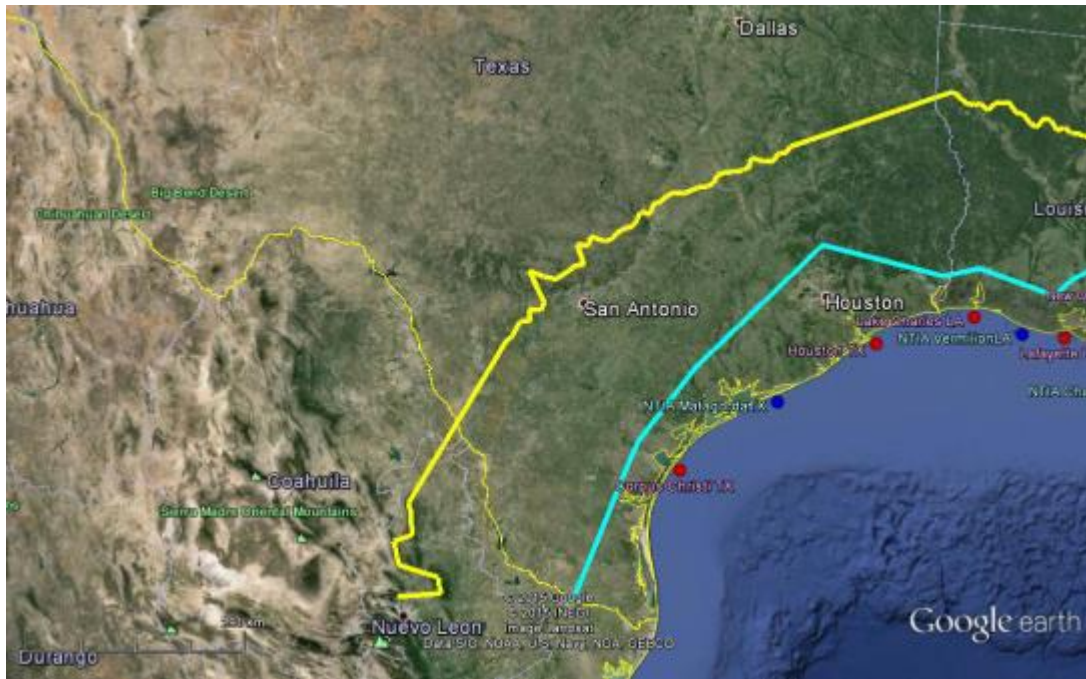


Figure B-9. Shipborne Radar 1–Exclusion zone western gulf coast (yellow line–fast track exclusion zone and blue line–revised exclusion zone).



Figure B-10. Shipborne Radar 4–Exclusion zone lower 48 states (yellow line–fast track exclusion zone and blue line–revised exclusion zone).

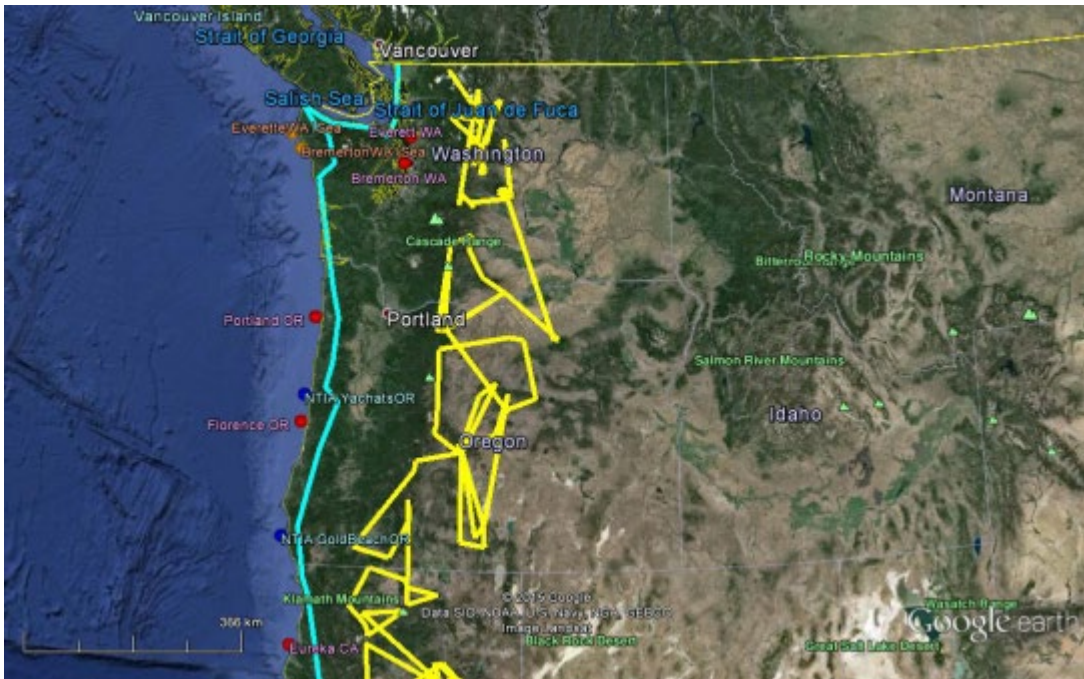


Figure B-11. Shipborne Radar 4–Exclusion zone upper west coast (yellow line–fast track exclusion zone and blue line–revised exclusion zone).

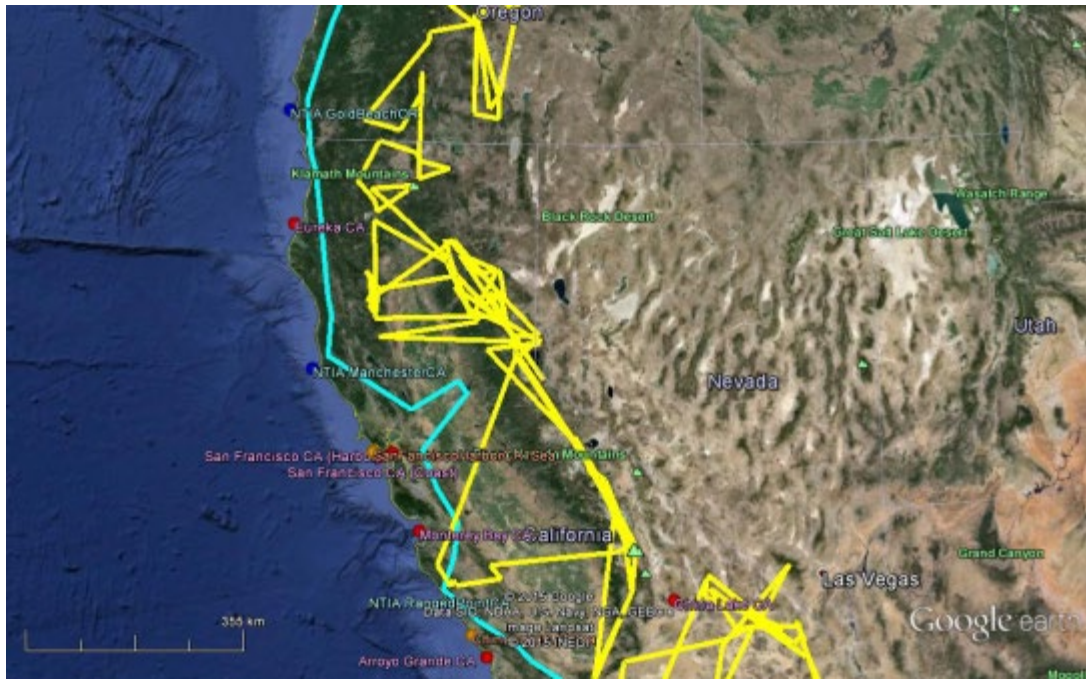


Figure B-12. Shipborne Radar 4–Exclusion zone middle west coast (yellow line–fast track exclusion zone and blue line–revised exclusion zone).

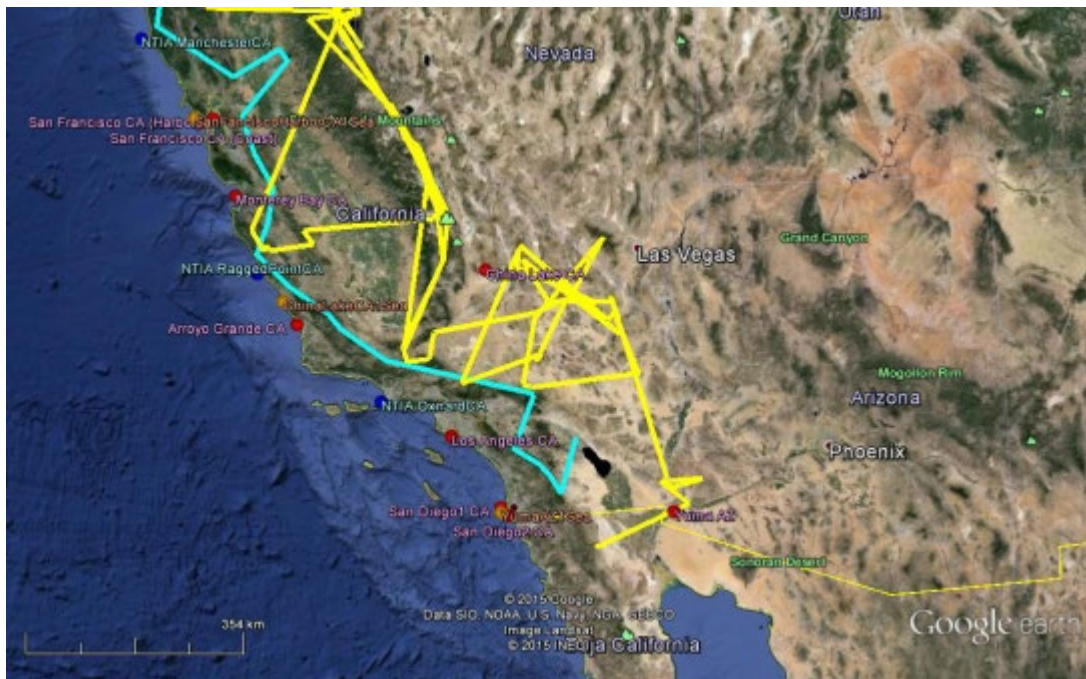


Figure B-13. Shipborne Radar 4–Exclusion zone lower west coast (yellow line–fast track exclusion zone and blue line–revised exclusion zone).

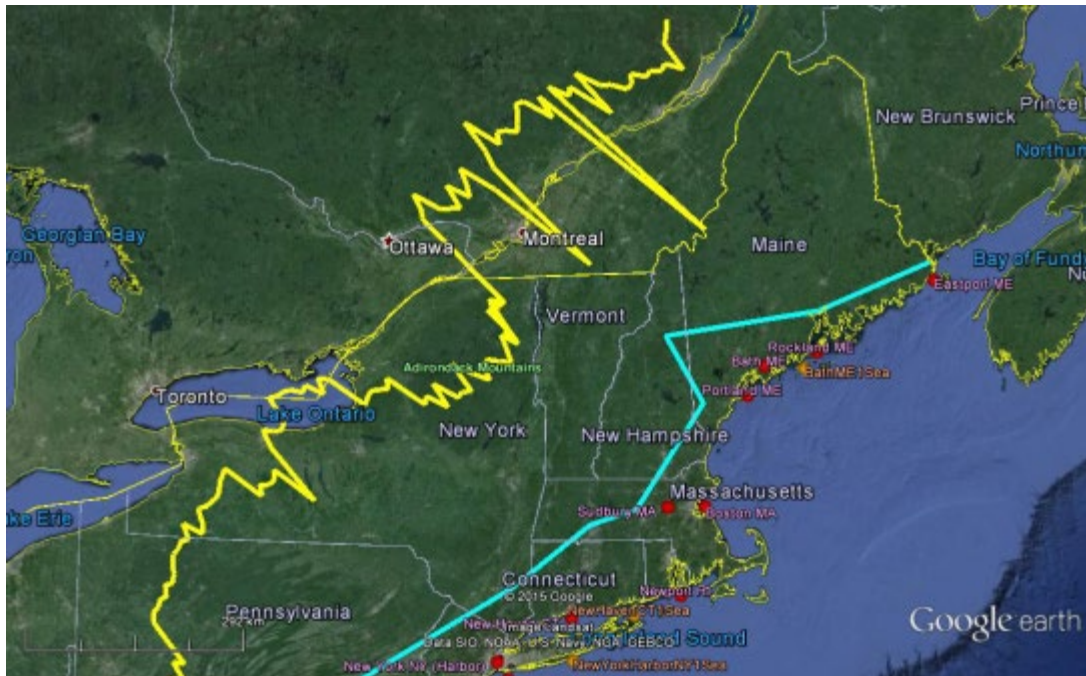


Figure B-14. Shipborne Radar 4–Exclusion zone upper east coast (yellow line–fast track exclusion zone and blue line–revised exclusion zone).



Figure B-15. Shipborne Radar 4–Exclusion zone middle east coast (yellow line–fast track exclusion zone and blue line–revised exclusion zone).

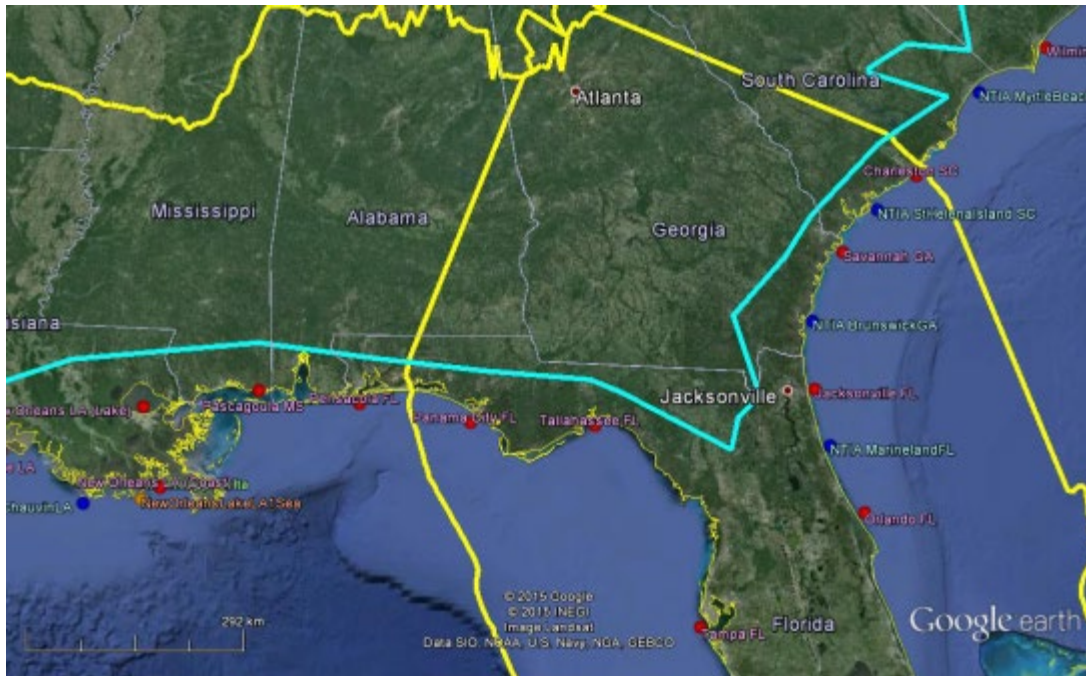


Figure B-16. Shipborne Radar 4–exclusion zone lower east coast (yellow line–fast track exclusion zone and blue line–revised exclusion zone).

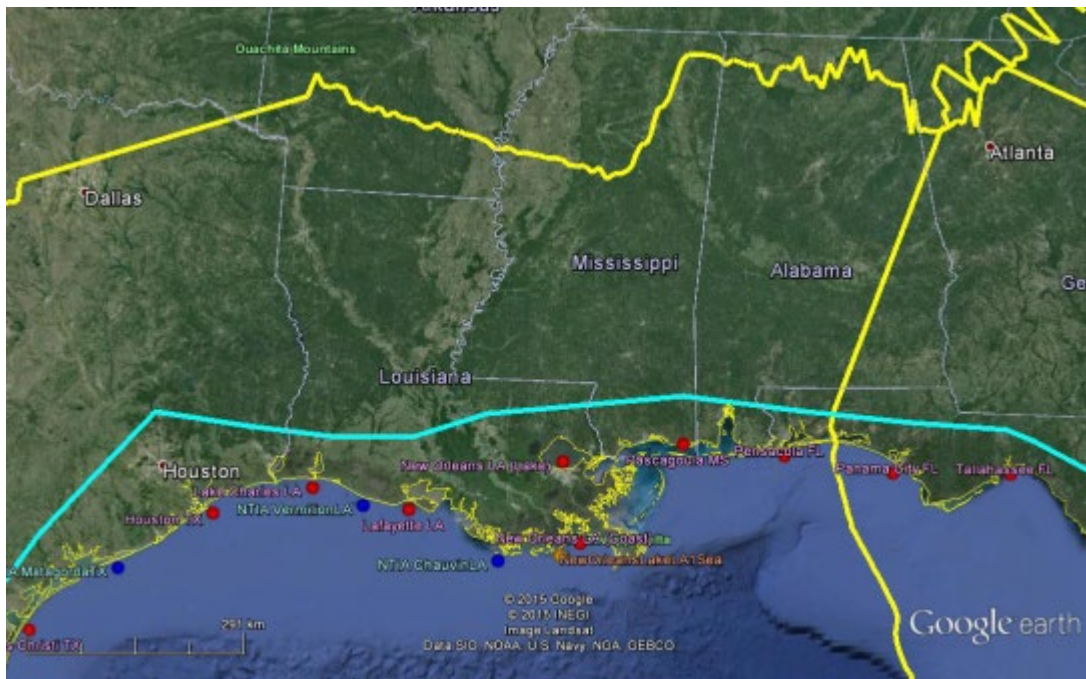


Figure B-17. Shipborne Radar 4–Exclusion zone eastern gulf coast (yellow line–fast track exclusion zone and blue line–revised exclusion zone).

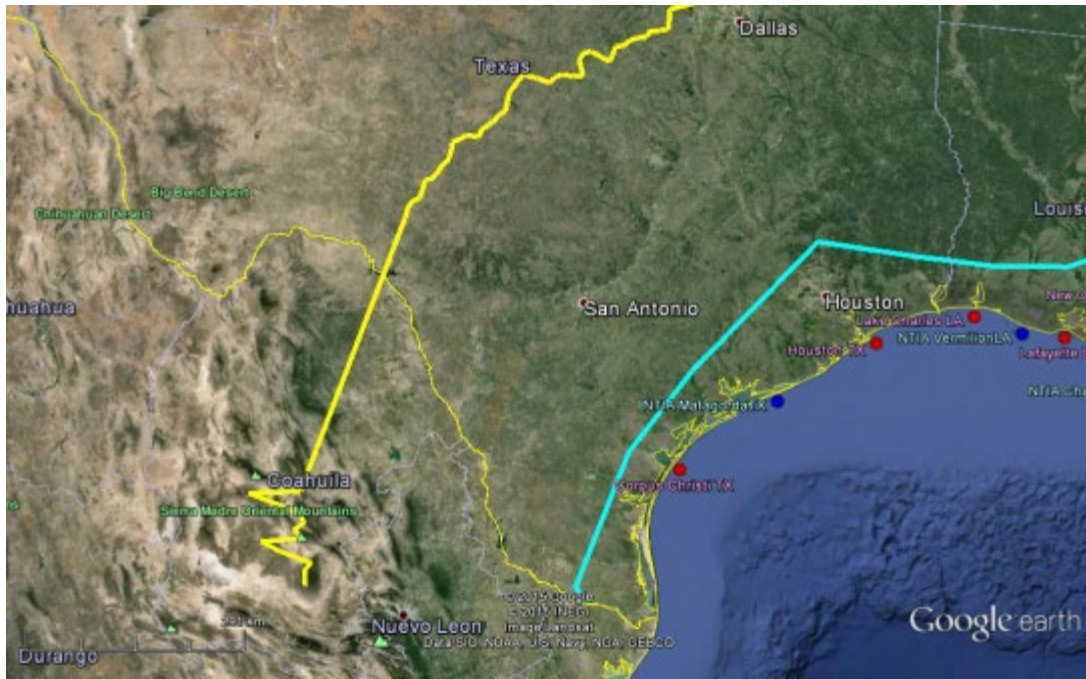


Figure B-18. Shipborne Radar 4–Exclusion zone eastern gulf coast (yellow line–fast track exclusion zone and blue line–revised exclusion zone).



Figure B-19. Shipborne Radar 5–Exclusion zone lower 48 states (yellow line–fast track exclusion zone and blue line–revised exclusion zone).

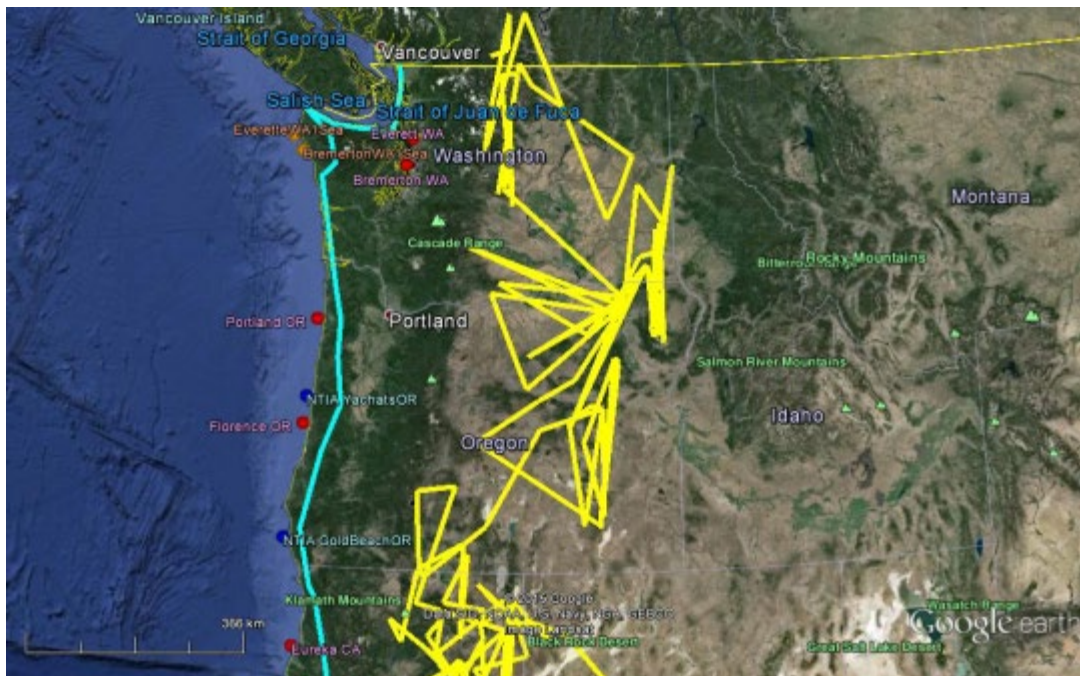


Figure B-20. Shipborne Radar 5–Exclusion zone upper west coast(yellow line–fast track exclusion zone and blue line–revised exclusion zone).

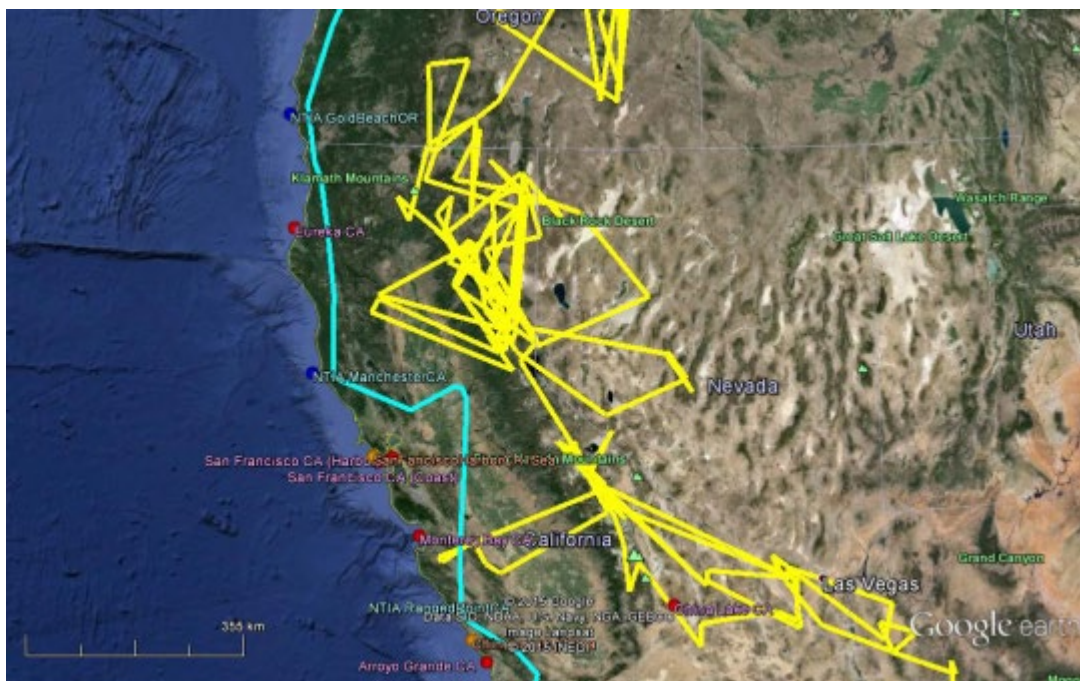


Figure B-21. Shipborne Radar 5–Exclusion zone middle west coast (yellow line–fast track exclusion zone and blue line–revised exclusion zone).

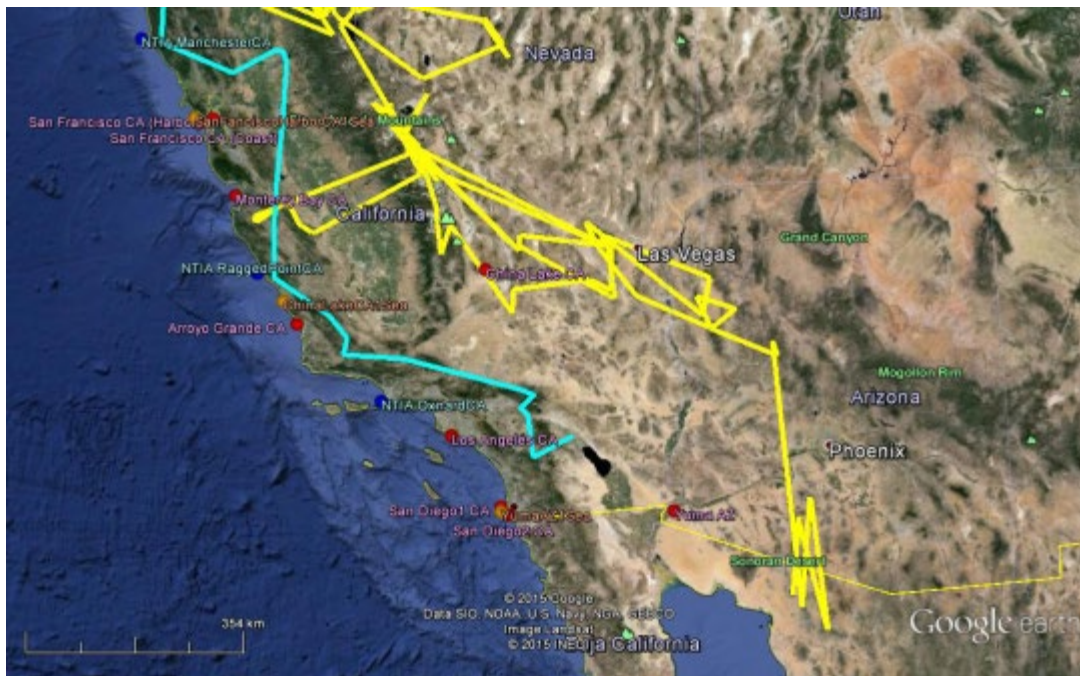


Figure B-22. Shipborne Radar 5–Exclusion zone lower west coast (yellow line–fast track exclusion zone and blue line–revised exclusion zone).

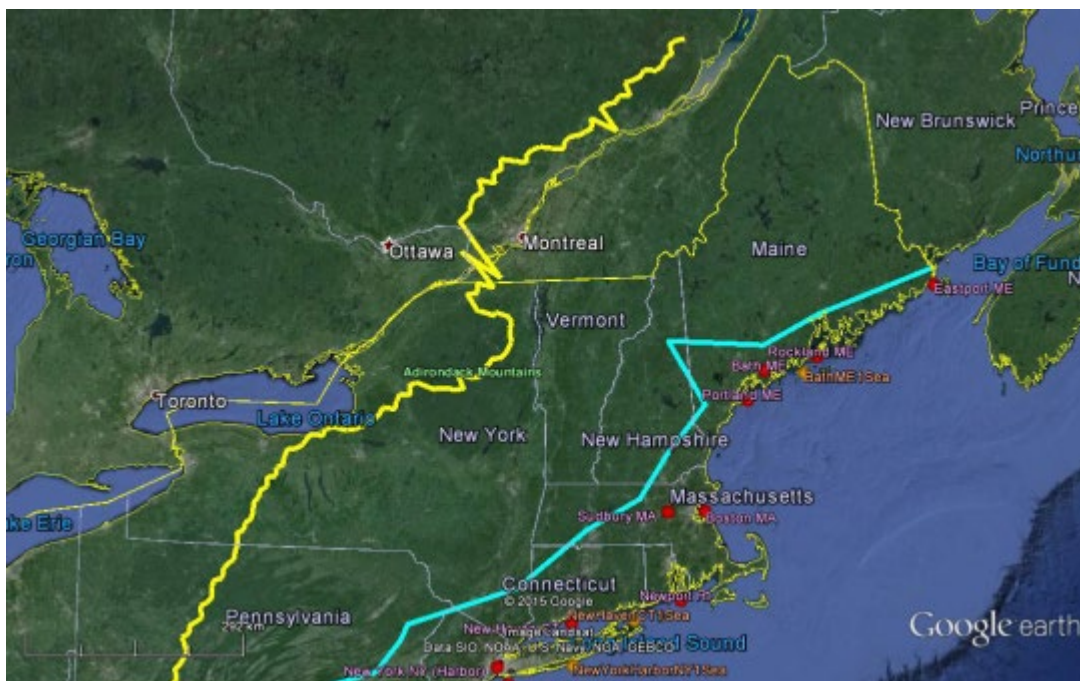


Figure B-23. Shipborne Radar 5–Exclusion zone upper east coast (yellow line–fast track exclusion zone and blue line–revised exclusion zone).



Figure B-24. Shipborne Radar 5–Exclusion zone middle east coast (yellow line–fast track exclusion zone and blue line–revised exclusion zone).

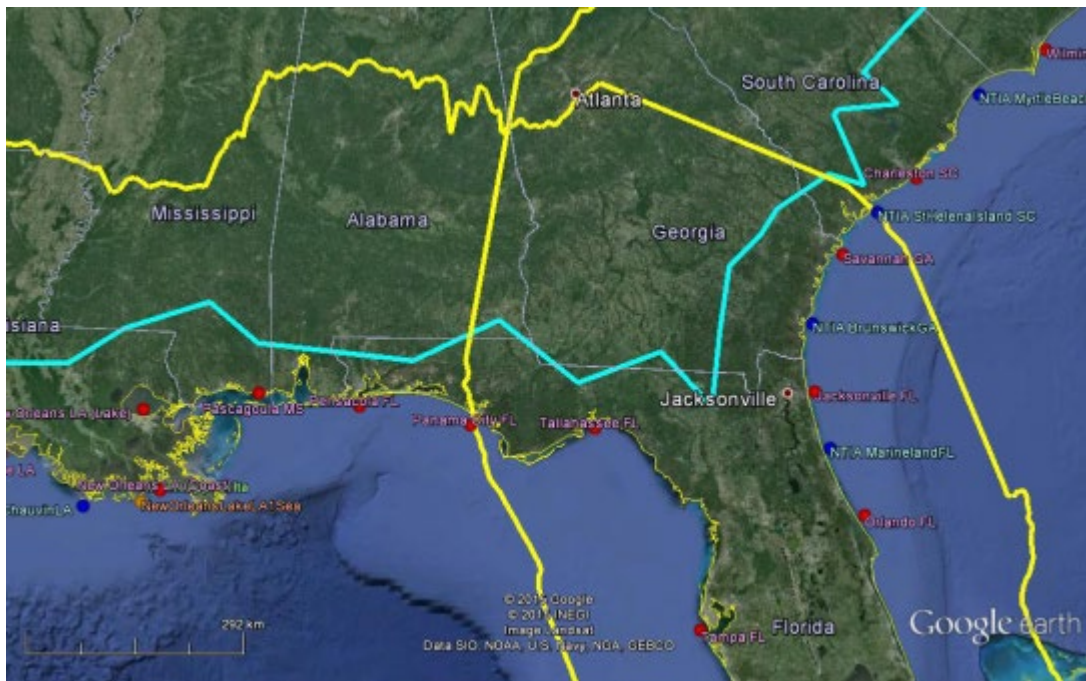


Figure B-25. Shipborne Radar 5–Exclusion zone lower east coast (yellow line–fast track exclusion zone and blue line–revised exclusion zone).

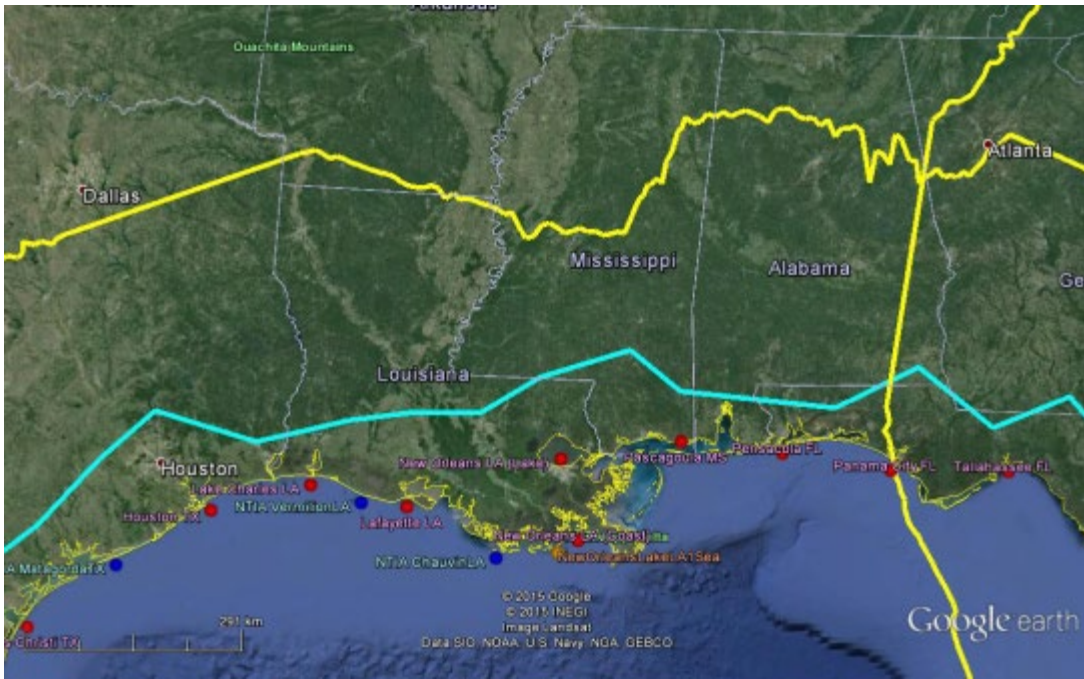


Figure B-26. Shipborne Radar 5–Exclusion zone eastern gulf coast (yellow line–fast track exclusion zone and blue line–revised exclusion zone).

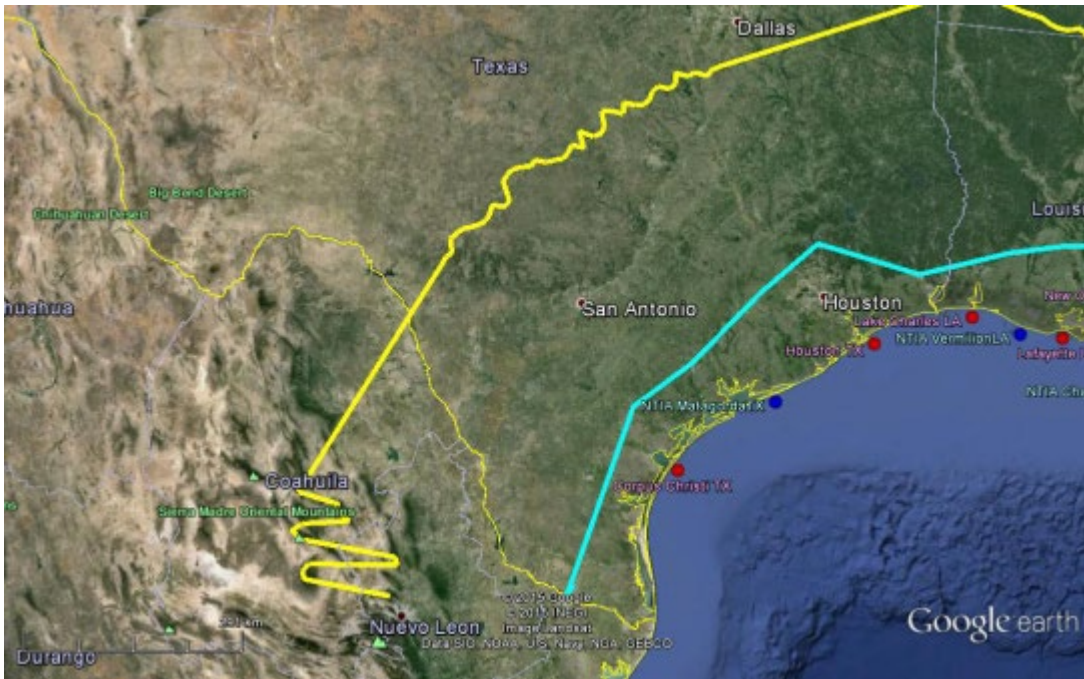


Figure B-27. Shipborne Radar 5–Exclusion zone western gulf coast (yellow line–fast track exclusion zone and blue line–revised exclusion zone).

The composite exclusion zones for the shipborne radars operating in the 3550–3650 MHz band are provided in Figures B-28 through B-36. The yellow line on each plot is the composite

exclusion zone distance based on the Fast Track Report and the blue line is the revised composite exclusion zone distance. Ship locations are not shown in these figures.

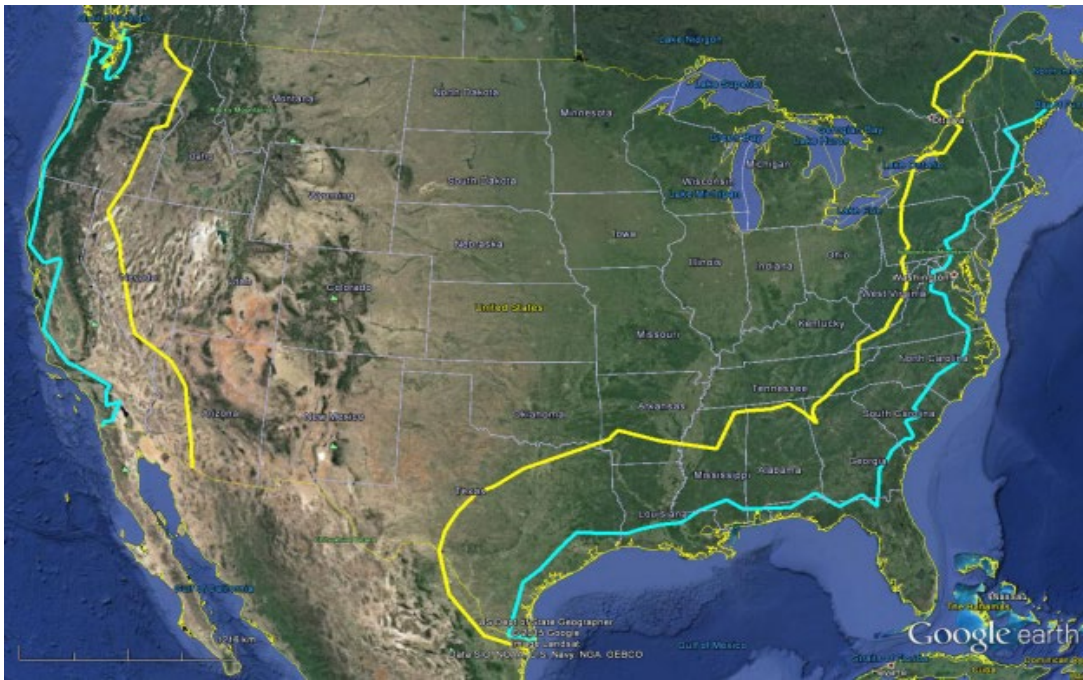


Figure B-28. Composite shipborne radar exclusion zone lower 48 states (yellow line—fast track exclusion zone and blue line—revised exclusion zone).

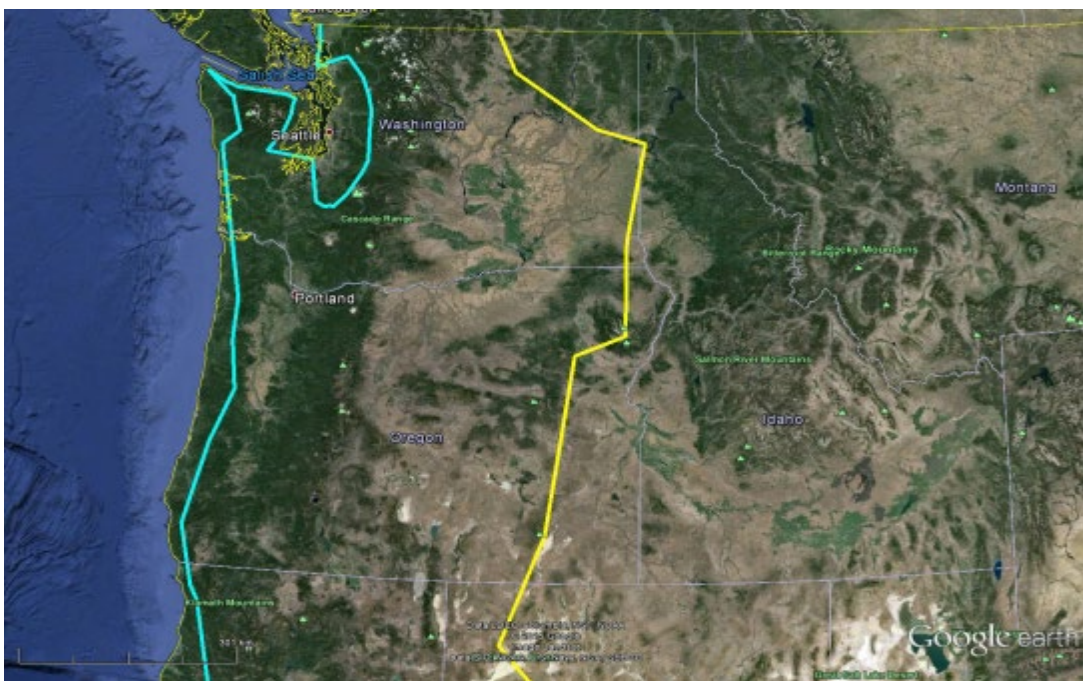


Figure B-29. Composite shipborne radar exclusion zone upper west coast (yellow line—fast track exclusion zone and blue line—revised exclusion zone).

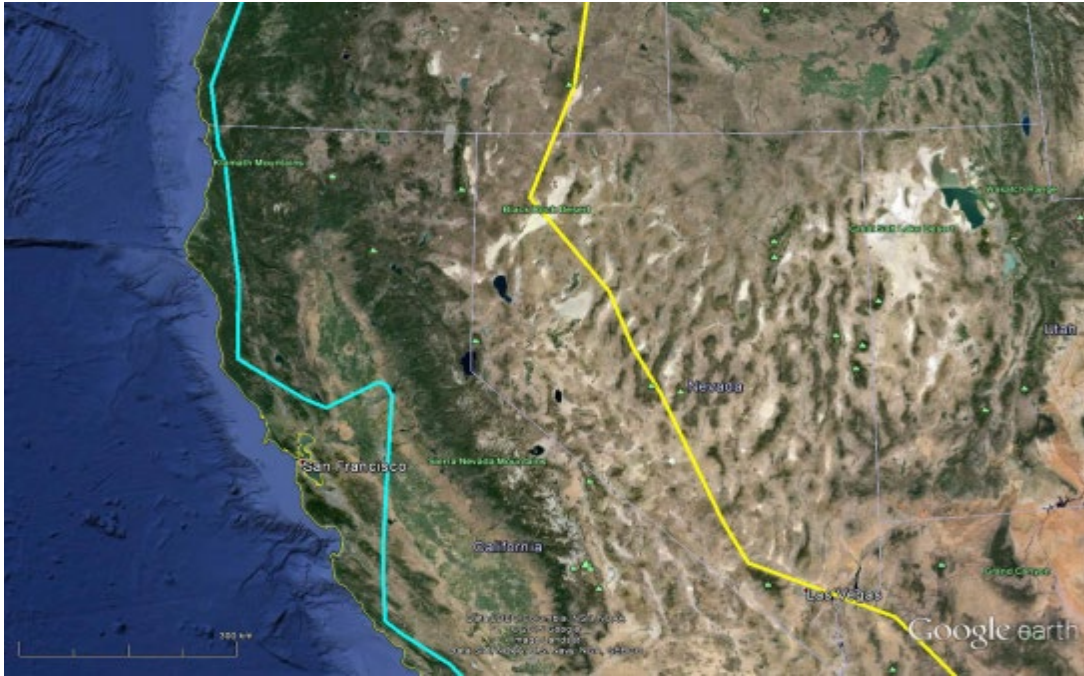


Figure B-30. Composite shipborne radar exclusion zone middle west coast (yellow line—fast track exclusion zone and blue line—revised exclusion zone).

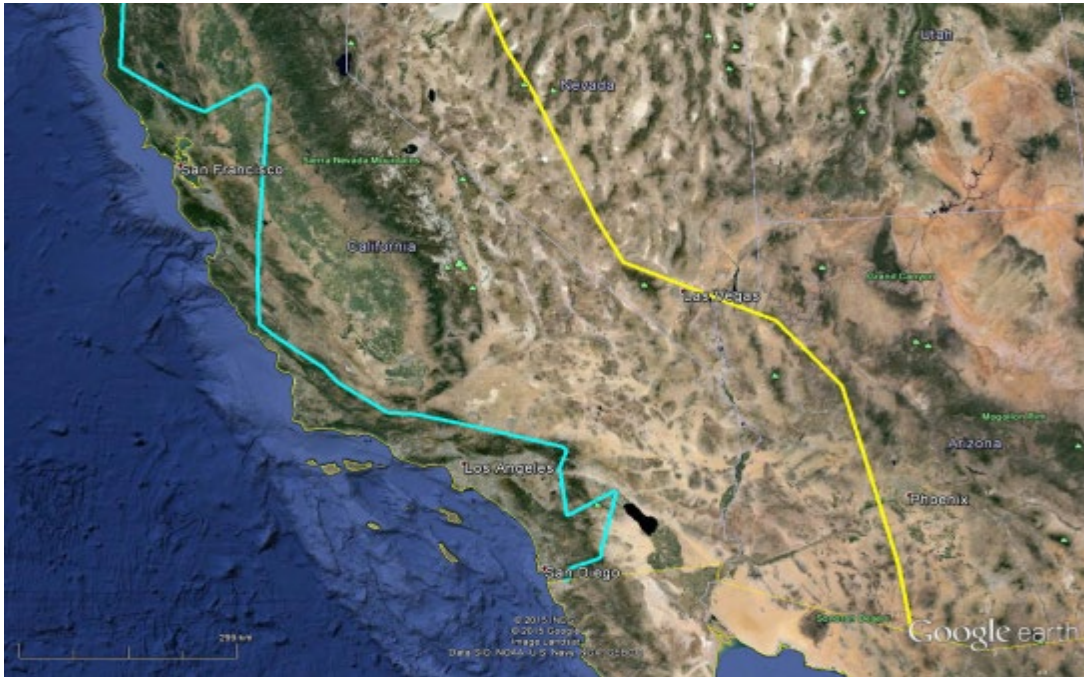


Figure B-31. Composite shipborne radar exclusion zone lower west coast (yellow line—fast track exclusion zone and blue line—revised exclusion zone).

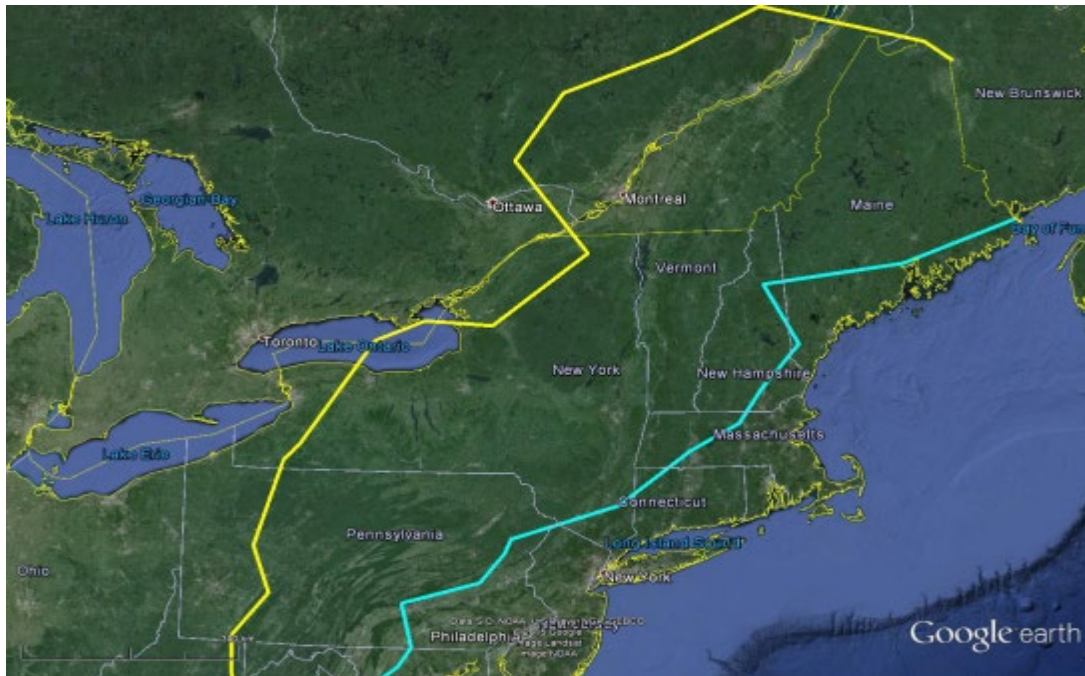


Figure B-32. Composite shipborne radar exclusion zone upper east coast (yellow line–fast track exclusion zone and blue line–revised exclusion zone).



Figure B-33. Composite shipborne radar exclusion zone middle east coast (yellow line–fast track exclusion zone and blue line–revised exclusion zone).

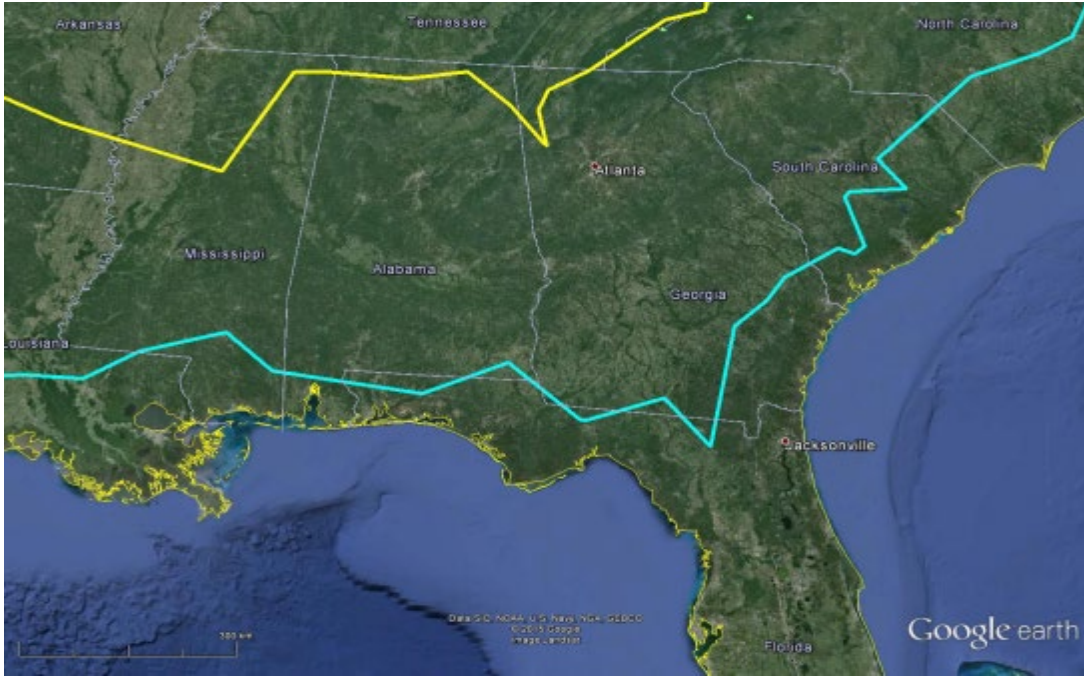


Figure B-34. Composite shipborne radar exclusion zone lower east coast(yellow line–fast track exclusion zone and blue line–revised exclusion zone).

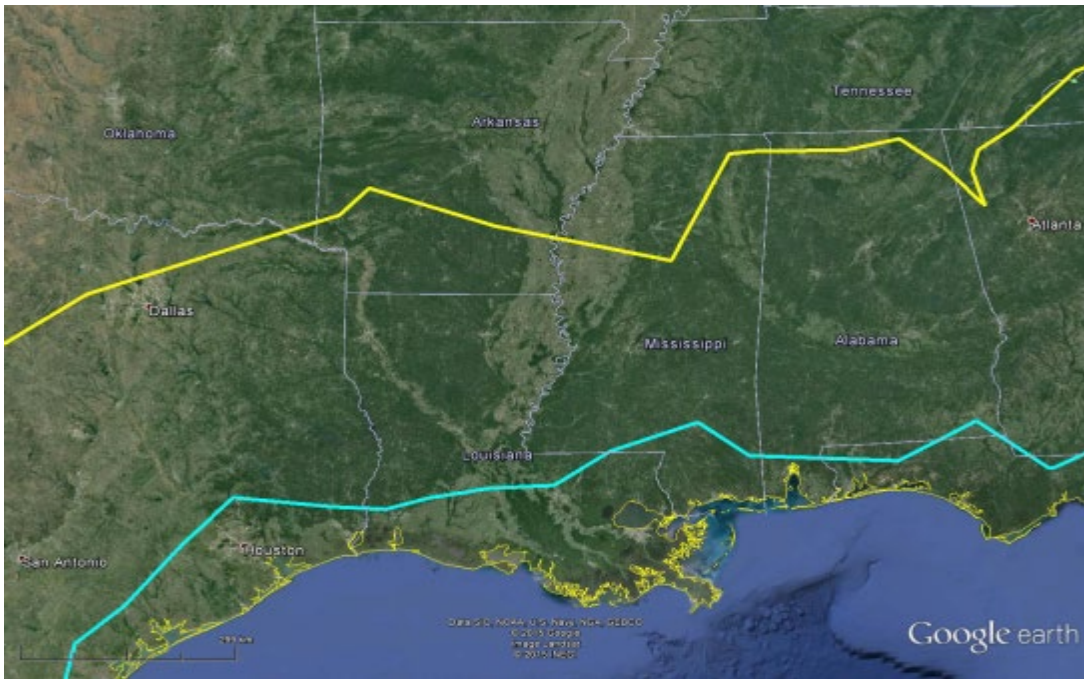


Figure B-35. Composite shipborne radar exclusion zone eastern gulf coast (yellow line–fast track exclusion zone and blue line–revised exclusion zone).

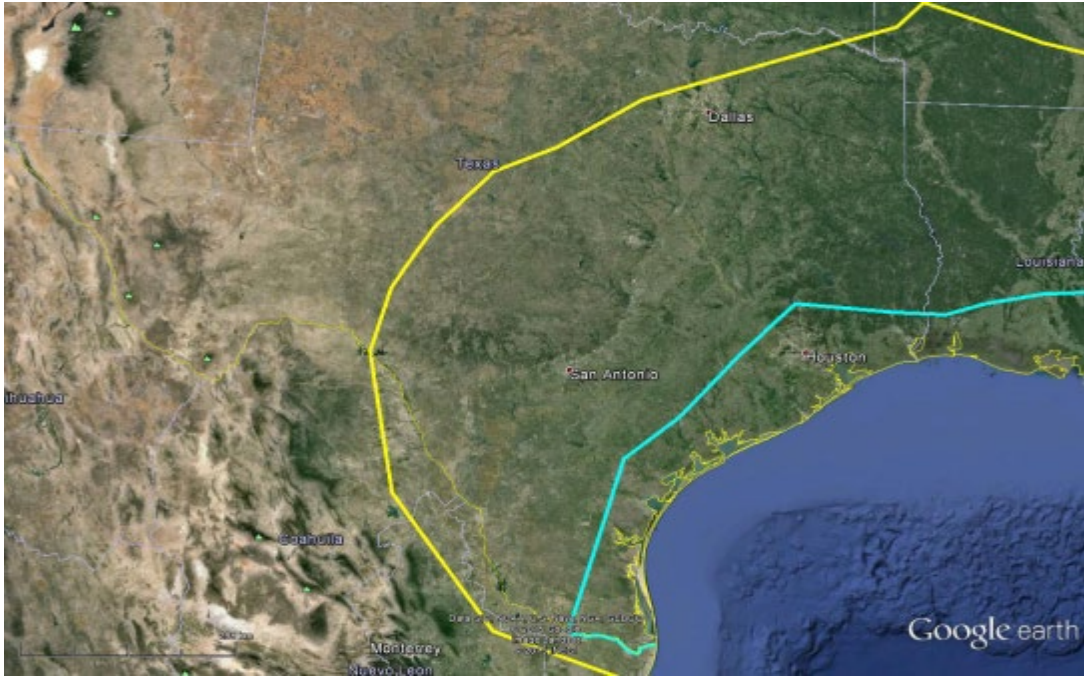


Figure B-36. Composite shipborne radar exclusion zone western gulf coast (yellow line–fast track exclusion zone and blue line–revised exclusion zone).

The results for the shipborne radar exclusion zone distance analysis compared to the Fast Track Report exclusion zone distances are provided in Tables B-1 to B-3. The results are presented for three parameters: percentage of area impacted, percentage of population impacted, and average exclusion zone distance.

Table B-1. Summary of Shipborne Radar Analysis Results

Radar Identifier	Geographic Area	Percentage of Area Impacted (km ²)		
		Fast Track ¹³ Report Analysis	Revised Analysis (3.5 GHz Study)	Reduction of Area Impacted
Shipborne Radar 1	East Coast	654,067	251,706	62 %
	West Coast	477,627	76,363	84 %
	Gulf Coast	528,374	167,936	68 %
Shipborne Radar 4	East Coast	1,081,389	299,243	72 %
	West Coast	611,070	79,729	87 %
	Gulf Coast	880,096	182,258	79 %
Shipborne Radar 5	East Coast	1,040,991	339,037	67 %
	West Coast	956,435	93,530	90 %
	Gulf Coast	718,117	211,218	71 %

¹³ [B-1] Table 5-4.

Table B-2. Comparison of Summary of Shipborne Radar Analysis Results

Radar Identifier	Geographic Area	Fast Track Report Analysis		Revised Analysis (3.5 GHz Study)		Reduction in Percentage of Total Population Impacted
		Population Impacted	Percentage of Total Population Impacted	Population Impacted	Percentage of Total Population Impacted	
Shipborne Radar 1	East Coast	58,562,753	28 %	48,387,330	23 %	17 %
	West Coast	41,164,529	20 %	27,112,935	13 %	34 %
	Gulf Coast	18,943,514	9 %	12,439,455	6 %	34 %
Shipborne Radar 4	East Coast	66,771,384	32 %	49,480,866	24 %	26 %
	West Coast	42,136,232	20 %	27,092,000	13 %	36 %
	Gulf Coast	29,342,307	14 %	12,812,822	6 %	56 %
Shipborne Radar 5	East Coast	66,589,823	32 %	50,391,618	24 %	24 %
	West Coast	45,145,947	22 %	28,447,839	14 %	37 %
	Gulf Coast	21,992,519	11 %	12,878,464	6 %	41 %

Table B-3. Summary of Shipborne Radar Analysis Results by Area Affected

Radar Identifier	Geographic Area	Average Exclusion Zone Distance		
		Fast Track Report Analysis	Revised Analysis (3.5 GHz Study)	Reduction in Average Exclusion Zone Distance
Shipborne Radar 1	East Coast	255	89	166
	West Coast	189	41	148
	Gulf Coast	248	64	184
Shipborne Radar 4	East Coast	426	117	309
	West Coast	245	39	206
	Gulf Coast	427	71	356
Shipborne Radar 5	East Coast	398	116	282
	West Coast	423	46	377
	Gulf Coast	359	94	265

B.3 References

- [B-1] U.S. Department of Commerce, National Telecommunications and Information Administration, *An Assessment of the Near-Term Viability of Accommodating Wireless Broadband Systems in the 1675-1710 MHz, 1755-1780 MHz, 3500-3650 MHz, and 4200-4220 MHz, 4380-4400 MHz Bands* (Nov. 15, 2010) (*Fast Track Report*), available at http://www.ntia.doc.gov/reports/2010/FastTrackEvaluation_11152010.pdf.

APPENDIX C GROUND-BASED RADAR ANALYSIS RESULTS

C.1 Introduction

Appendix C provides the results of the exclusion zone distance analysis and the exclusion zones needed to protect the ground-based radars operating adjacent to the 3550–3650 MHz band.

C.2 Ground-Based Radar Analysis Results

Exclusion zones around ground-based radars are defined as a fixed distance outside the perimeters of the installations listed in Tables C-1 and C-2.

Table C-1. Ground-Based Radar 1 Locations

Location of Military Facility
Aberdeen PG, MD
Camp Shelby, MS
Camp Sherman, OH
Camp Smith, NY
Fort Benning, GA
Fort Bragg, NC
Fort Campbell, KY
Fort Carson, CO
Fort Drum, NY
Fort Indiantown Gap, PA
Fort Irwin, CA
Fort Hood, TX
Fort Lewis, WA
Fort Polk, LA
Fort Riley, KS
Fort Sill, OK
Fort Stewart, GA
Letterkenny, PA
Morristown, NJ
Pohakuola Training Area, HI
Yakima Firing Center, WA
Yuma PG, AZ
Schofield Barracks, HI
Knoxville, TN
Pinon Canyon, CO
Tupelo, MS
White Sands Missile Range, NM

Table C-2. Ground-Based Radar 3 Locations

Location of Military Facility
MCB Camp Pendleton, CA
MCAS Miramar, CA
MAGTFTC Twenty Nine Palms, CA
MCAS Yuma, AZ
MCB Camp Lejeune, NC
MCAS Cherry Point, NC
MCAS Beaufort, SC
Virginia Beach, VA (reserve unit)
Fort Worth, TX (reserve unit)
Fort Sill, OK
Naval Air Station, Patuxent River, MD
Eglin AFB, FL
Naval Air Station China Lake, CA

Table C-3. Results of Ground-Based Radar Analyses

Military Base	Radar	Nearby City	Exclusion Zone
Fort Carson CO	GB-1	Colorado Springs CO	2 km
Fort Riley KS	GB-1	Junction City KS	3 km
Fort Riley KS	GB-1	Manhattan KS	2 km
Fort Sill OK	GB-3	Lawton OK	2 km
Camp Pendleton CA	GB-3	Oceanside/Carlsbad CA	4 km

Based on these results, a 3 kilometer exclusion zone around the perimeter of each of the installations listed in Tables C-1 and C-2 is needed to protect these radars. The exclusion zones for ground-based radars in the Fast Track Report were between 40 and 60 km.¹⁴

The exclusion zones for the ground-based radar systems are provided in Figures C-1 through C-8.

¹⁴ [C-1] Table 5-2.

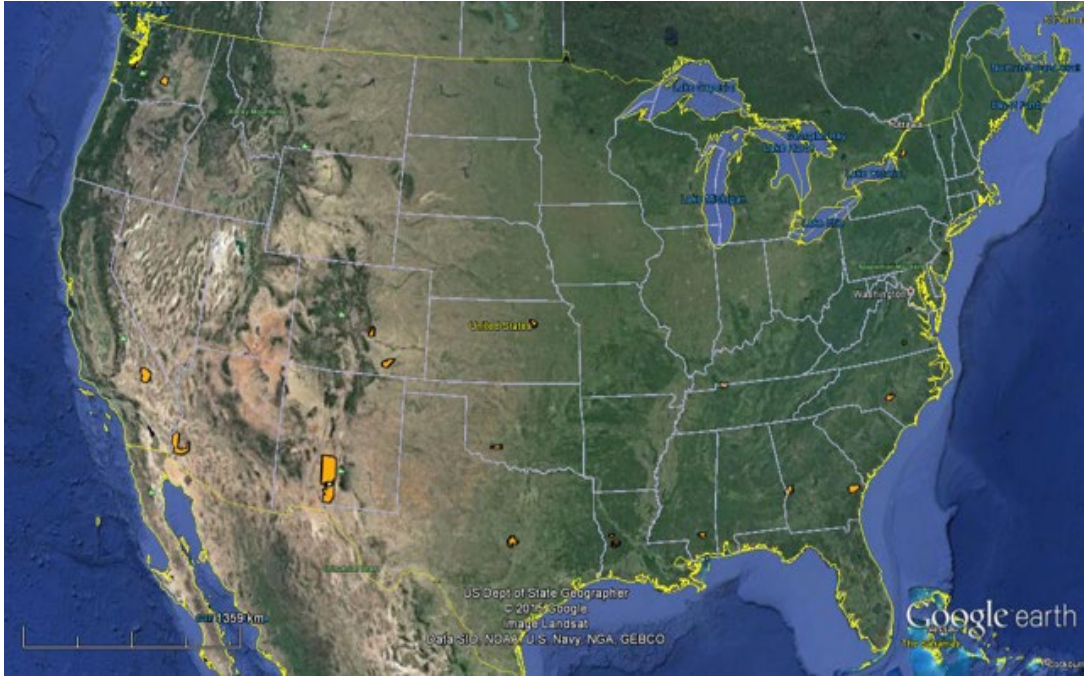


Figure C-1. Ground-based radar exclusion zone lower 48 states.

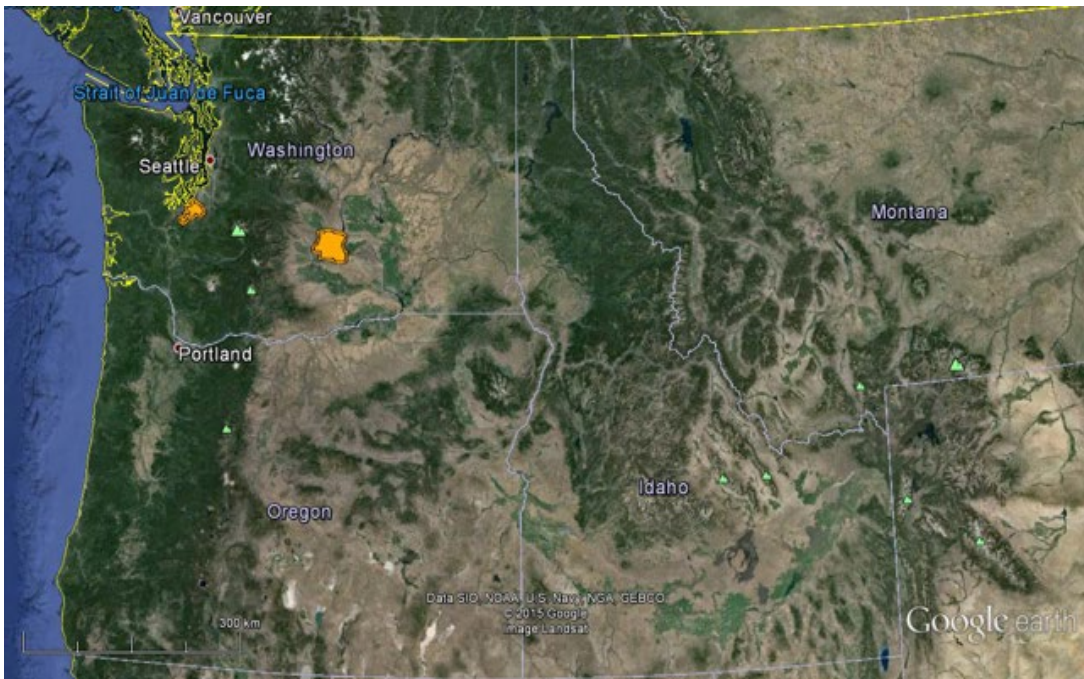


Figure C-2. Ground-based radar exclusion zone upper west coast.



Figure C-3. Ground-based radar exclusion zone middle west coast.



Figure C-4. Ground-based radar exclusion zone upper central.

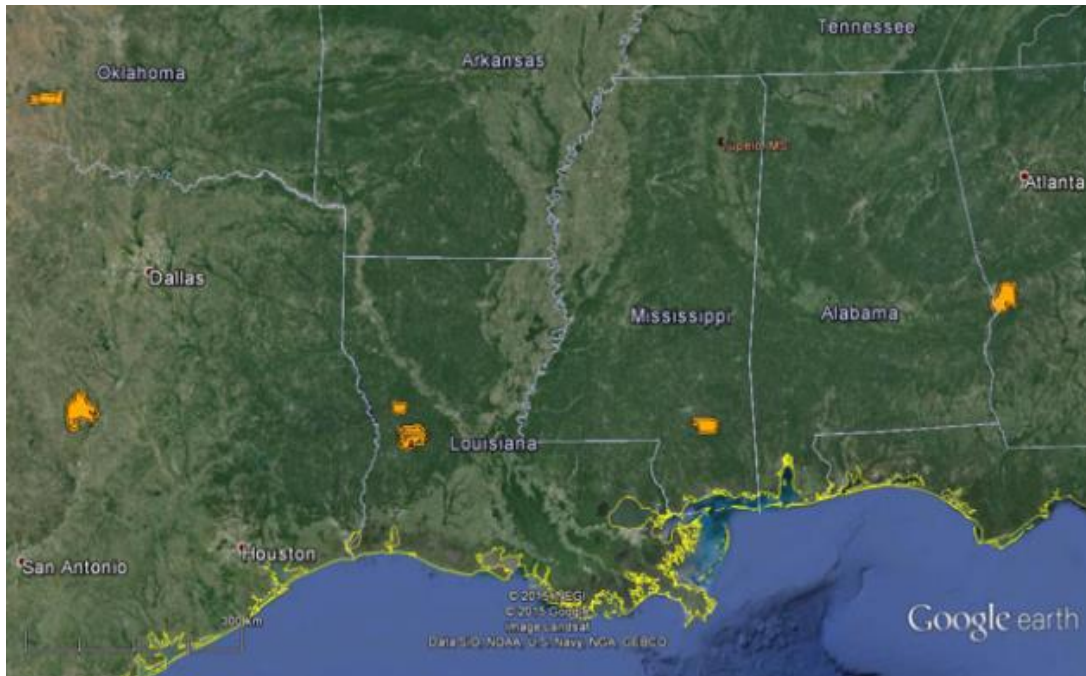


Figure C-5. Ground-based radar exclusion zone lower central.

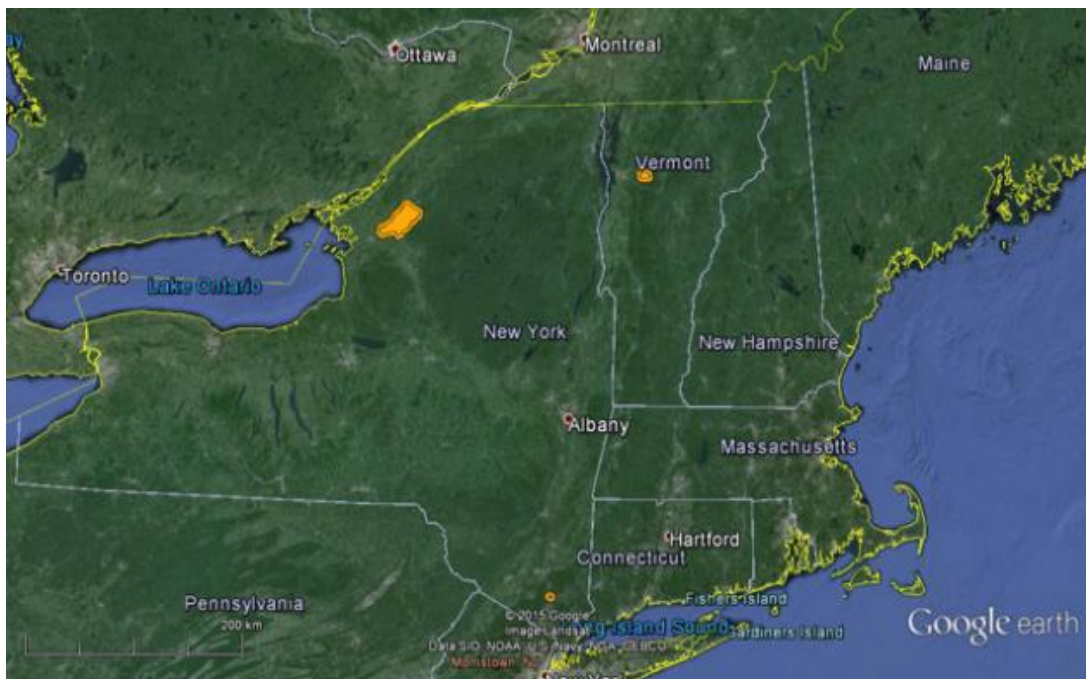


Figure C-6. Ground-based radar exclusion zone upper east coast.

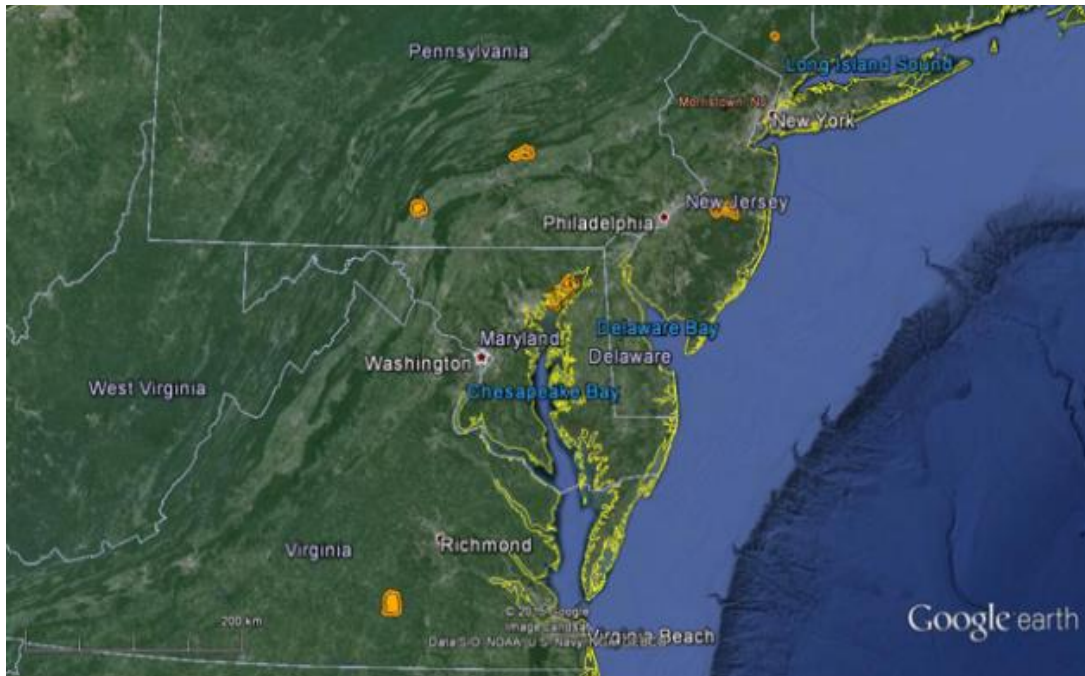


Figure C-7. Ground-based radar exclusion zone middle east coast.

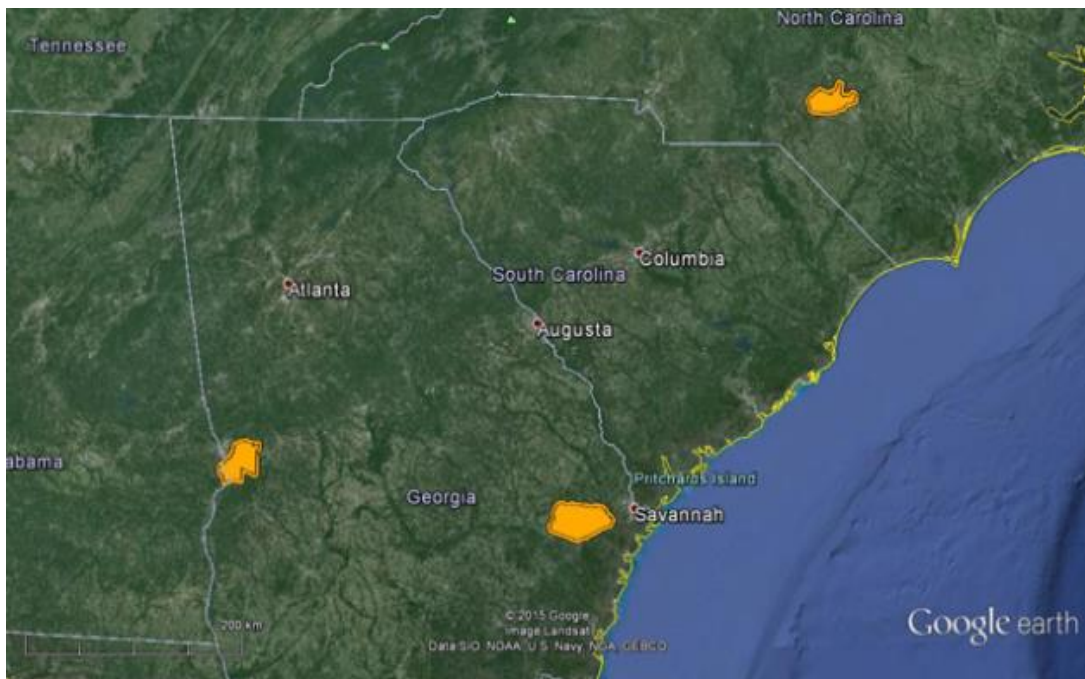


Figure C-8. Ground-based radar exclusion zone lower east coast.

C.3 References

- [C-1] U.S. Department of Commerce, National Telecommunications and Information Administration, *An Assessment of the Near-Term Viability of Accommodating Wireless Broadband Systems in the 1675-1710 MHz, 1755-1780 MHz, 3500-3650 MHz, and 4200-4220 MHz, 4380-4400 MHz Bands* (Nov. 15, 2010) (*Fast Track Report*), available at http://www.ntia.doc.gov/reports/2010/FastTrackEvaluation_11152010.pdf.

BIBLIOGRAPHIC DATA SHEET

1. PUBLICATION NO. TR-15-517	2. Government Accession No.	3. Recipient's Accession No.
4. TITLE AND SUBTITLE 3.5 GHz Exclusion Zone Analyses and Methodology		5. Publication Date June 2015, Reissued March 2016
		6. Performing Organization Code NTIA/OSM
7. AUTHOR(S) E. Drocella, J. Richards, R. Sole, F. Najmy, A. Lundy, and P. McKenna		9. Project/Task/Work Unit No. 6469000-200
8. PERFORMING ORGANIZATION NAME AND ADDRESS Institute for Telecommunication Sciences National Telecommunications & Information Administration U.S. Department of Commerce 325 Broadway Boulder, CO 80305		10. Contract/Grant Number.
		12. Type of Report and Period Covered
11. Sponsoring Organization Name and Address National Telecommunications & Information Administration Herbert C. Hoover Building 14 th & Constitution Ave., NW Washington, DC 20230		12. Type of Report and Period Covered
14. SUPPLEMENTARY NOTES		
15. ABSTRACT (A 200-word or less factual summary of most significant information. If document includes a significant bibliography or literature survey, mention it here.) This report describes the 3.5 GHz Study. It explains the assumptions, methods, analyses, and system characteristics used to generate the revised exclusion zones for small-cell commercial broadband systems to protect federal radar operations (ship and land based) from aggregate interference in the band 3550–3650 MHz. The 3.5 GHz Study's exclusion zones are compared with the exclusion zones that were generated in the Fast Track Report, which considered macro-cell operations.		
16. Key Words (Alphabetical order, separated by semicolons) NTIA, FCC, radar, exclusion zones, CBRS, CBSD, spectrum, sharing, 3550–3650 MHz		
17. AVAILABILITY STATEMENT <input checked="" type="checkbox"/> UNLIMITED. <input type="checkbox"/> FOR OFFICIAL DISTRIBUTION.	18. Security Class. (This report) Unclassified	20. Number of pages 103
19. Security Class. (This page) Unclassified		21. Price: N/A

NTIA FORMAL PUBLICATION SERIES

NTIA MONOGRAPH (MG)

A scholarly, professionally oriented publication dealing with state-of-the-art research or an authoritative treatment of a broad area. Expected to have long-lasting value.

NTIA SPECIAL PUBLICATION (SP)

Conference proceedings, bibliographies, selected speeches, course and instructional materials, directories, and major studies mandated by Congress.

NTIA REPORT (TR)

Important contributions to existing knowledge of less breadth than a monograph, such as results of completed projects and major activities.

JOINT NTIA/OTHER-AGENCY REPORT (JR)

This report receives both local NTIA and other agency review. Both agencies' logos and report series numbering appear on the cover.

NTIA SOFTWARE & DATA PRODUCTS (SD)

Software such as programs, test data, and sound/video files. This series can be used to transfer technology to U.S. industry.

NTIA HANDBOOK (HB)

Information pertaining to technical procedures, reference and data guides, and formal user's manuals that are expected to be pertinent for a long time.

NTIA TECHNICAL MEMORANDUM (TM)

Technical information typically of less breadth than an NTIA Report. The series includes data, preliminary project results, and information for a specific, limited audience.

For information about NTIA publications, contact the NTIA/ITS Technical Publications Office at 325 Broadway, Boulder, CO, 80305 Tel. (303) 497-3572 or e-mail info@its.bldrdoc.gov.